SKI Report 02:62

Research

Exploration of Important Issues for the Safety of SFR 1 using Performance Assessment Calculations

Philip R. Maul
Peter C. Robinson

June 2002

ISSN 1104–1374
ISRN SKI-R-02/62-SE

SKI perspective

Background

The Swedish repository of low and intermediate-level radioactive waste, SFR 1, is used for final disposal of waste produced by the Swedish nuclear power programme, industry, medicine and research. The repository is located near to the Forsmark nuclear power plant about 160 km north of Stockholm.

As part of the license for the SFR 1 repository a renewed safety assessment should be carried out at least every ten years for the continued operation of the SFR 1 repository. The safety assessment shall include both the operation and long-term aspect of the repository. SKB has during year 2001 finalised their renewed safety assessment (project SAFE) which evaluates the performance of the SFR 1 repository system. The current safety assessment is the first renewal carried out by SKB for the SFR 1 repository.

Purpose of the project

The purpose of this project is to use the radionuclide transport model (AMBER) that has been developed to investigate important issues of long-term safety regarding the SFR 1 repository system. This work is valuable for SKI in its review of SKB's calculations for SFR 1 done in the project SAFE. It should be noted that the performance assessment calculations that have been undertaken in the current project are by no means comprehensive and does not represent an alternative assessment of potential radiological impacts to that produced by SKB.

Results

Some of the key issues that have been identified can be summarised as follows:

- It is important that all relevant time-dependent processes are represented in system modelling.
- Because of the complexity of the system, it is not always possible to define what choices of modelling assumptions and parameter values can be regarded as 'conservative'.
- Peak impacts are likely to be sensitive to the assumptions made about groundwater flow rates through the vaults.

Effect on SKI's work

The development of the radio nuclide transport compartment model, AMBER, for SFR 1 is a good base in developing models for the repository for spent fuel and the repository for long-lived low and intermediate level waste SFL 3-5.

Project information

Responsible at SKI has been Benny Sundström.
SKI ref.: 14.9-010239/01065

Relevant SKI report: Chapman, N. A., Maul, P. R., Robinson, P. C., Savage D., SKB's Project SAFE for the SFR 1 Repository - A Review by Consultants to SKI -, SKI Report 02:61, Swedish Nuclear Power Inspectorate, Stockholm, Sweden, 2002.

SKI Report 02:62

Research

Exploration of Important Issues for the Safety of SFR 1 using Performance Assessment Calculations

Philip R. Maul
Peter C. Robinson

Quintessa Limited
Dalton House
Newton Road
Henley-on-Thames
Oxfordshire RG9 1HG
United Kingdom

June 2002

Executive Summary

SKB (The Swedish Nuclear Fuel and Waste Management Company) has produced a revised safety case for the SFR 1 disposal facility for low and intermediate level radioactive wastes at Forsmark: project SAFE (Safety Assessment of Final Repository for Radioactive Operational Wastes). This assessment includes a Performance Assessment (PA) for the long term post-closure safety of the facility. SKI (The Swedish Nuclear Power Inspectorate) has a responsibility to scrutinise SKB's safety case that is shared with SSI (the Swedish Radiation Protection Authority).

Quintessa has undertaken a review of SKB's case for the long term safety of SFR 1 to assist SKI's evaluation of SAFE, and this is given in Chapman et al. (2002), henceforth referred to as the Quintessa Review. The current report describes the independent PA calculations that provided an input to that review.

Since 1999 SKI has been developing a PA capability for SFR 1 using the AMBER software. Two key features of the approach taken have been:

- To represent the whole system in a single model; and
- To allow the time-dependency of all key features, events and processes to be represented.

These capabilities allow a better understanding of the key features of the system to be obtained for different future evolutions (scenarios).

This report presents a summary of the work undertaken to provide SKI with a PA capability for SFR 1 and the calculations undertaken with it. Calculations have been undertaken for radionuclides transported in groundwater and gas, but not for direct intrusion by humans into the wastes.

It should be emphasised that the purpose of the Performance Assessment calculations described in this report is not to provide an alternative assessment of potential radiological impacts to that produced by SKB. The aim is to use the models that have been developed to investigate the important features of the system and to help SKI scrutinise the case put to them by SKB. The PA calculations that have been undertaken are by no means comprehensive, and various issues could be investigated further if required.

The key issues that have been identified can be summarised as follows:

1. The SFR 1 system has a number of different timescales that can affect the magnitude of potential radiological impacts. These include: repository resaturation and gas evolution timescales, the rate at which the Baltic is retreating, the rates of engineered barrier degradation, and groundwater residence times in the geosphere. It is important that all relevant time-dependent processes are represented in system modelling.

2. Because of the complexity of the system, it is not always possible to define what choices of modelling assumptions and parameter values can be regarded as 'conservative'.

3. Radiological impacts when radionuclide discharges are to the Baltic are likely to be orders of magnitude lower than those when the discharges are to the terrestrial environment.

4. If overpressurisation of the Silo takes place due to gas generation, this could lead to increased early releases of short-lived radionuclides into the environment, but this is unlikely to lead to significantly increased radiological impacts as these releases would take place when SFR 1 is below the Baltic. Physical damage of the engineered barriers, might, however, be important on longer timescales by affecting groundwater flows through the facility.

5. Dose rates of the order of 0.1 mSv y^{-1} are possible when radionuclides from SFR 1 enter the terrestrial environment. The precise value of the calculated maximum dose rate will depend upon a number of assumptions about biosphere characteristics and critical group behaviour. The use of contaminated well water may give rise to significant exposures.

6. Long-lived actinide radionuclides (particularly in the Silo) may be retained by sorption processes on very long timescales. If this is the case, peak impacts are likely to be dominated by long-lived beta-gamma radionuclides such as Mo-93, Nb-93m, Ni-59, Cl-36, Se-79, Cs-135 and C-14.

7. For most of the PA calculations organic C-14 appears to be the dominant radionuclide primarily because it is assumed not to be sorbed in the near-field. Further consideration needs to be given to the behaviour of this radionuclide throughout the system in order to be able to provide better estimates of potential radiological impacts.

8. Peak impacts are likely to be sensitive to the assumptions made about groundwater flow rates through the vaults.

9. Illustrative calculations to investigate the potential importance of permafrost suggest that impacts are unlikely to be greater than those calculated in its absence.

10. Calculations to investigate potential impacts on very long timescales when the wastes may be brought close to the surface by erosive processes have shown that such impacts are likely to be small, being dominated by very long-lived radionuclides and their daughters such as Nb-94, Tc-99, Ra-226, Th-229, Th-230, Pa-233, Np-237, Pu-239 and Pu-242.

Contents

1 Introduction

SKB (The Swedish Nuclear Fuel and Waste Management Company) has produced a revised safety case for the SFR 1 disposal facility for low and intermediate level radioactive wastes at Forsmark: project SAFE (Safety Assessment of Final Repository for Radioactive Operational Wastes). This assessment includes a Performance Assessment (PA) for the long term post-closure safety of the facility. SKI (The Swedish Nuclear Power Inspectorate) has a responsibility to scrutinise SKB's safety case that is shared with SSI (the Swedish Radiation Protection Authority).

Quintessa has undertaken a review of SKB's case for the long term safety of SFR 1 to assist SKI's evaluation of SAFE, and this is given in Chapman et al. (2002), henceforth referred to as the Quintessa Review. The current report describes the independent PA calculations that provided an input to that review.

Figure 1.1 shows the general layout of SFR 1 with five individual vaults (the Silo, BMA, two BTF vaults and the BLA). A general description of the SFR facility is given in the Quintessa Review. In this report it is assumed that the reader is familiar with the general layout of SFR.

The need for an independent PA capability is recognised by SKI. This assists the process of reviewing proponent's safety cases, and helps to identify key issues in guiding the proponent's research and development activities.

Since 1999 SKI has been developing a PA capability for SFR 1 using the AMBER software. Two key features of the approach taken have been:

- To represent the whole system in a single model; and
- To allow the time-dependency of all key features, events and processes to be represented.

These capabilities allow a better understanding of the key features of the system to be obtained for different future evolutions (scenarios).

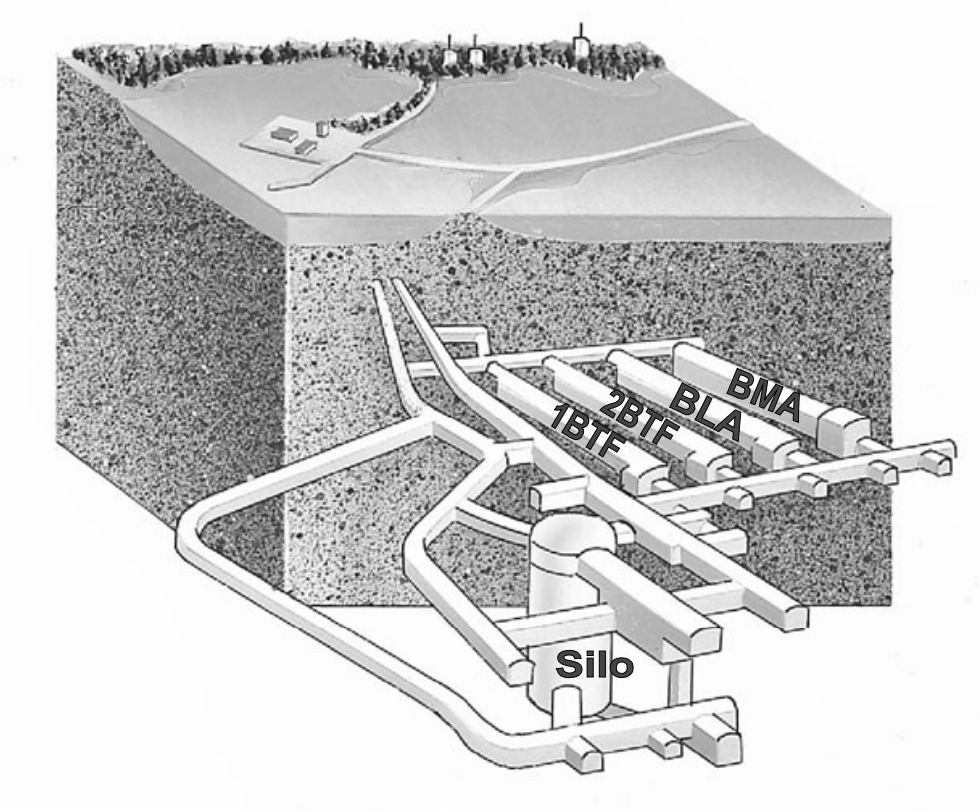

Figure 1.1 *The Layout of the SFR 1*

This report presents a summary of the work undertaken to provide SKI with a PA capability for SFR 1 and the calculations undertaken with it. It is structured as follows:

- Section 2 summarises the general approach to modelling the SFR 1 system that has been developed. Further mathematical details are given in Appendix A.
- Section 3 summarises the preliminary PA calculations that were undertaken in the period from 1999 to 2000.
- Section 4 then summarises the Final set of calculations undertaken in December 2001. These remain independent of SKB's calculations; no comparisons have been made with the calculations described in the SAFE documentation.
- Finally, Section 5 discusses the overall conclusions that can be drawn.

Calculations have been undertaken for radionuclides transported in groundwater and gas, but not for direct intrusion by humans into the wastes.

It should be emphasised that the purpose of the Performance Assessment calculations described in this report is not to provide an alternative assessment of potential

radiological impacts to that produced by SKB. The aim is to use the models that have been developed to investigate the important features of the system and to help SKI scrutinise the case put to them by SKB. The PA calculations that have been undertaken are by no means comprehensive, and various issues could be investigated further if required.

2 Modelling the SFR 1 with AMBER

In this Section the general approach that has been taken to modelling the SFR 1 system with the AMBER software (version 4.3) is described, based on the AMBER Case File that was used in the Final set of calculations for the Reference Scenario in Section 4. More detailed information is given in Appendix A. The preliminary calculations used slightly different models: these are described in Section 3 and Appendices 2-4.

2.1 AMBER

The AMBER software (QuantiSci and Quintessa, 2000) uses a compartmental modelling approach. The system to be modelled is represented by a number of compartments in which contaminants can be assumed to be uniformly mixed. Compartments may represent a fixed volume of the system being studied, but it may also be advantageous for a compartment to represent a part of the system whose physical boundaries change with time. The verification of the AMBER software is summarised in QuantiSci and Quintessa (2001).

AMBER was developed for the modelling of contaminant transport with potential radiological impacts to humans being estimated from calculated radionuclide concentrations in environmental materials. It is not currently suitable for modelling the transport of bulk materials around the system. For example, groundwater flows cannot be conveniently calculated in AMBER. If such information is required in order to calculate contaminant transport it must be supplied as input information, obtained from expert judgement or from calculations undertaken by supporting computer codes.

The general modelling approach that is used can be summarised as follows:

- The system to be modelled is represented by a number of compartments.
- The transport of contaminants between compartments is modelled, with information on the transport of bulk materials within the system being provided as input information.
- Potential radiological impacts are estimated from calculated radionuclide concentrations in environmental materials.

AMBER has a number of facilities that make it a powerful tool for undertaking this type of modelling. These include:

- The ability to represent time dependent processes. The evolution of compartment characteristics and the variation with time of contaminant transfer rates can be modelled. This is very important for SFR 1 as many of the characteristics of the system change significantly with time.
- The ability to structure the system as a number of sub-systems. This greatly helps to clarify the modelling of the SFR 1 system which can naturally be split up into a number of separate parts.
- The ability to undertake model calculations with all radionuclides of interest at the same time in an acceptable run time. Some general purpose modelling tools do not have an in-built understanding of radionuclides and decay chains, and may require separate model calculations for different groups of radionuclides.
- An in-built capability to undertake multiple runs for probabilistic or sensitivity calculations. This capability has been used to help identify some of the key model parameters and associated processes for the SFR 1 system.
- The capability to represent some non-linear processes. This has been used to investigate whether solubility limitations are important for SFR 1.

2.2 The SFR 1 System

The Quintessa Review includes a summary of work undertaken by SKI to analyse a Process Influence Diagram for SFR 1. This work is described in more detail by Stenhouse et al. (2001), and the analysis undertaken for the biosphere by Egan (1999). This work helped to identify some of the key processes that need to be modelled in PA calculations. As previously stated, however, it is not the intention to produce a comprehensive assessment of the SFR 1 facility, but to enable important issues to be identified.

In the future the environment in the Öregrunsgrepen region will change as a result of factors such as post glacial uplift. Brydsten (1999) has reported a study of how land uplift and changing sea levels will affect the Öregrunsgrepen region generally, and the area around the SFR 1 facility in particular. Key conclusions for modelling environmental change can be summarized as follows:

- At present the SFR 1 facility is 1 km off the coastline below the Öregrunsgrepen.
- Current land uplift rates are in the region of 6 mm y^{-1}, and are reducing. This is resulting in a gradual retreat of the coastline.

- The current rate of coastline retreat in the region of SFR 1 is around 1 m y^{-1}.
- The land immediately above SFR 1 will start to drain in around 400 years time, and will have completely drained in around 1500 years time.
- As sea levels fall a number of lakes will form in the Öregrunsgrepen. Some will be shallow, and these may form peaty areas or bogs.
- A small lake is expected to form about 1 km to the north of the SFR 1 location (lake number 20 in the inner area referred to by Brydsten (1999)). This lake is expected to have an area of around 160 000 m^2 and a mean depth of 1.4 m. It will form in around 1800 years time.

Sub-systems

The SFR 1 system has been divided into four sub-systems as shown in Figure 2.1, with the corresponding screen shot in AMBER shown in Figure 2.2. Figure 2.1 shows the main processes by which radioactivity can be moved around the system. The four sub-systems considered are:

- The Repository sub-system which includes models for each of the vaults (Silo, 1BTF, 2BTF, BMA and BLA), together with associated near-field rock;
- The Geosphere sub-system which represents the far-field rock;
- The Terrestrial Biosphere; and
- The Marine Biosphere.

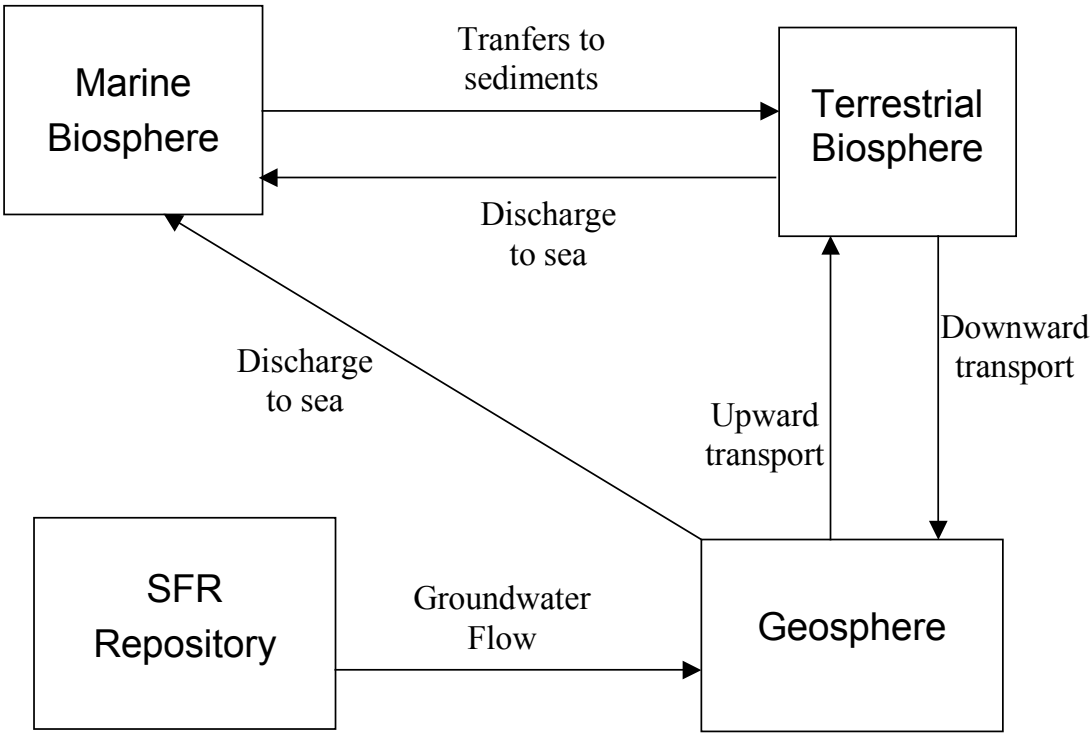

Figure 2.1 *The AMBER System Model for SFR 1*

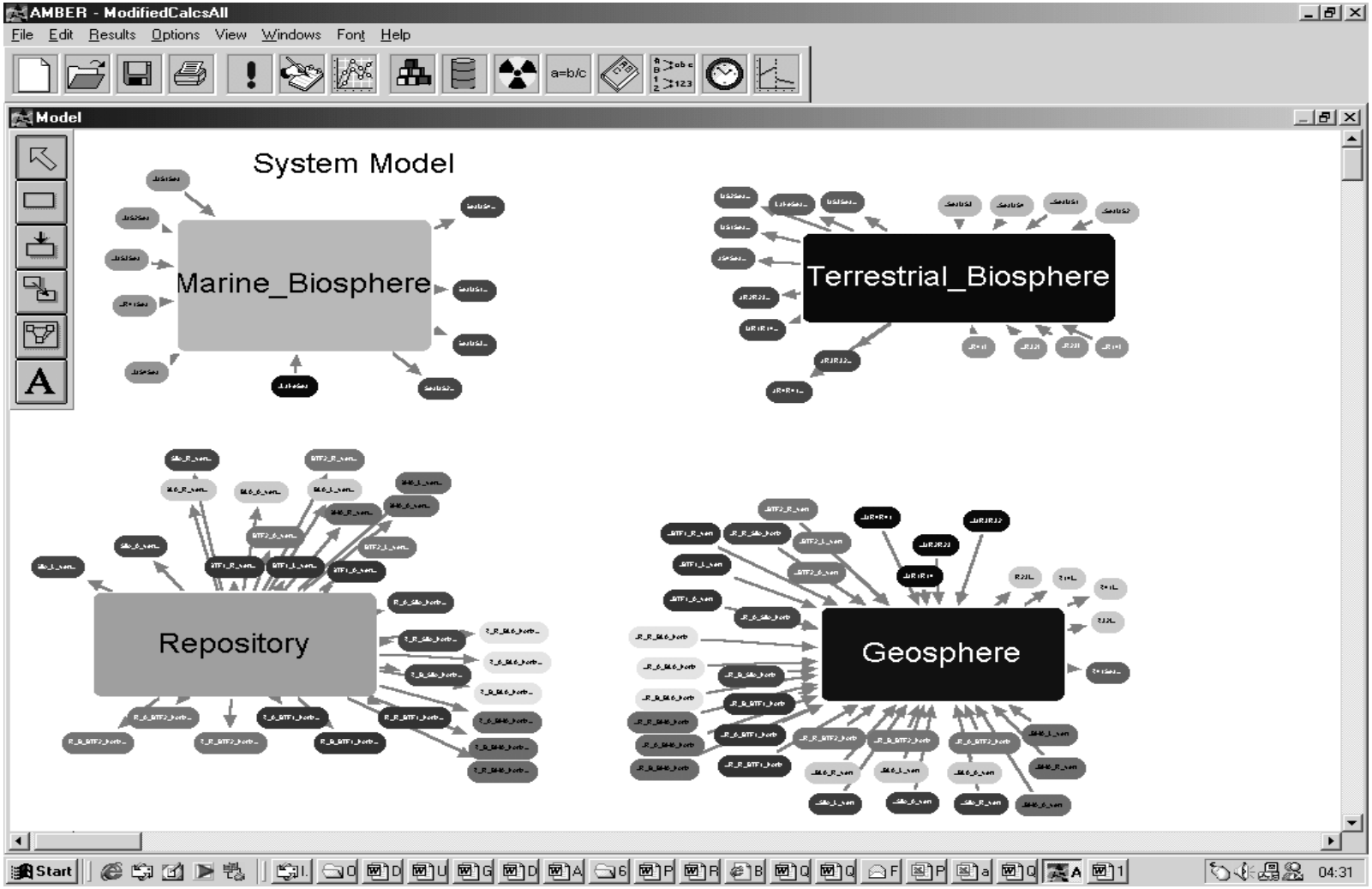

Figure 2.2 *Screenshot of the AMBER System Model for SFR 1*

Figure 2.3 shows the sub-model hierarchy used in AMBER. The Repository sub-system is broken down into a sub-model for each vault, and a distinction is made between the engineered facility and the near-field rock around that facility.

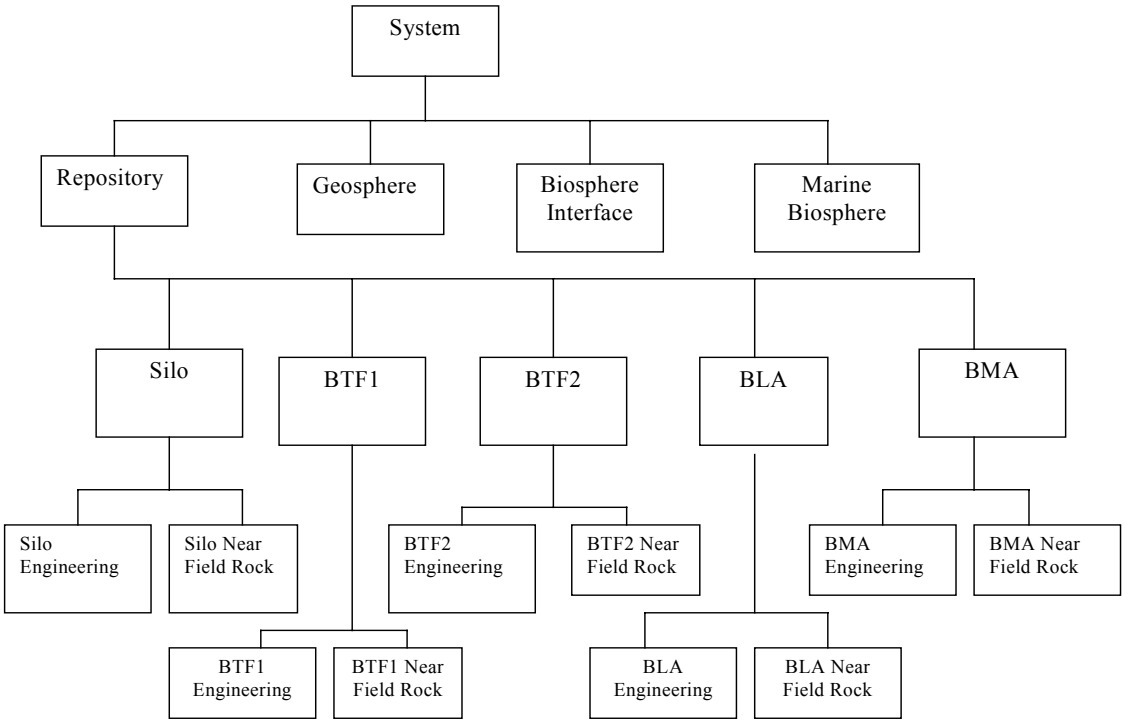

Figure 2.3 *The AMBER Model Hierarchy*

Groundwater Flow

The system is represented in three dimensions, but only discretised in two. All groundwater flows are assumed to be in the 2D plane that is discretised. The direction of the groundwater flow is assumed to vary over a 90 degree angle as the system evolves, so that components in the positive x- and y- directions have been assumed.

Figures 2.4 and 2.5 show schematically how the groundwater flow direction is assumed to vary from generally upwards from the repository region to the overlying sea initially to almost horizontal when the Baltic has retreated and the lake referred to above is assumed to have formed. In the AMBER calculations it was assumed that this lake

may persist for the period of interest of the PA calculations, or it may silt up; exposure calculations for both possibilities are considered.

In the following sub-sections details are given for how the various parts of the system have been modelled.

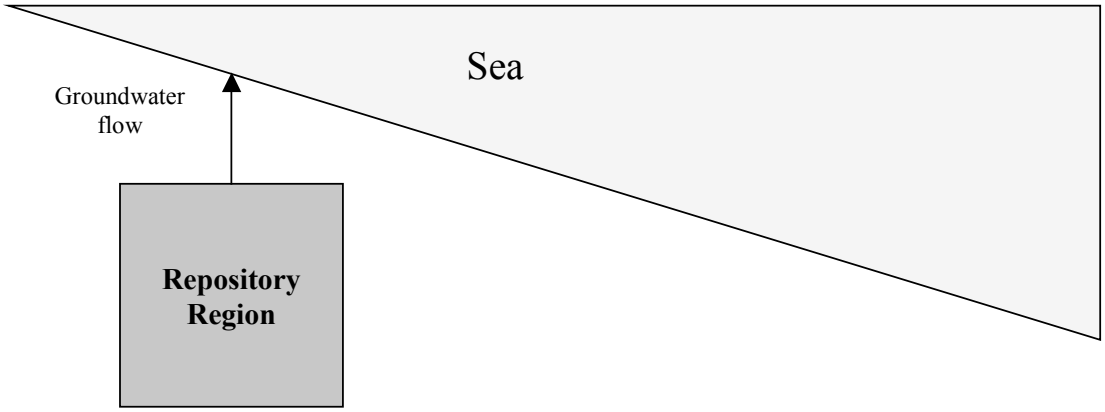

Figure 2.4 *Groundwater Flows when the Repository is below the Baltic*

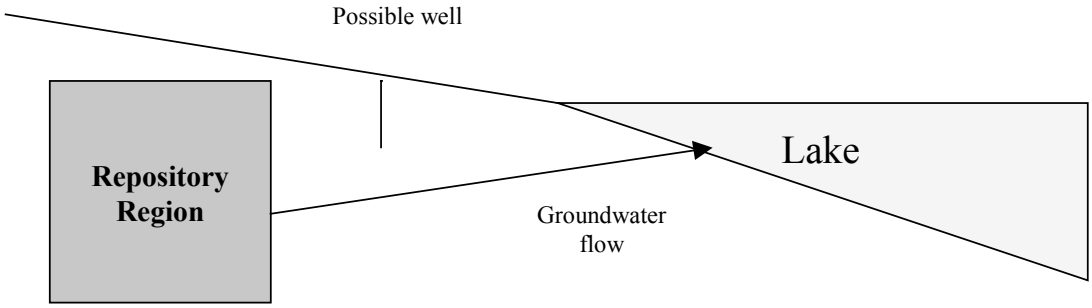

Figure 2.5 *Groundwater Flows when the Baltic has Retreated*

2.3 The Silo

Figure 2.6 shows the arrangement of near-field rock compartments around the engineered part of the system in the AMBER model. Advective transfers out of the sub-model are to the Geosphere sub-model.

Figure 2.7 shows the general layout of the Silo and Figure 2.8 shows the representation in AMBER of the engineered structure, with a screenshot of this sub-system in AMBER given in Figure 2.9. Interactions between compartments with only a small common area (e.g. base and walls) have not been included in the model. All radionuclide transfers out of the sub-model are to the Silo near-field rock sub-model. In the Final calculations described in Section 4, the Silo Backfill was assumed to be crushed rock (or similar material).

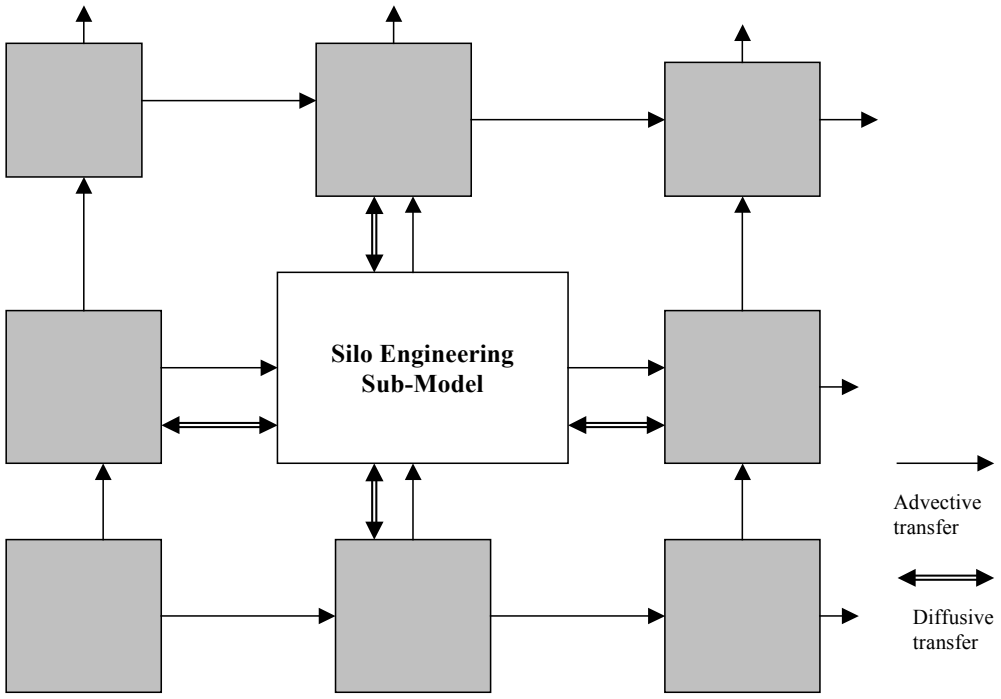

Figure 2.6 *The Silo Sub-Model*

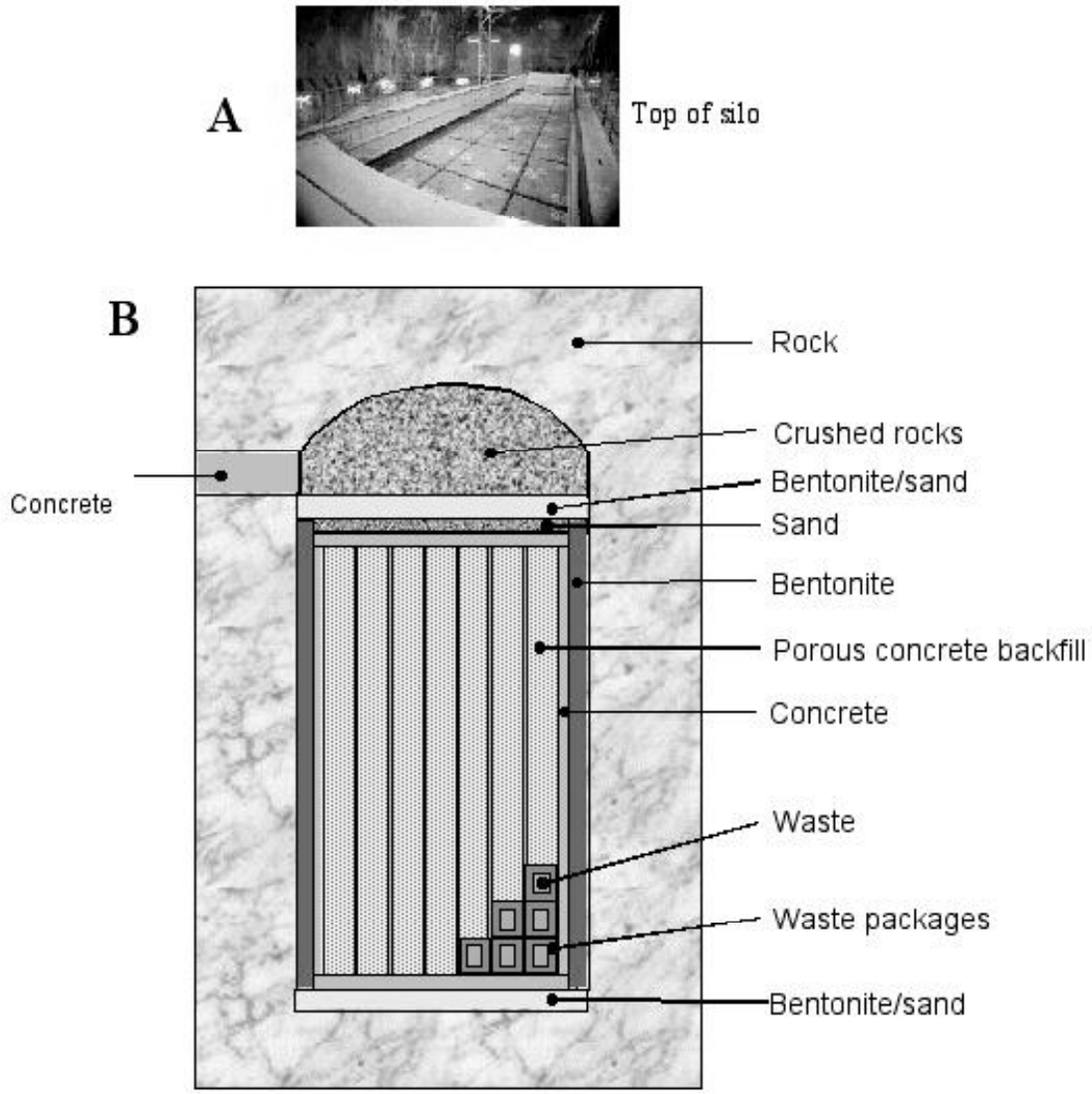

Figure 2.7 *The Layout of the Silo*

A*: photograph, Swedish Nuclear Fuel and Waste Management Co.*

B*: disposal system*

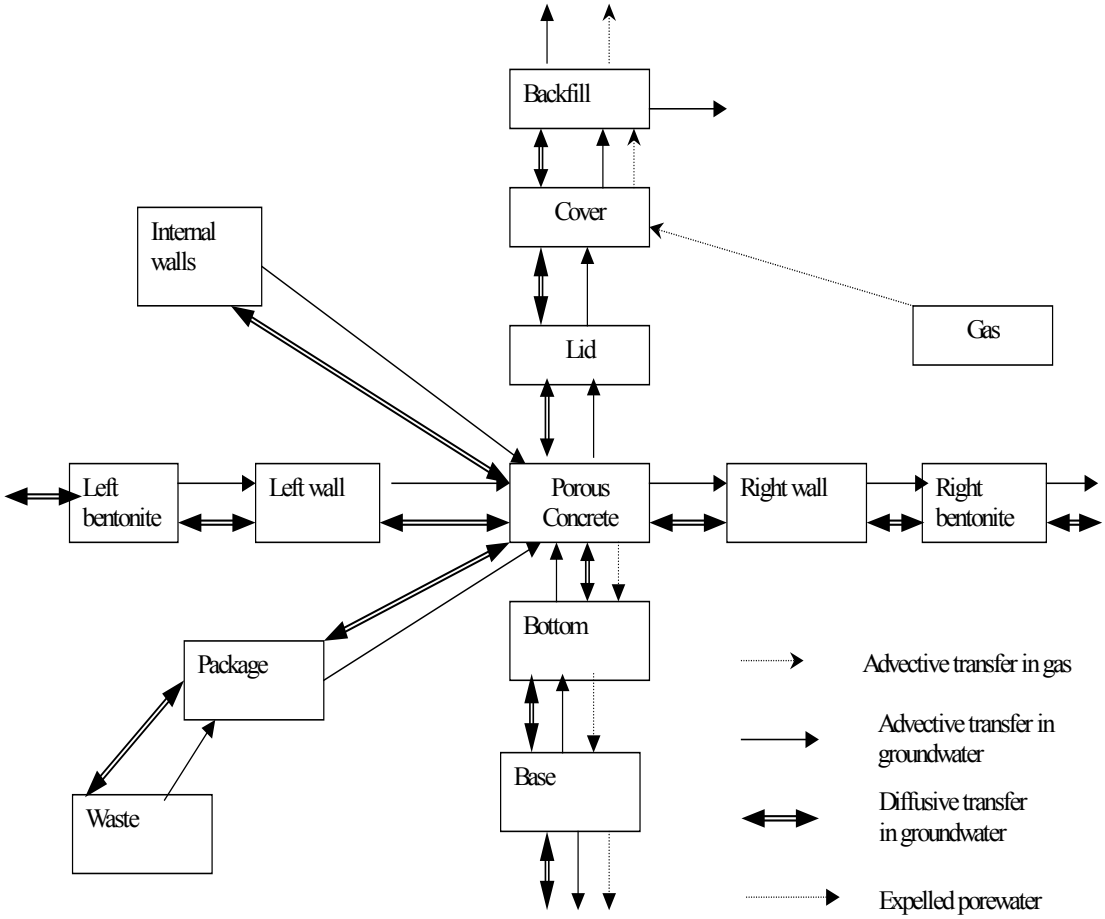

Figure 2.8 *The Silo Engineering Sub-Model*

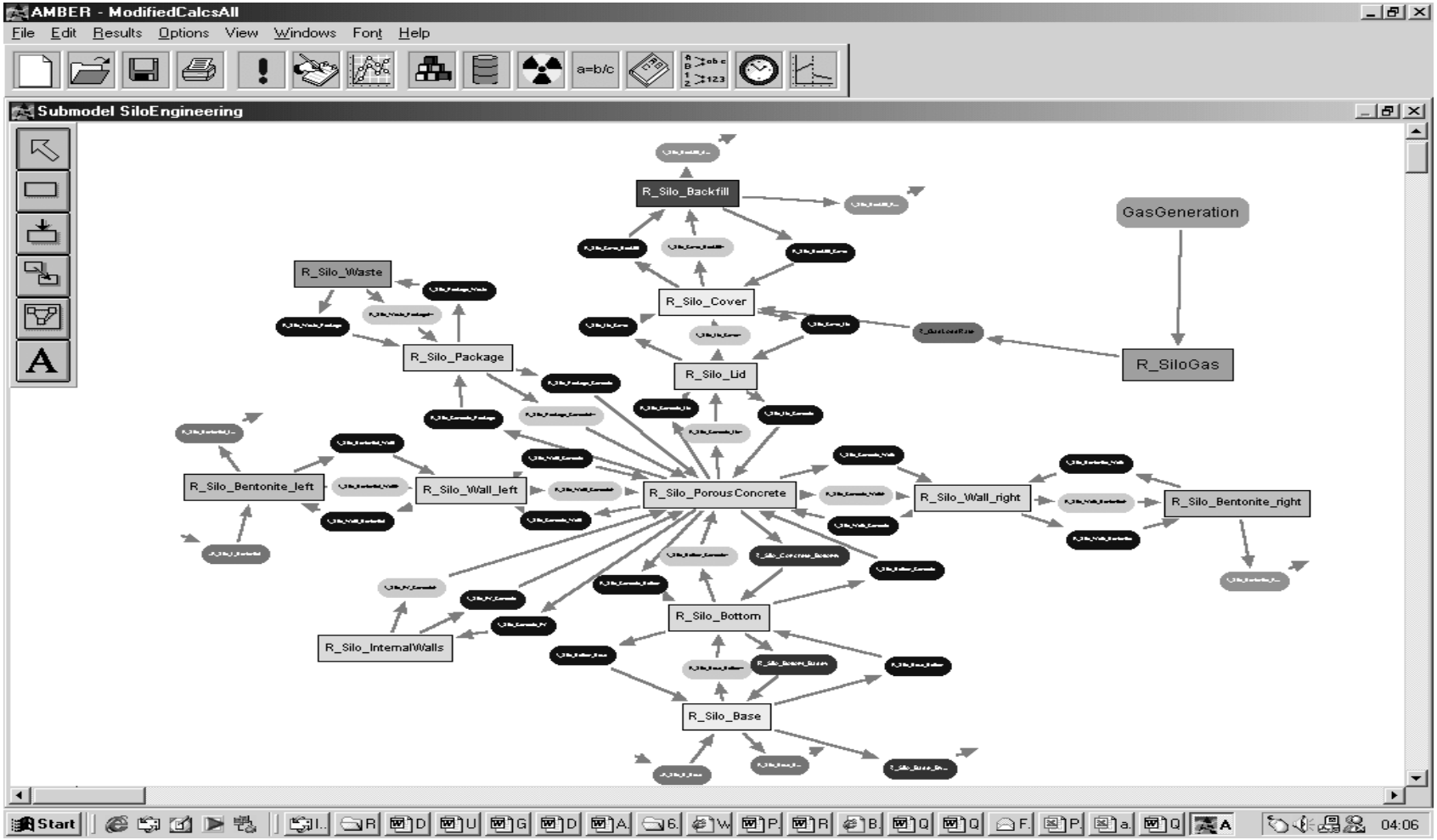

Figure 2.9 *AMBER Screenshot for the Silo Engineering Sub-Model*

Resaturation and Gas Evolution

When the repository is closed it will initially be unsaturated, and resaturation will begin to take place. In addition gas may be produced, primarily from the corrosion of metals in the repository. The Silo may have gas vents included in the lid, but there is the possibility that these vents could become blocked. The processes of resaturation and gas evolution could be most important for the Silo because the use of bentonite could slow down the rate of resaturation and limit the rate at which gas can escape. For this reason these processes have been included in the AMBER model for the Silo.

Details of the modelling that has been undertaken are given in Appendix A and a discussion of the importance of processes associated with gas production and transport are included in the Scoping calculations summarised in Section 3.

It is assumed that when SFR 1 is closed there will initially be a residual volume of air in the Silo at close to atmospheric pressure, and that water will flow into the system until the pressure equilibrates. Figure 2.10 gives a simplified representation of the system being modelled.

It is assumed that there will be a gas layer at the top of the Silo and that there will be an initial resaturation period during which water enters the Silo at an assumed rate (in reality this not be constant but will depend upon the pressure differences between the Silo and the outside). As the Silo resaturates the gas pressure increases and one can envisage four possible states of the system:

1. Initial resaturation is taking place and there is no gas flow through the lid (the overpressure is less than that required to initiate flow or barrier failure).
2. Initial resaturation is taking place at the same time that gas flow has been initiated.
3. Initial resaturation has been completed but there is no gas flow.
4. Initial resaturation has been completed and there is gas flow through the lid. When gas flow starts this may result in a further flow of groundwater into the system.

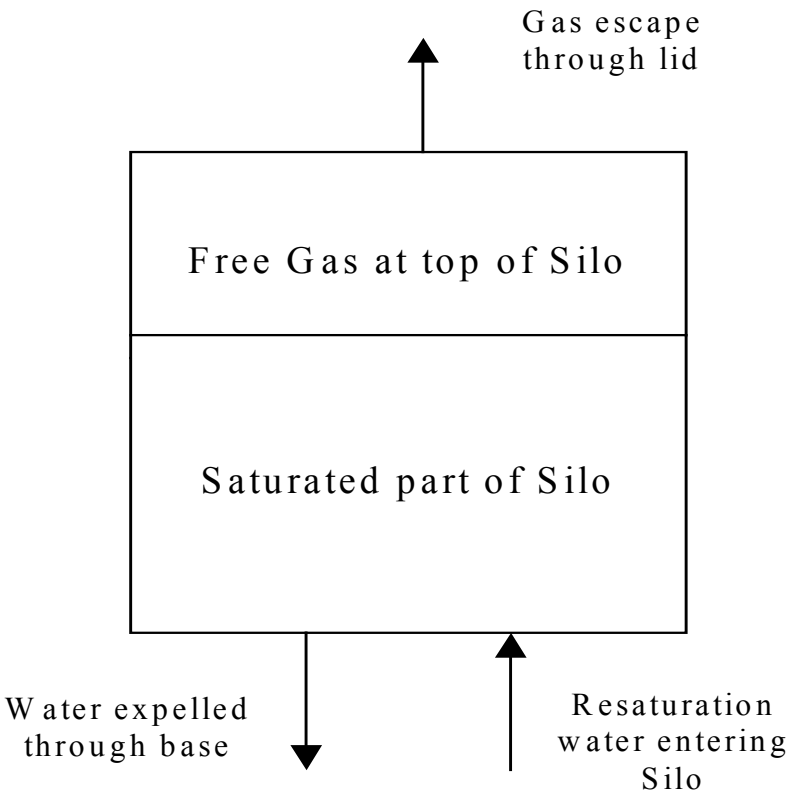

Figure 2.10 *A Simplified Representation of the Evolution of the Silo System*

The possibility that the engineered barriers could be damaged by gas over-pressurisation, leading to some groundwater flow through the barriers is represented in the model.

Physical and Chemical Degradation of Engineered Barriers

It is assumed that at any time Darcy flow through a vault is a fraction *f* of that in the surrounding geosphere. It is also assumed that as the engineered barriers degrade physically, *f* will increase. The barriers are assumed to degrade at the same rates; no distinction is made between the concrete and bentonite barriers, although alternative assumptions could be made if required.

As the concrete in the Silo ages its chemical properties change. Savage and Stenhouse (2001) refer to three stages of chemical evolution and these have been used in defining model parameters for the AMBER Case File. Further details are given in Appendix A.

This is an example of how AMBER allows time-dependent modelling of the system to be undertaken.

Radionuclide Transport in Groundwater

The Waste, Package, Porous Concrete and Internal Walls are represented using single compartments with volumes and surface areas representative of the whole 'Silo Contents', with radionuclides being uniformly distributed within them. The conceptual model for radionuclide transport is determined by following the path of the radionuclides out from the Waste. The key modelling issues are to represent radionuclide migration from the Waste into the Porous Concrete and, once in the Porous Concrete, to represent radionuclide migration out of the Silo.

Figure 2.8 shows both advective and diffusive transfers. Transfers between the Waste and the Package occur over the short distances relevant to individual waste packages. The area over which diffusive transfers take place is the total surface area for all the waste, derived by multiplying the area for a single package by the number of packages. Diffusive transport of radionuclides within and out of the Silo may be important before groundwater starts to flow once barriers start to degrade physically. The model also allows for the possibility that radionuclide transfers from the Waste could be solubility limited.

Similar arguments apply to transfers from the Package to the Porous Concrete, with the area for diffusion being the total surface area of all the packages, with the advection distance being the diameter of a single package.

Advection to the Internal Walls is neglected, but diffusion from the Porous Concrete to the Internal Walls occurs over the area of the walls (both sides), and the diffusion distance is the average thickness of the Internal Walls and the Porous Concrete. The advective transfer from the Internal Walls to the Porous Concrete uses the wall thickness as the length scale.

Contaminants can migrate from the Porous Concrete through the following routes:

- through the top of the Silo via the Lid, the sand/bentonite Cover and the Backfill;
- through the bottom of the Silo via the Silo Bottom and the sand/bentonite; and
- through the mantle (the side walls) through the concrete walls and the bentonite buffer.

Radionuclide Transfers due to Gas Generation

Figure 2.8 includes additional radionuclide transfers due to gas generation. Radionuclides can be transported in the gas itself, or in porewater expelled from the Silo due to the build-up of gas pressure in the Silo.

Groundwater Flows in Near-Field Rock

Groundwater flows in the near-field rock around the repositories are derived from the vertical and horizontal components of the Darcy flow in the geosphere. A simple approach was taken based on the following assumptions:

- For horizontal flows when the Silo is less conductive than the surrounding rock, it was assumed that additional flows through the backfill compensate for the flow deficit through the Silo bentonite.
- For horizontal flows when the Silo was more conductive than the surrounding rock, it is assumed that extra water is drawn into the system 'upstream' to allow for the additional flow through the Silo bentonite and backfill.
- For vertical flows when the Silo is less conductive than the surrounding rock, it was assumed that additional flows through the near-field rock to either side of the Silo would compensate for the flow deficit through the Silo itself. No attempt was made to model the modifications to flows above the Silo.
- For vertical flows when the Silo is more conductive than the surrounding rock, it was assumed that extra water would be drawn into the system 'upstream' to allow for the additional flow through the Silo.

2.4 1BTF and 2BTF

The AMBER sub-model for the engineered parts of the 1BTF repository is shown in Figure 2.11, based on a simple representation of the engineered structures shown in Figure 2.12; that for 2BTF is identical. As with the Silo, additional near-field rock compartments are included, and the modelling of groundwater flows in these is similar; all radionuclide transfers out of the BTF Engineering sub-model are to the BTF near-field rock compartments. In the calculations presented in Section 4, it is assumed that the BTF backfill material would be sand (or similar). In the BTF (and other) vaults, the effects of gas generation have not been modelled, and no detailed consideration is given to the post-closure resaturation period; it is implicitly assumed that resaturation is rapid.

The waste and packages are represented using a single compartment with volume and surface area representative of the whole repository.

Once radioactivity has migrated out of the waste Package it can leave the BTF repository through the following routes:

- through the top of the BTF via the Lid and the Backfill;
- through the bottom of the BTF via the BTF Base; and
- through the side walls.

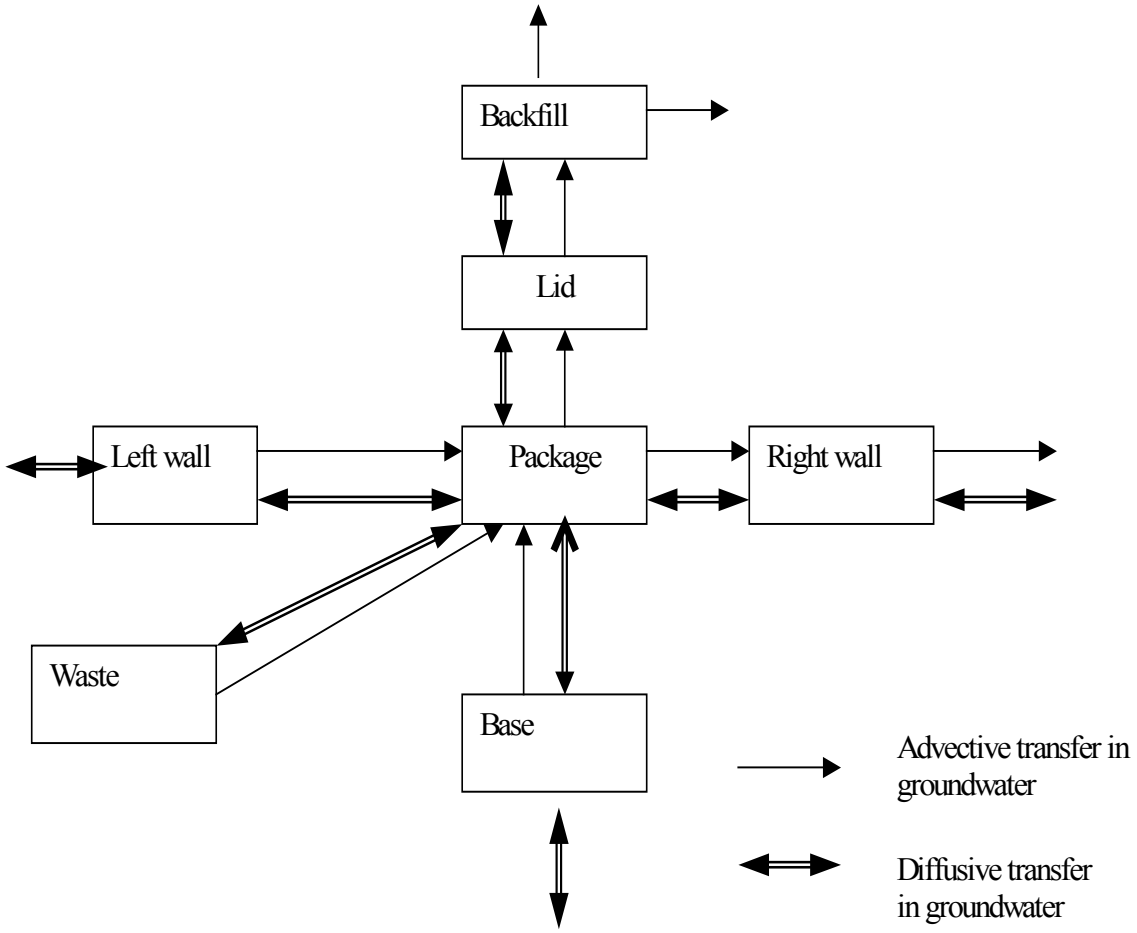

Figure 2.11 *The BTF Engineering Sub-Model*

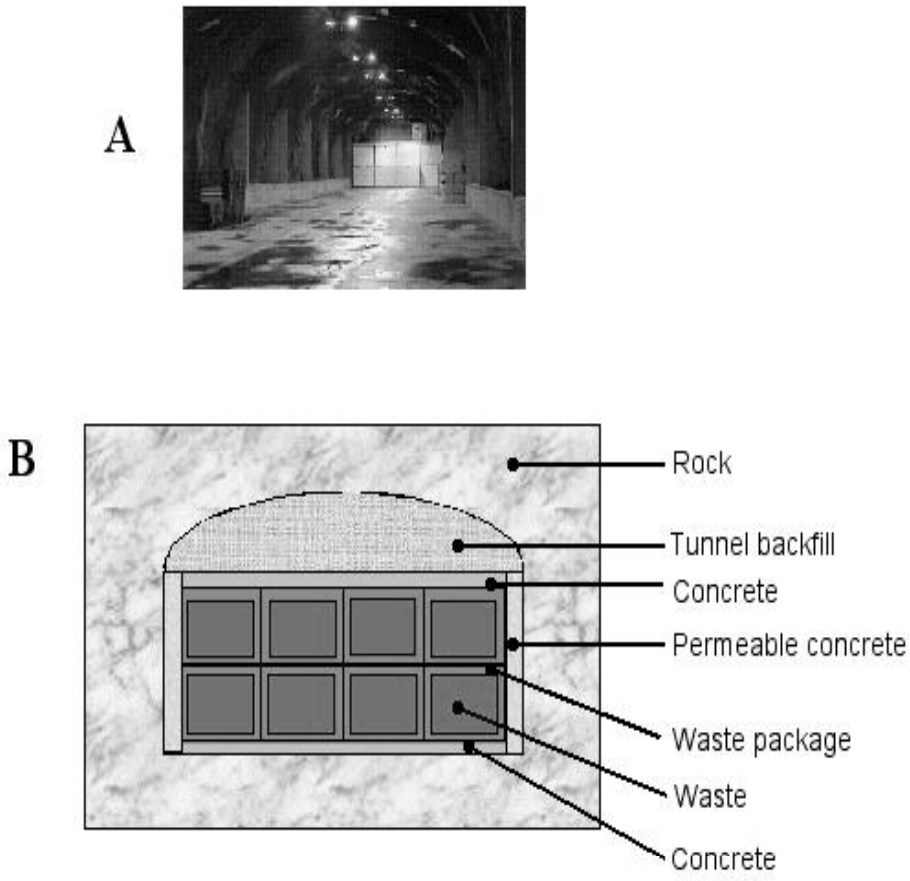

Figure 2.12 *The Layout of the BTF*

A*: photograph, Swedish Nuclear Fuel and Waste Management Co.;*

B*: disposal system*

2.5 The BMA

The AMBER sub-model for the engineered parts of the BMA is shown in Figure 2.13, based on a simple representation of the engineered features in Figure 2.14. As with the Silo, additional near-field rock compartments are included; all radionuclide transfers out of the BMA Engineering sub-model are to the BMA near-field rock compartments. In the calculations described in Section 4, it was assumed that no backfill would be used, so that the space above the lid would be occupied by groundwater. The overall modelling approach is similar to that employed for the BTF vaults.

The waste Packages are represented using a single compartment with volume and surface area representative of the whole repository. Once radioactivity has migrated out of the waste Package it can leave the BMA repository through the following routes:

- through the top of the BMA via the Lid the and the Backfill;
- through the bottom of the BMA via the BMA Base; and
- through the side walls and the surrounding sand.

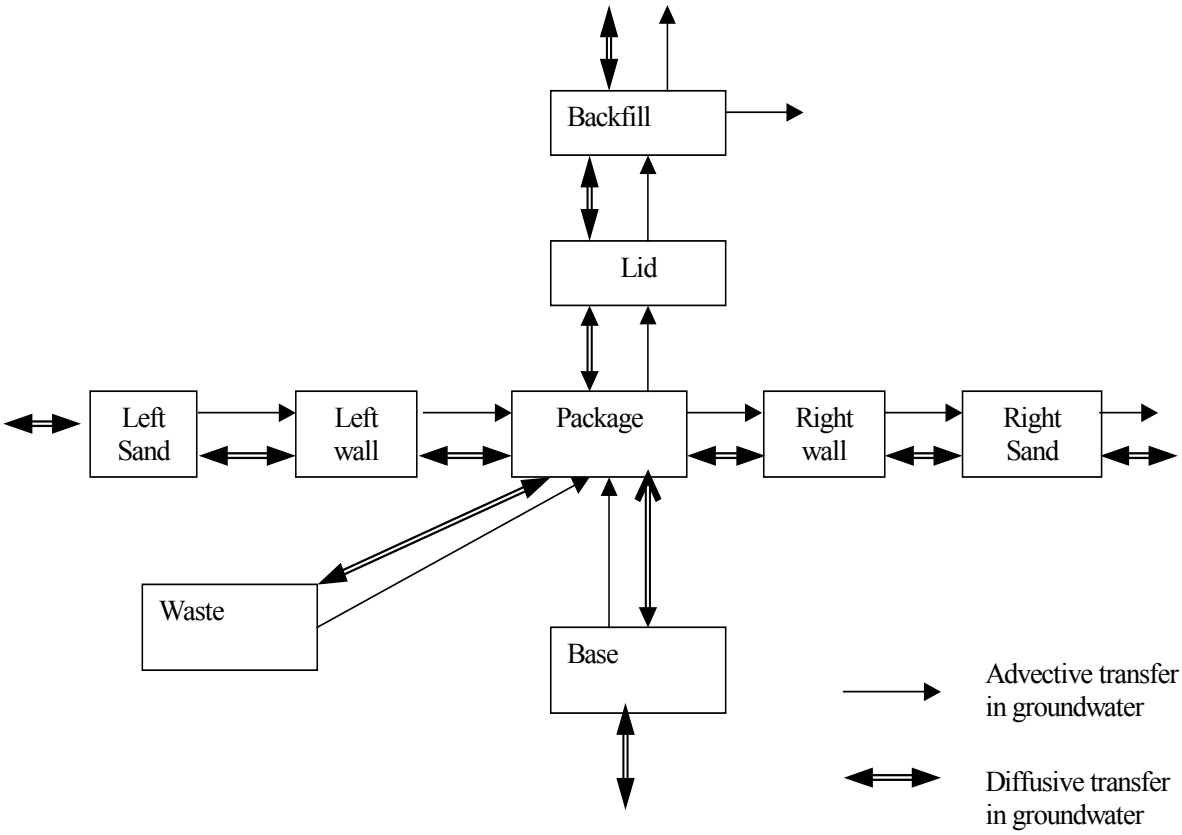

Figure 2.13 *The BMA Engineering Sub-Model*

A

B

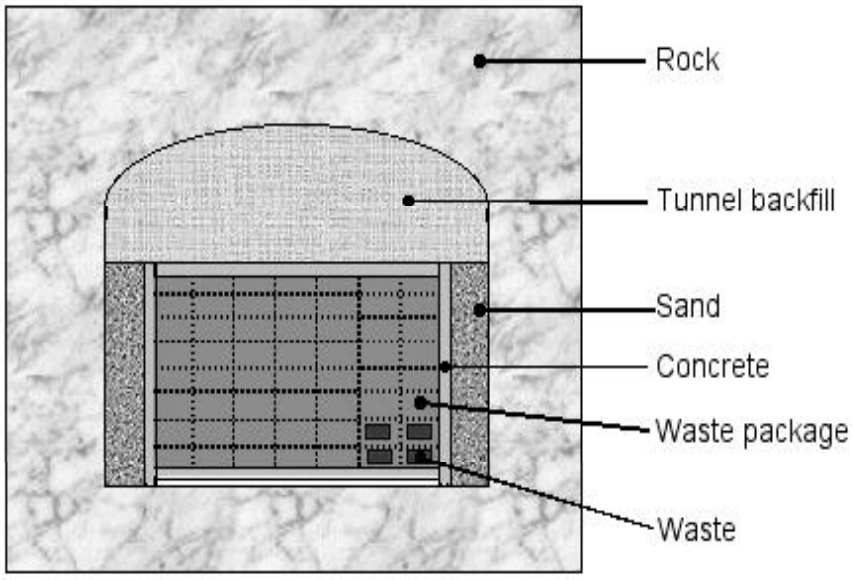

Figure 2.14 *The Layout of the BMA*

A*: photograph, Swedish Nuclear Fuel and Waste Management Co.;*

B*: disposal system*

2.6 The BLA

The AMBER sub-model for the engineered parts of the BLA is shown in Figure 2.15 based on a simple representation of the engineered features in Figure 2.16. This model is much simpler than that for the other repositories as there are essentially no engineered barriers. All radionuclide transfers out of the sub-model are to the BLA near-field rock compartments. In the calculations described in Section 4 it was assumed that no backfill would be used, so that the space above the waste would be filled with groundwater. Near-field rock compartments are included as for the other repositories.

The Waste is represented using single a compartment with volume and surface area representative of the whole repository. Once radioactivity has migrated out of the Waste it can leave the BLA repository through the following routes:

- through the top of the BLA directly into the Backfill; and
- through the side walls.

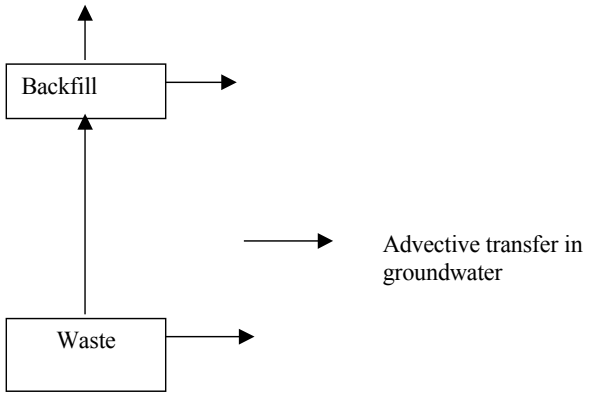

Figure 2.15 *The BLA Engineering Sub-Model*

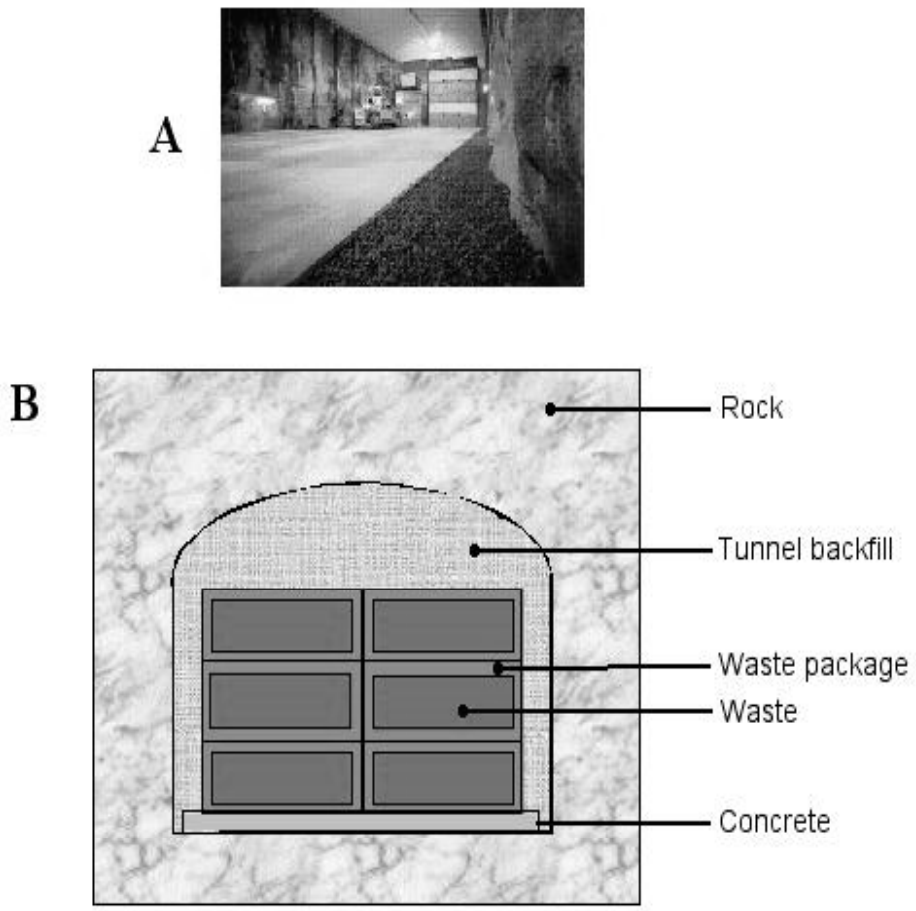

Figure 2.16 *The Layout of the BLA*

A*: photograph, Swedish Nuclear Fuel and Waste Management Co.;*

B*: disposal system*

2.7 The Geosphere

The structure of the Geosphere sub-system is shown in Figure 2.17, derived from the simple schematic representation of the system in Figures 2.4 and 2.5. There are eight compartments representing a region of fractured rock, each with associated rock matrix compartments.

The compartments Rock13 and Rock14 are directly above the Repository sub-model. Groundwater transport through the crystalline rock is assumed to be rapid, so that only advective transfers between rock fractures (i.e. the 'Rock' compartments in Figure 2.17) are considered. Radionuclide transfers between the rock fractures and rock matrix (i.e. between the 'Rock' and 'Matrix' compartments in Figure 2.17) are diffusive. Radionuclide sorption in the rock matrix is modelled, but sorption on fracture walls is neglected.

The degree of discretisation chosen for the geosphere was based on a desire to keep the representation consistent with the level of detail required for the calculations, enabling the importance of the variation of the magnitude and direction of the Darcy velocity with time to be investigated.

Groundwater Flow

The magnitude and direction of the Darcy velocity in the geosphere are assumed to vary linearly from an initial value (taken to be vertical) to a final value (taken to be close to horizontal) on a specified timescale (determined by the time assumed for the transition to an 'inland' environment to be completed).

By assuming uniform mixing of radionuclides in the model compartments, the possibility for focussed flows through one or several highly conductive fractures cannot be represented directly. This is not considered to be a major limitation because the areas of the surface compartments in the Terrestrial Biosphere are relatively small, and radiation exposures are unlikely to be significantly underestimated even if there are such focussed flows.

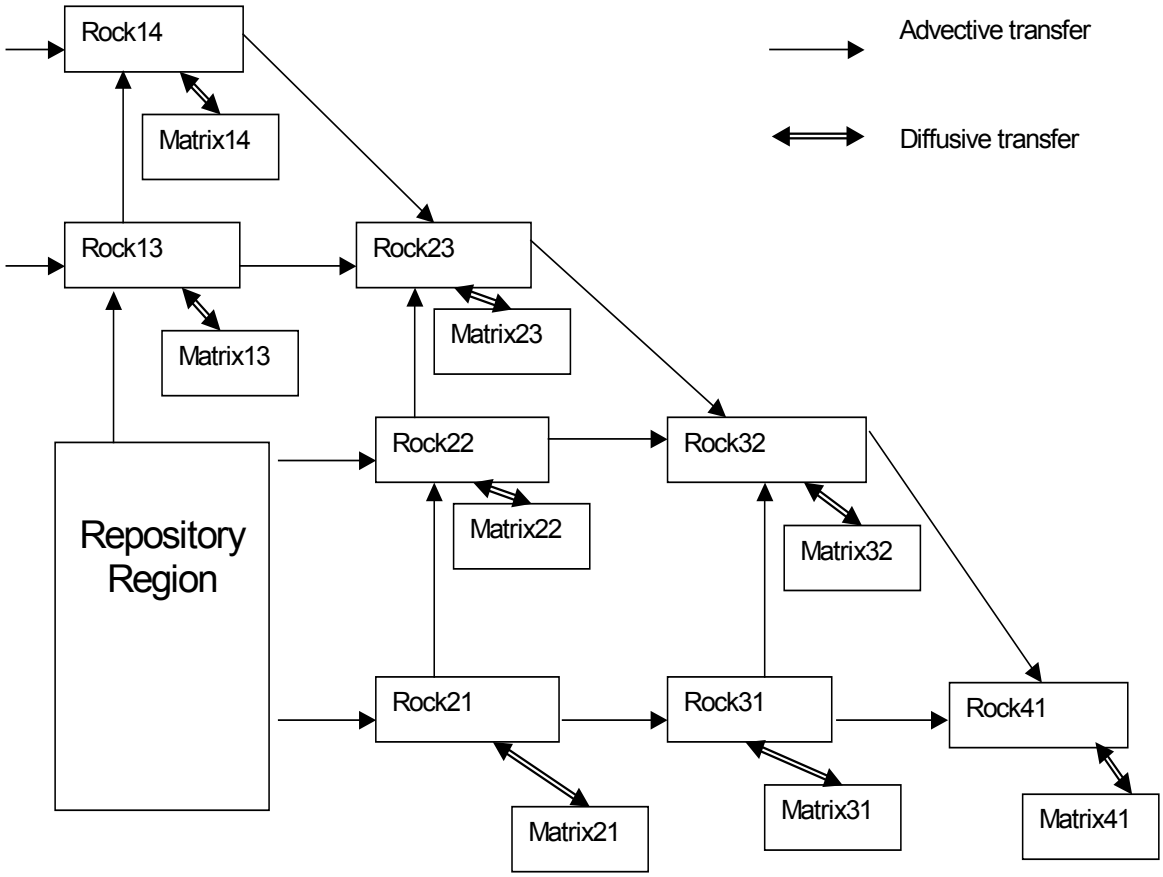

Figure 2.17 *The Geosphere Sub-System*

Note: The Figure does not show transfers into the Terrestrial and Marine Biosphere systems

2.8 The Terrestial Biosphere

The structure of the Terrestrial Biosphere sub-system is shown in Figure 2.18.

Four areas of land are considered in the modelling plane. The choice of the parts of the system that are included in the Terrestrial Biosphere sub-model is, to a large extent, arbitrary. Initially the whole of the system being modelled is under the sea, but subsequently individual areas become exposed as the land rises and relative sea level falls. The pragmatic choice has been made to include in the Terrestrial Biosphere sub-system the top-most parts of the land surface which may become partially saturated when the sea retreats; rock which is saturated at all times is included in the Geosphere sub-system, but rock which may become unsaturated at some time is included in the Terrestrial Biosphere sub-system.

The different types of compartments are:

- The Upper Sediments compartments which represent the top layer of sediments when the area concerned is under the sea; these are treated as Upper Soil compartments when the sea has retreated. Soil can be used to grow crops and be grazed. The choice of the depth of the upper sediments is based on typical rooting depths and ploughing depths in soil.
- The Lower Sediments compartments which represent the lower layer of sediments when the area concerned is under the sea; these are treated as Lower Soil compartments when the sea has retreated.
- The Top Rock compartments which represent the top-most layer of saturated rock when the area concerned is under the sea; these may become partially saturated when the sea has retreated.
- The Lake compartment.

The specification of the groundwater flows in this part of the system (see Appendix A) maintains an approximate water balance as the system evolves.

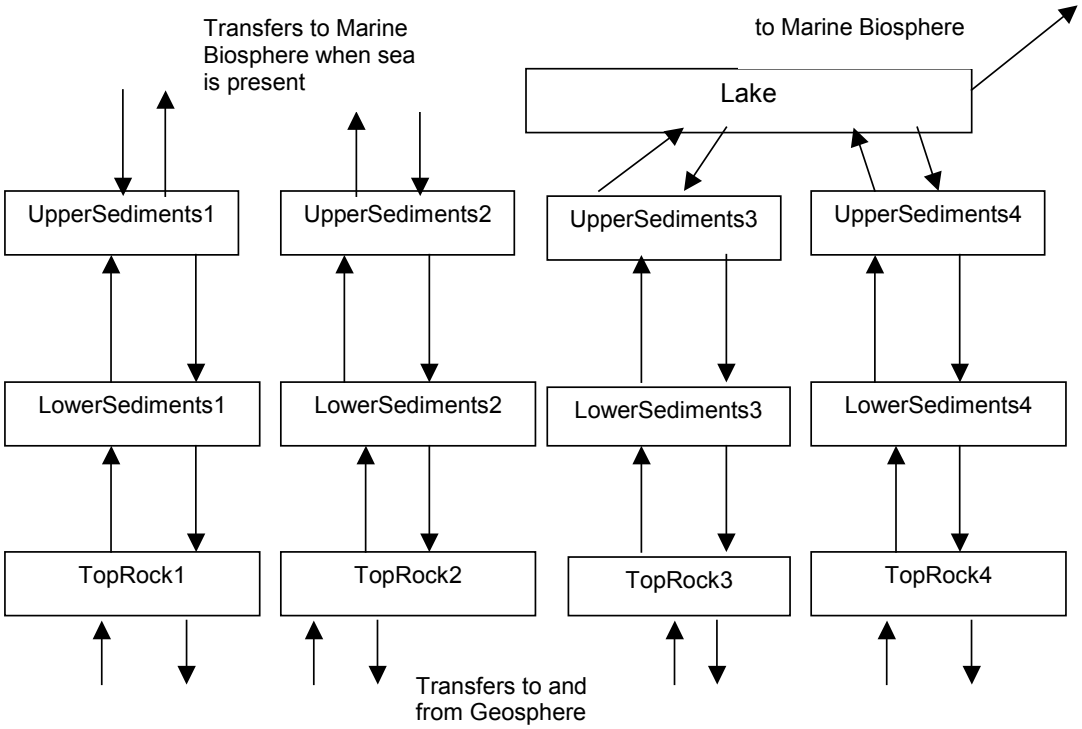

Figure 2.18 *The Terrestrial Biosphere Sub-System*

Transition Times

The transition times between the different states of the system are taken to be related to the rate of land uplift U (m y^{-1}). The time when the first two areas in the Terrestrial Biosphere sub-system become dry land area given by $t_i = \frac{d_i}{U}$, where d_i is the initial depth of the sea above area i (m). It is assumed that the Lake is formed when the sea recedes from the second area of land.

Once an area has become dry land, it is assumed that in Areas 1 and 2, the water table falls at a rate determined by the rate of land uplift until it reaches the bottom of the Top Rock compartment. The treatment of each compartment changes from being saturated to being partially saturated when the water table drops below the base of the compartment in question.

2.9 The Marine Biosphere

The structure of the Marine Biosphere sub-model is shown in Figure 2.19.

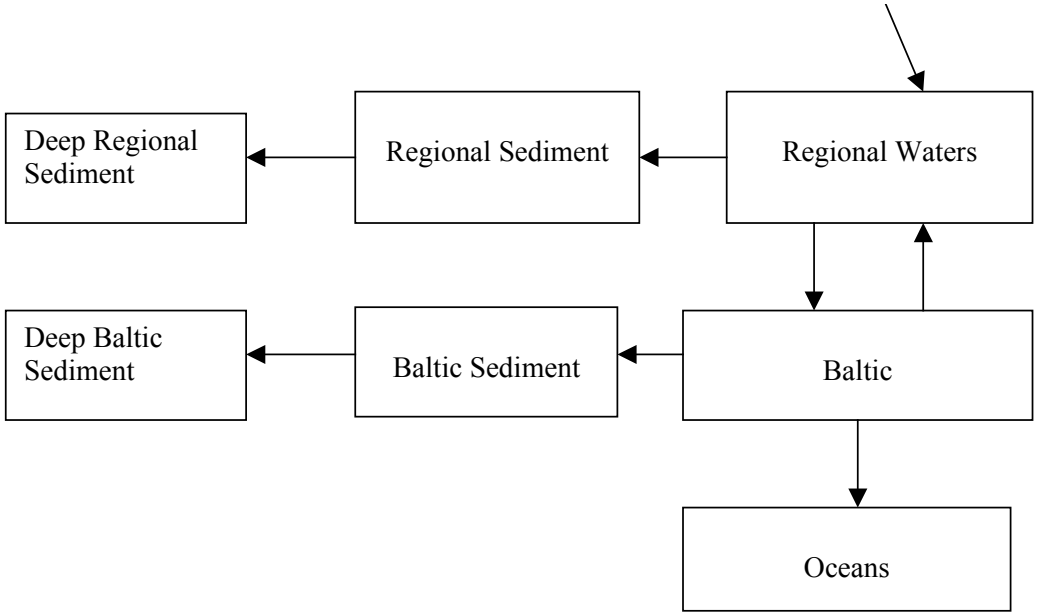

Figure 2.19 *The Marine Biosphere Sub-System*

Note: The Figure does not show transfers from the Terrestrial Biosphere system

There are model compartments for an area of Regional Waters and the Baltic, each with associated compartments for bottom sediments. The compartment for other Oceans is effectively a sink compartment i.e. contaminants entering other oceans are assumed to have left the system of interest and are no longer considered. The simplicity of the Marine Biosphere sub-system reflects the fact that the most significant radiological impacts are likely to arise directly from radionuclide concentrations in environmental materials in the Terrestrial Biosphere sub-system rather than the Marine Biosphere sub-system.

2.10 Radiological Impact Calculations

Individual doses are derived from the AMBER calculations of radionuclide concentrations in environmental materials; details are given in Appendix A. The intention is not to undertake a detailed assessment of potential doses, but to use representative pathways to enable comparisons to be made between the impacts for different modelling assumptions. Consistent with this aim, the representative pathways considered are external exposure over contaminated soils or sediments, inhalation of contaminated soil or sediment, the consumption of drinking water from a well, and the

consumption of lake and sea fish. Other pathways (for example the consumption of crops and animal products) could readily be added if required.

The model is not currently designed to provide information on either collective doses or radiological impacts to non-human biota.

2.11 Radionuclide Inventory

In the Final calculations described in Section 4, the radionuclide inventory given in SKB (2001) was used. Preliminary calculations used the inventory given in SKB (1987b). These inventories are reproduced in Appendices A and B respectively.

3 Preliminary PA Calculations

Before the Final PA calculations were undertaken to investigate the important issues for the Safety of SFR 1 (Section 4), three sets of preliminary calculations were undertaken as follows:

- The first Demonstration calculations were undertaken in 1999. These calculations demonstrated the capability of the AMBER software to reproduce the key features of the PA modelling undertaken by SKB at the time of the original licensing of SFR 1, and are described in Appendix B.
- A set of Prototype calculations was also undertaken in 1999. These calculations gave confidence in the capability of the AMBER software to meet SKI's requirements for a PA code and highlighted some important modelling issues for SFR 1. These calculations are described in Appendix C.
- Scoping calculations were undertaken in 2000; these included consideration of the effects of gas generation and the evolution of the Silo near-field. These are described in Appendix D.

3.1 Demonstration Calculations

The modelling undertaken at the time of the original safety case submission for SFR 1 considered two periods: the Saltwater Period, when fluxes of radionuclides to the biosphere entered the local marine environment, and the Inland Period, when radionuclides entered a lake or a well. The change occurred due to land rise resulting in changes in the surface environment. Two separate sets of calculations were undertaken for the two different periods; no attempt was made to model the transition between the two cases. One of the main aims of applying AMBER to the SFR 1 system was to represent the transition from the Saltwater to Inland environments better, considering the various time dependent processes in more detail. Nevertheless, producing AMBER models for these two environments and comparing the results with SKB calculations was extremely valuable, giving confidence in the use of AMBER for SFR 1.

3.2 Prototype Calculations

The main aim of these calculations was to set up PA models for SFR 1 that did not rely on previous work undertaken by SKB in order to investigate whether AMBER could be used effectively as a system-level code with a full representation of the time-

dependency of all the important processes. The AMBER models that were developed were similar in most respects to those used in the Final calculations (as described in Section 2 and Appendix A).

Demonstrating that a system as complex as SFR 1 with full time dependency could be represented in AMBER was a major step forward. Some of the time dependent processes that were modelled include:

- Groundwater flows through the vaults that vary with time according to both the position of the sea and the state of the engineered barriers;
- The chemical properties of the near-field environment;
- The location of the discharge to the biosphere changes as the biosphere evolves, in particular due to land rise and the resulting retreat of the sea; and
- The properties of the biosphere change with time; land that was under the sea can subsequently be farmed and new lakes can be formed.

3.3 Scoping Calculations

Building on the experience gained in the Prototype calculations, a set of Scoping calculations was undertaken to investigate some particular issues for SFR1 of interest to SKI. The AMBER Case File produced considered only the Silo repository, but incorporated a number of refinements including the representation of gas generation and transport and radionuclide solubility limitations. In addition, the use of the data from a 'vault database' commissioned by SKI (Savage and Stenhouse, 2001) avoided the need to rely totally on SKB data. This work suggested representing the chemical evolution of the engineered barriers in three stages.

The main conclusions from these calculations were:

5. The reference set of Scoping calculations suggested that potential doses would be very small when the SFR 1 is below the Baltic, but once the sea has retreated dose rates of around 0.1 mSv y^{-1} are possible.
6. For the reference calculations one of the most significant pathways could be the consumption of contaminated drinking water, although it is not certain that this pathway would actually be present.
7. Doses were generally dominated by long-lived mobile radionuclides such as C-14, Tc-99 and I-129.
8. If overpressurisation of the Silo takes place this could lead to increased early releases of short-lived radionuclides into the environment, but this is unlikely

to lead to significantly increased radiological impacts as these releases take place when the SFR 1 is below the Baltic and radionuclides released into the sea are rapidly dispersed.

9. The (chemical) sorbing properties of engineered barriers appear to be at least as important as their (physical) ability to limit groundwater flows. Calculated peak dose rates are sensitive to the choice of radionuclide sorption coefficients.

These conclusions helped to identify priorities for the Final set of calculations described in the next Section.

4 The Final PA Calculations

The preliminary calculations summarised in Section 3 provided the foundation for undertaking a Final set of PA calculations for SFR 1. The revised SKB inventory used in the SAFE calculations was used in these calculations (see Appendix A), rather than the inventory used in the preliminary calculations (see Appendix B). The revised inventory has several additional potentially important radionuclides, and for some radionuclides the assumed inventories are larger than in the original inventory.

Section 4.1 describes calculations for a Reference Scenario and a reference set of parameter values. The models used have already been described in Section 2, and details of the parameter values employed are given in Appendix A. These calculations provide a reference point against which other variant calculations can be compared. Section 4.2 includes a description of a number of such variant cases, designed to investigate further the importance of groundwater flows through the repositories, barrier lifetimes and radionuclide sorption.

Additional calculations are presented in Section 4.3 to 4.5. Section 4.3 describes a Permafrost scenario designed to investigate whether permafrost could be important in the future evolution of the system. Section 4.4 describes a long term calculation designed to illustrate the potential consequences if most of the radioactivity in SFR 1 remained in situ for very long periods of time until surface erosion resulted in waste materials in the repository entering the accessible environment. In Section 4.5 some calculations are presented to investigate the sensitivity of the Reference Scenario calculations to the way that time dependent processes are represented.

Finally Section 4.6 summarises the conclusions that can be drawn from the calculations presented.

4.1 The Reference Scenario and Reference Case

This calculation case is designed to provide the basis against which variant assumptions and calculations can be compared. The data used for these calculations are given in Appendix A.

Figure 4.1 shows the calculated flux of radionuclides from the different vaults. The peak flux from the Silo, 5.5E8 Bq y^{-1}, occurs at around 1600 years after repository closure. The flux calculations from the Silo can be compared with those for the Scoping calculations. There the peak flux was 1.4E8 Bq y^{-1} at around 3400 years after

repository closure. The main reason for the differences is the revised radionuclide inventory, although changes in some model parameter values are also significant. The peak flux from the BLA occurs at very early times and cannot be seen in the Figure. Except for the BLA, peak fluxes into the terrestrial environment occur at around the time that can be expected to result in the highest doses, relatively soon after the Baltic has retreated.

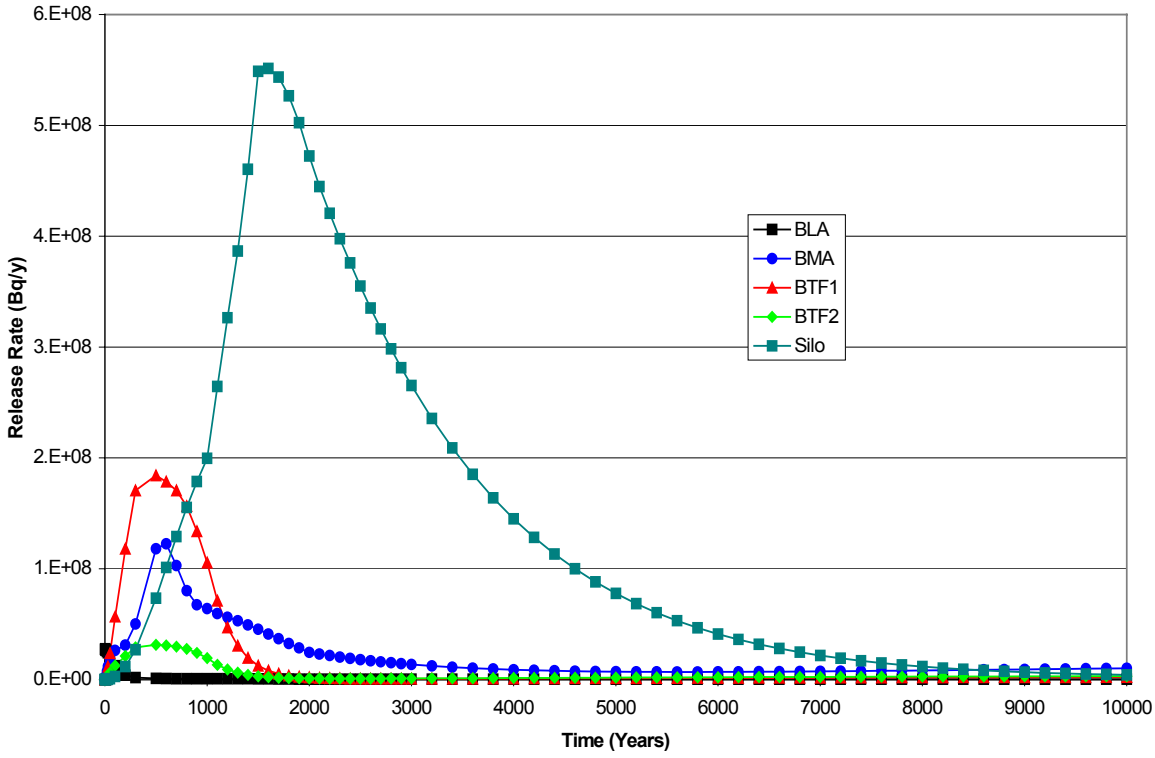

Figure 4.1 *Radionuclide Fluxes from the Vaults in the Reference Calculations*

Figure 4.2 shows some calculated environmental concentrations in soils/sediments. The concentrations relate to the solid phase. These show that the highest calculated concentration is only just over 100 Bq kg^{-1} in the fourth region of the Terrestrial Biosphere part of the system. These concentrations are comparable with typical background concentrations of radioactivity. Figure 4.3 shows the most important radionuclides involved. These are all long-lived beta/gamma radionuclides: Mo-93, Nb-93m, Ni-59, Cl-36, Se-79 and Cs-135. Because the concentrations are in the solid phase, radionuclides that are assumed not to be sorbed (such as organic C-14) are not shown in this Figure. It is interesting to note that concentrations for Ni-59 (and some other radionuclides) are still increasing after 10 000 years.

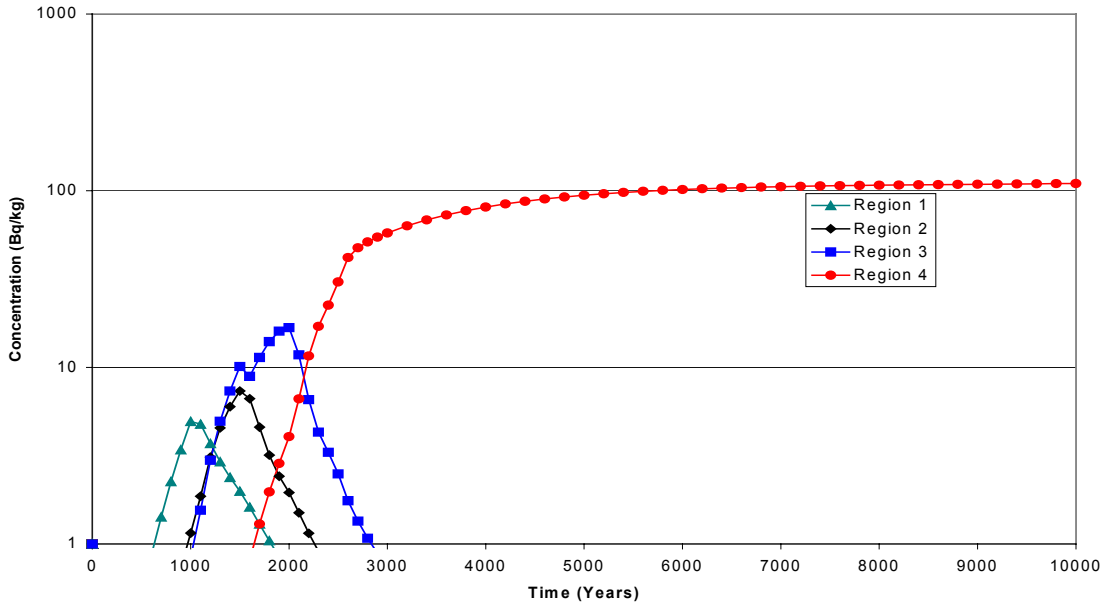

Figure 4.2 *Environmental Concentrations in Soils/Sediments for the Reference Calculations*

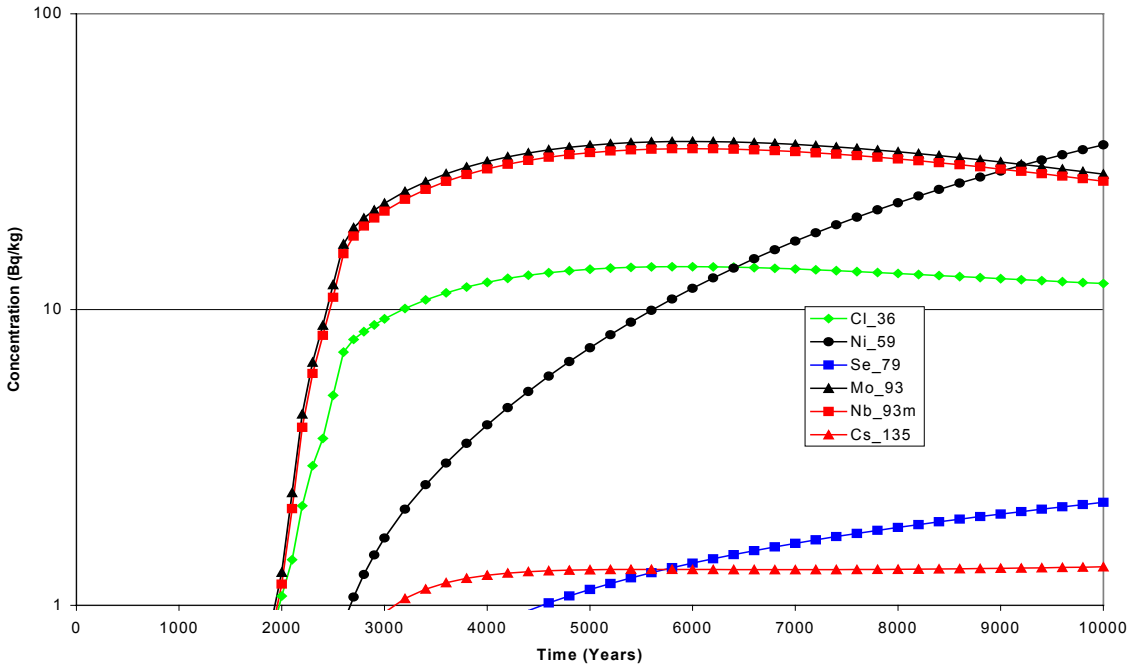

Figure 4.3 *Radionuclide Concentrations in Soil/Sediment in the Fourth Region of the Terrestrial Biosphere Sub-Model for the Reference Calculations*

Figure 4.4 gives illustrative dose calculations for the selected 'terrestrial' pathways. The doses appear to be dominated by organic carbon-14. As described in Appendix A, the calculations include a 'well dilution factor' to allow for the dilution of contaminated groundwater with uncontaminated groundwater. Previous calculations did not include this factor. The precise value of the dose calculated for the Lake Fish pathway will depend upon parameters such as the Lake volume and turnover time, both of which have default parameter values that are likely to be pessimistic.

The calculations confirm the conclusion drawn from the Scoping calculations that once the Baltic has retreated from above the repository (after 1000 years with the reference parameter values) dose rates of the order of 0.1 mSv y^{-1} are possible.

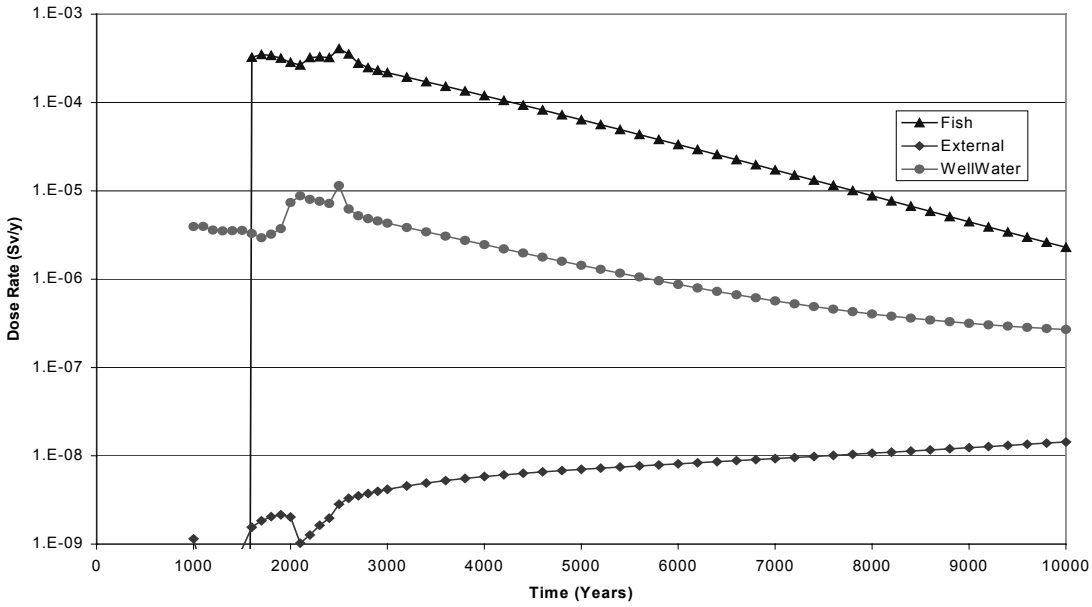

Figure 4.4 *Illustrative Dose Calculations for Terrestrial Pathways for the Reference Calculations*

Figure 4.5 gives illustrative calculations for the selected 'Marine' pathways. On the scale employed, only the dose for the sea fish consumption pathway can be seen. The doses are much lower than those calculated for the Terrestrial pathways. The sea fish consumption pathway is dominated by organic C-14 from the Silo.

With the reference parameter values chosen, retention in the geosphere by matrix diffusion is not an important process. The calculated dose rates shown in Figures 4.4 and 4.5 are little affected if matrix diffusion is 'switched off' by choosing a very low

value of the flow wetted surface area. Matrix diffusion can be more important, however, for long-lived actinides on much longer timescales.

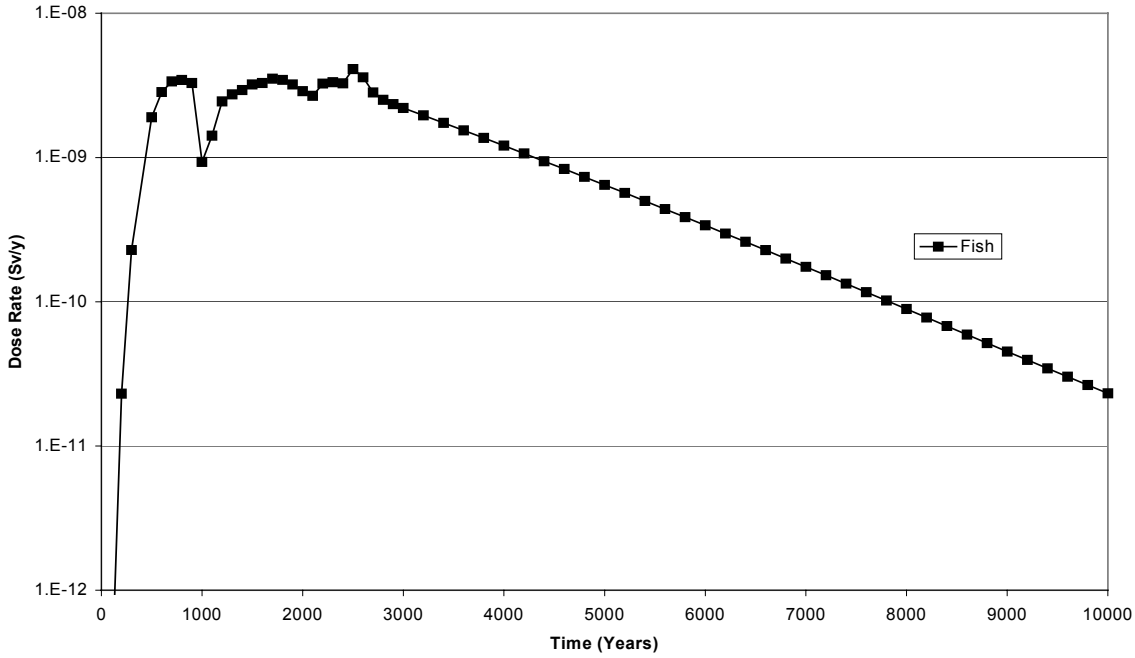

Figure 4.5 *Illustrative Dose Calculations for Marine Pathways for the Reference Calculations*

4.2 The Reference Scenario Variants

Based on the experienced gained in the Scoping calculations (Section 3) a number of variant calculations were undertaken to investigate three issues that appeared to be potentially important for the overall safety of SFR 1. These were: the groundwater flow rates through the vaults; the timescales for the physical and chemical degradation of the engineered barriers, and the sorption of radionuclides in the near-field. In each case sensitivity analyses were undertaken. These sensitivity analyses involved investigating how chosen measures of system performance varied with the choice of model parameters.

4.2.1 Repository Flows Sensitivity Calculations

In order to investigate the importance of the assumptions about groundwater flows through the repositories, a set of variant calculations were undertaken with a few key parameters being varied. The parameters that were varied were:

- The time when the physical degradation of the Silo is assumed to commence. This was varied between 100 and 5000 years after repository closure.
- The regional Darcy velocity. The final regional Darcy velocity varied from 0.0005 to 0.05 m y^{-1}. The well dilution factor was taken to vary inversely with the magnitude of the Darcy velocity.
- The final flow rate through the vaults when barriers have physically degraded compared with the surrounding rock. The final repository flow rates varied from a factor of 0.2 to a factor of 20 of the flow rates through the surrounding rock.

The peak dose rate from all the terrestrial pathways (whenever this occurs in the first ten thousand years) has been taken as an indicator of potential impacts. The variation of the start of the physical degradation of the Silo barriers did not greatly influence peak dose rates, but the variation of the second two parameters did. Figure 4.6 gives a scatter plot for the variation of the peak dose rate with the magnitude of the regional Darcy vector. As the Darcy velocity varies over two orders of magnitude, there is an increase in the peak dose rate of around one-and-a-half orders of magnitude. A very similar situation is shown in Figure 4.7 that gives the corresponding scatter plot for the final repository flow factor.

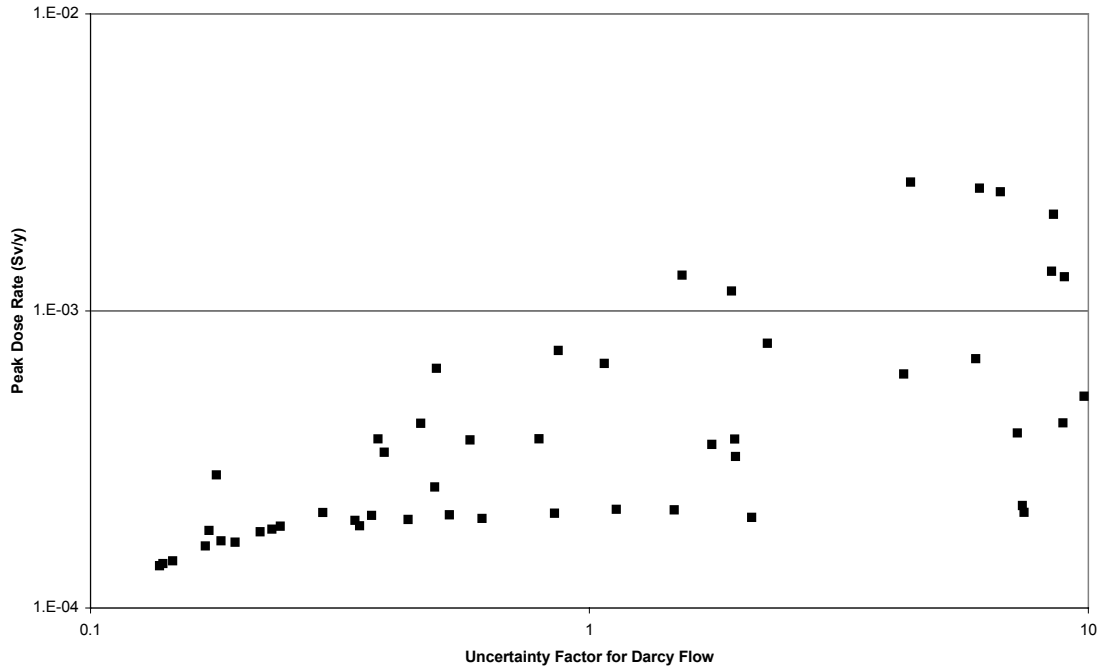

Figure 4.6 *Scatter Plot for Peak Dose Rate for Terrestrial Pathways against Uncertainty Factor for the Regional Darcy Flow*

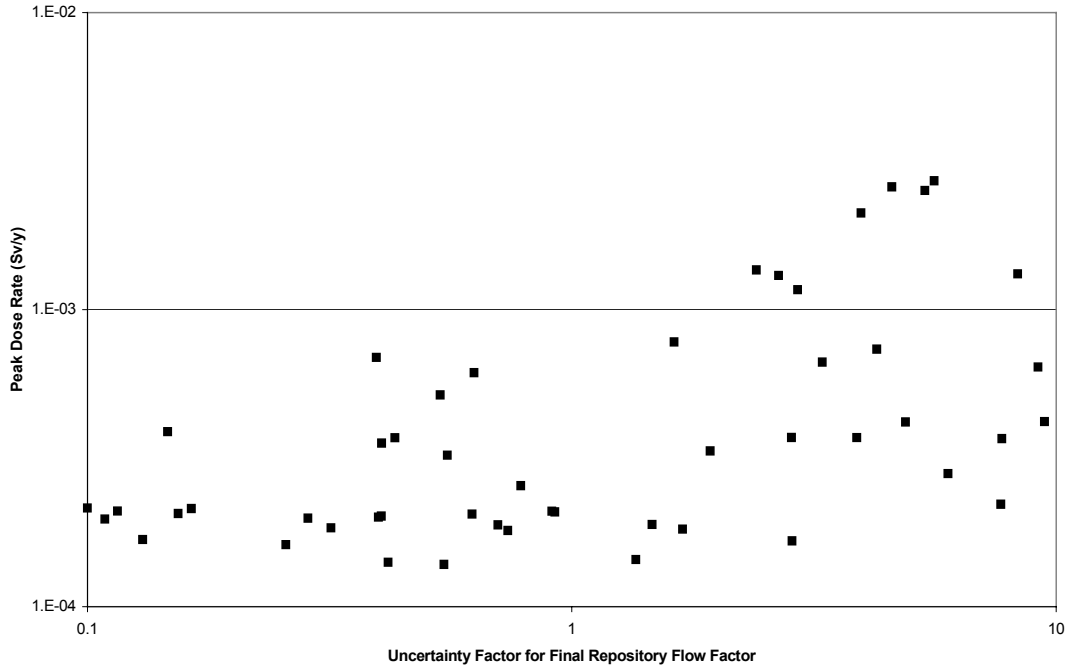

Figure 4.7 *Scatter Plot for Peak Dose Rate for Terrestrial Pathways against Uncertainty Factor for the Final Flow Factor for the Vaults*

The dependence of the peak dose rate on vault flows is most clearly demonstrated by considering the product of the uncertainties used in Figures 4.6 and 4.7, i.e. the net uncertainty factor for the final flow rate through the repositories. The relevant scatter plot is shown in Figure 4.8. As the overall uncertainty factor varies from 0.01 to 100, this corresponds to final Darcy flow rates through the vaults of 10^{-4} to 1 m y^{-1}. It is interesting to note that the two samples with the highest flow rates actually give lower peak dose rates. This would appear to be due to the very high flow rates resulting in a large fraction of the radionuclide inventories being transported into the Baltic before it has retreated from above the repository. This emphasises again the importance of the timing of the radionuclide fluxes into the environment.

It is clear that the assumptions made about groundwater flow rates through the vaults will be important in determining calculated radiological impacts.

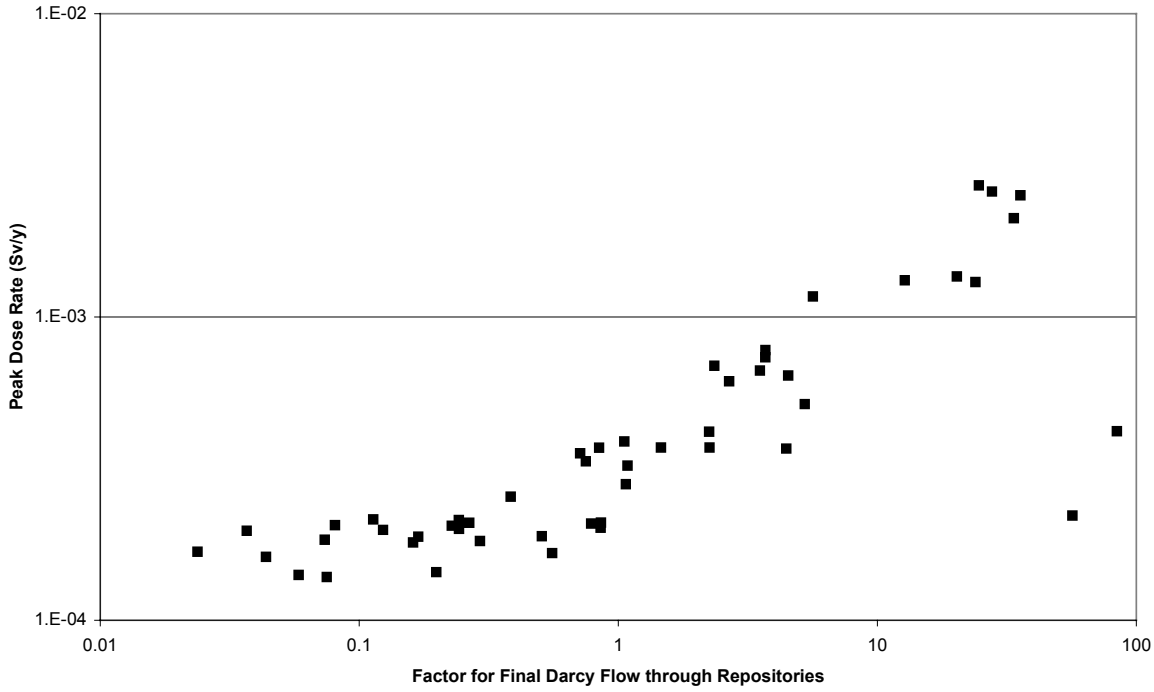

Figure 4.8 *Scatter Plot for Peak Dose Rate for Terrestrial Pathways against uncertainty factor for the Final Darcy Flow through the Vaults*

4.2.2 Barrier Degradation Sensitivity Calculations

In order to investigate the importance of the assumptions about engineered barrier degradation, a set of variant calculations was undertaken with a few key parameters being varied. The parameters that were varied were:

- The timescale for Silo engineered barriers to undergo complete physical degradation. This parameter was varied from 100 to 10 000 years.
- The timescale for the other vault engineered barriers (where present) to undergo complete physical degradation. This parameter was varied over the same range as the corresponding parameter for the Silo.
- The timing of the second and third stages of the chemical degradation of concrete barriers. The commencement of Stage 2 varying from 100 to 10 000 years after repository closure for all vaults, and the start of Stage 3 varying from 1000 to 100 000 years.

The sensitivity calculations showed the expected dependencies, but with much less variation than for the flow sensitivities. For example, Figure 4.9 shows how the peak Terrestrial dose rate varies with the Silo physical degradation timescale. No strong dependency is shown, with a total variation in peak dose rates of only a factor of around 5. This is consistent with the Scoping calculations, where it was noted that changing the timescales for barrier degradation altered the timing of peak fluxes and doses but did not greatly alter their magnitude.

Figure 4.10 gives the corresponding scatter plot for the uncertainty in chemical degradation timescales. In general, the shorter the chemical degradation timescale the higher the peak uncertainty in dose rate, although the overall variation is not very great. However, care should be exercised in drawing firm conclusions from these calculations, as the sorbing properties of several key radionuclides are assumed not to vary significantly as the concrete barriers degrade. With the default parameter values used for sorption coefficients, the chemical barrier produced by the large mass of cement, particularly in the BMA and Silo, remains very important for several long-lived alpha-emitting radionuclides.

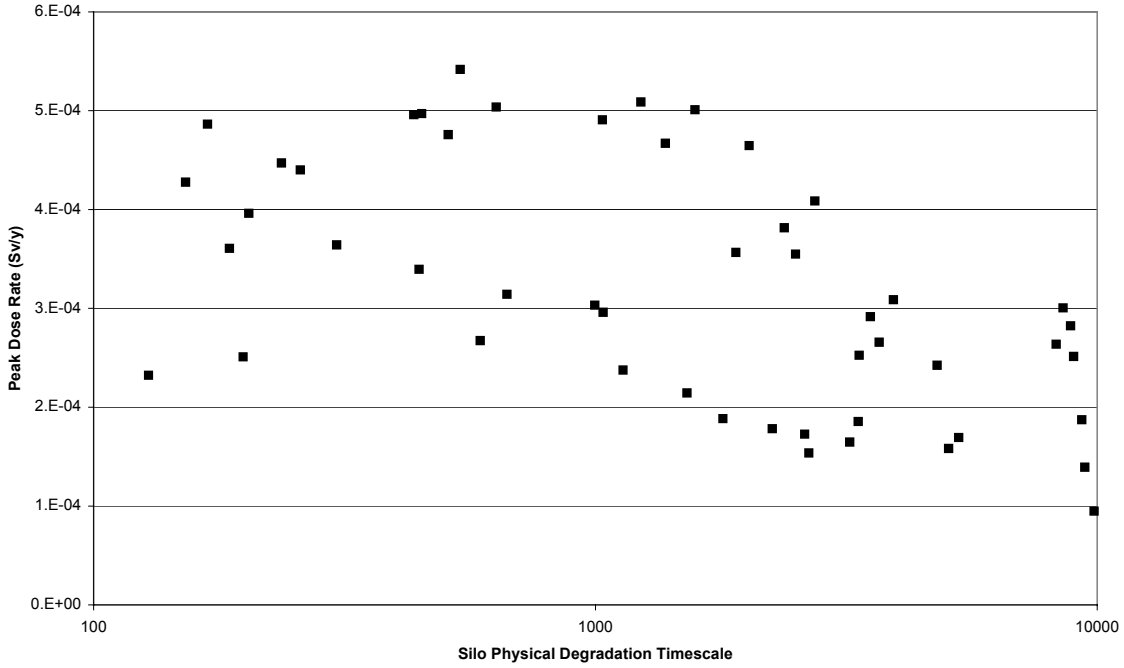

Figure 4.9 *Scatter Plot for Peak Dose Rate for Terrestrial Pathways against the Silo Physical Degradation Timescale*

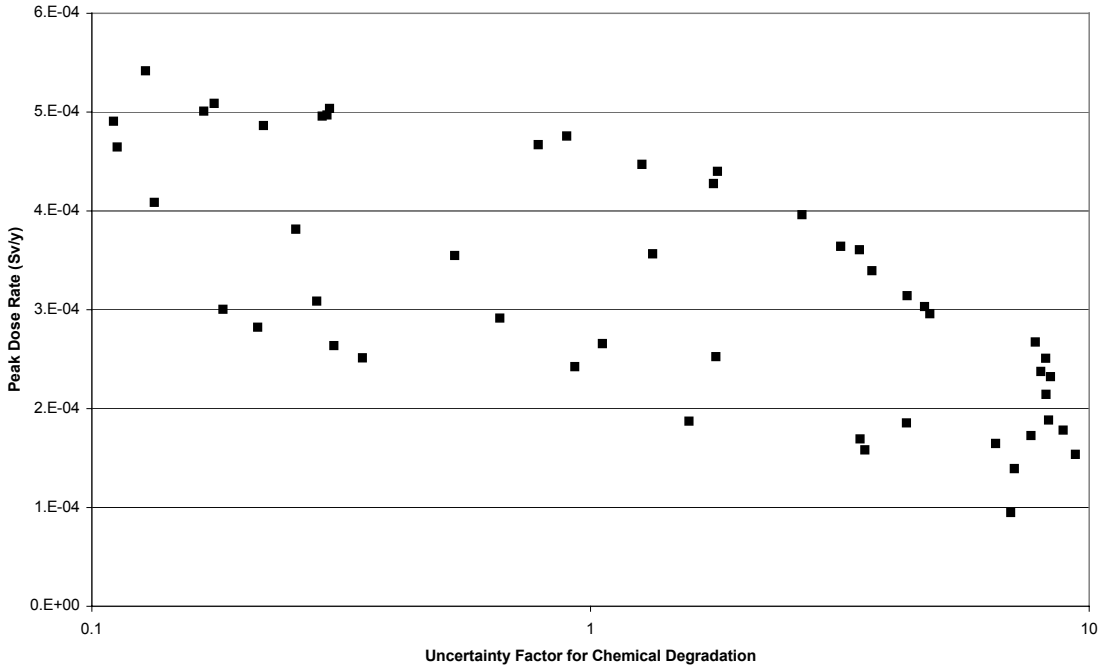

Figure 4.10 *Scatter Plot for Peak Dose Rate for Terrestrial Pathways against the Uncertainty Factor for Chemical Degradation Timescale*

4.2.3 Sorption Sensitivity Calculations

The Scoping calculations emphasised the importance of the chemical containment of long-lived radionuclides in the Silo. In this final round of calculations the importance of chemical containment has been investigated for the Silo by varying the sorption coefficients used in radionuclide transport over a range of four orders of magnitude by using a multiplicative uncertainty factor.

Figure 4.11 shows how the peak dose rate for Terrestrial Pathways varies with this sorption uncertainty factor for the Silo source term alone. Figure 4.12 shows how the timing of that peak dose varies. It can be seen that for 'low' values of the sorption coefficients (uncertainty factor less than about 0.1) peak dose rates increase, and occur much later typically around 11 000 years after closure. The reason the peak dose rate is later for the lowest values of Kd is that it is now dominated by long-lived radionuclides that are now able to reach the biosphere on the timescales of interest. The overall maximum increase in the peak dose rate is, however, less than a factor of three.

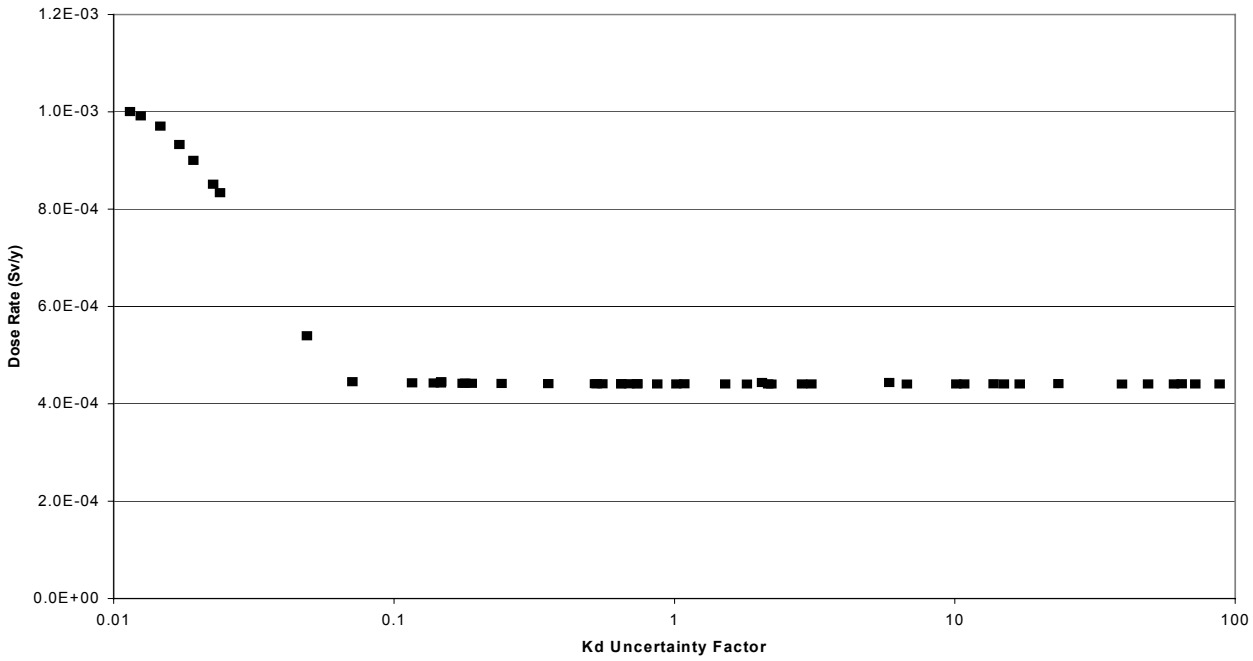

Figure 4.11 *Scatter Plot for Peak Dose Rate for Terrestrial Pathways against the Uncertainty Factor for Radionuclide Sorption for the Silo Source Term*

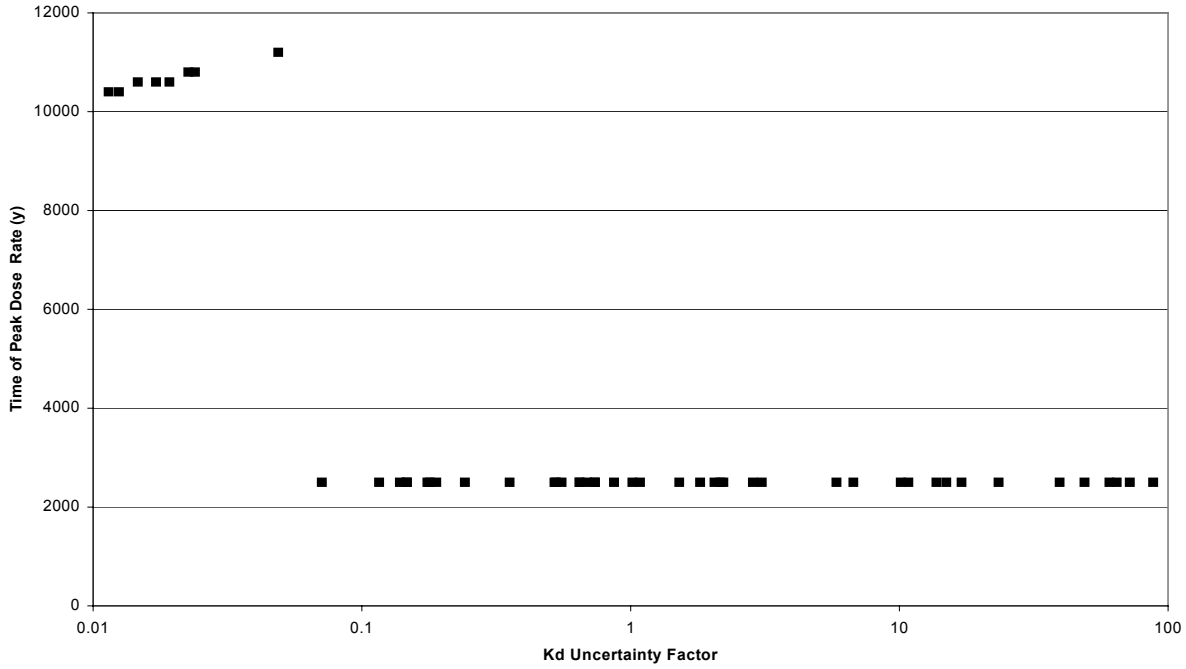

Figure 4.12 *Scatter Plot for the Timing of the Peak Dose Rate for Terrestrial Pathways against the Uncertainty Factor for Radionuclide Sorption for the Silo Source Term*

The reason for the relatively small change in overall peak dose rate is that the dose rate at relatively early times (around 2000 years after repository closure) is dominated by long-lived beta-gamma radionuclides whose transport is not so sensitive to the assumed sorption coefficients as the long-lived actinides.

Pathways where the long-lived actinides are important are very sensitive to the assumed sorption coefficients, as illustrated in Figure 4.13. This Figure shows how calculated dose rate for the inhalation pathway for Pu-239 at a particular time, 10 000 years after repository closure, varies with the assumed sorption coefficients. As the sorption coefficients are reduced over two orders of magnitude, the calculated dose rate varies by no less than four orders of magnitude. With lower sorption coefficients, the long-lived actinides provide a greater contribution to the overall calculated dose rates, and the peak dose rate occurs longer after repository closure due to the time needed for these radionuclides to be transported into the accessible environment.

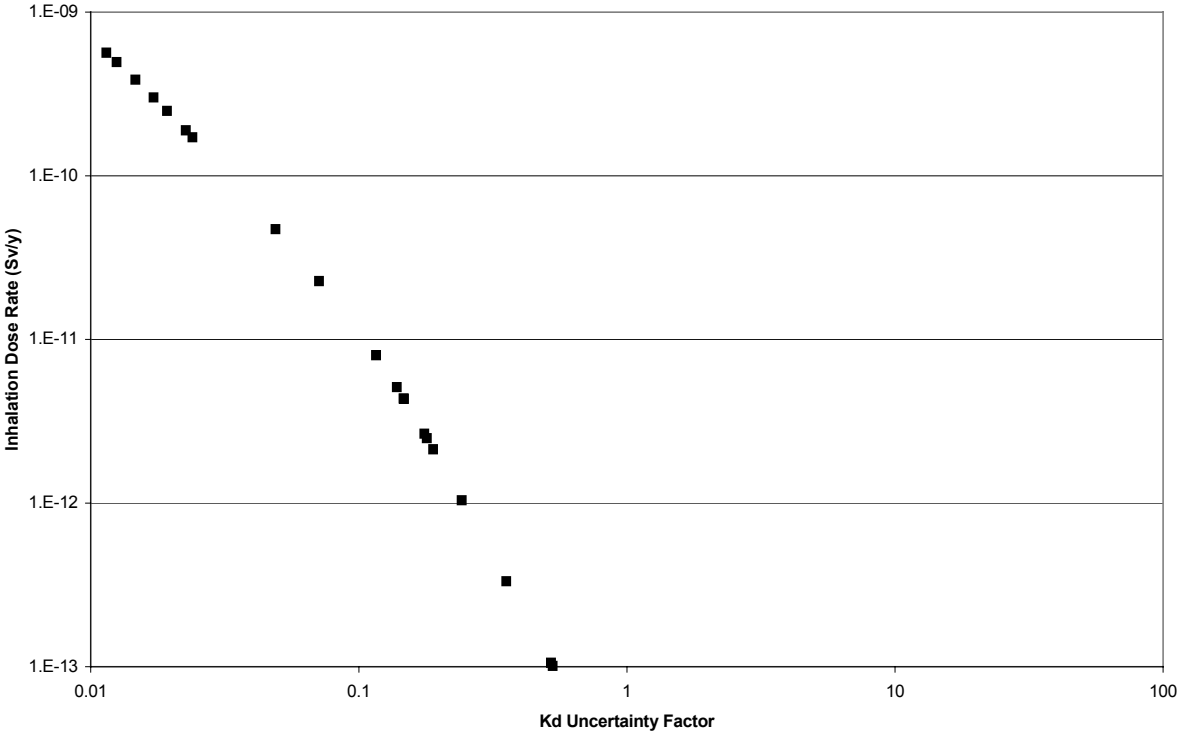

Figure 4.13 *Scatter Plot for the Inhalation Dose Rate for Terrestrial Pathways for Pu-239 at 10 000 Years against the Uncertainty Factor for Radionuclide Sorption for the Silo Source Term*

4.2.4 Discussion

The variant calculations show that slightly higher radiological impacts than those calculated in the Reference Case with the default choice of parameter values could be calculated with more conservative choices of some key parameters. However, the reference calculation is close to the most pessimistic 'worst case' that can be defined by choosing (probably unrealistic) combinations of model parameters.

4.3 The Permafrost Scenario

In this scenario it is assumed that the engineered barriers remain physically intact until the repository is subject to permafrost. Following the thawing of the permafrost it is assumed that the barriers are degraded.

Figure 4.14 gives the illustrative calculations for the situation where permafrost is initiated 5000 years after repository closure and thaws 1000 years later. Before 5000

years the doses are a result of releases from the BLA (where there are no engineered barriers) and diffusive releases from the other repositories. There is a peak in the release rate when the permafrost thaws.

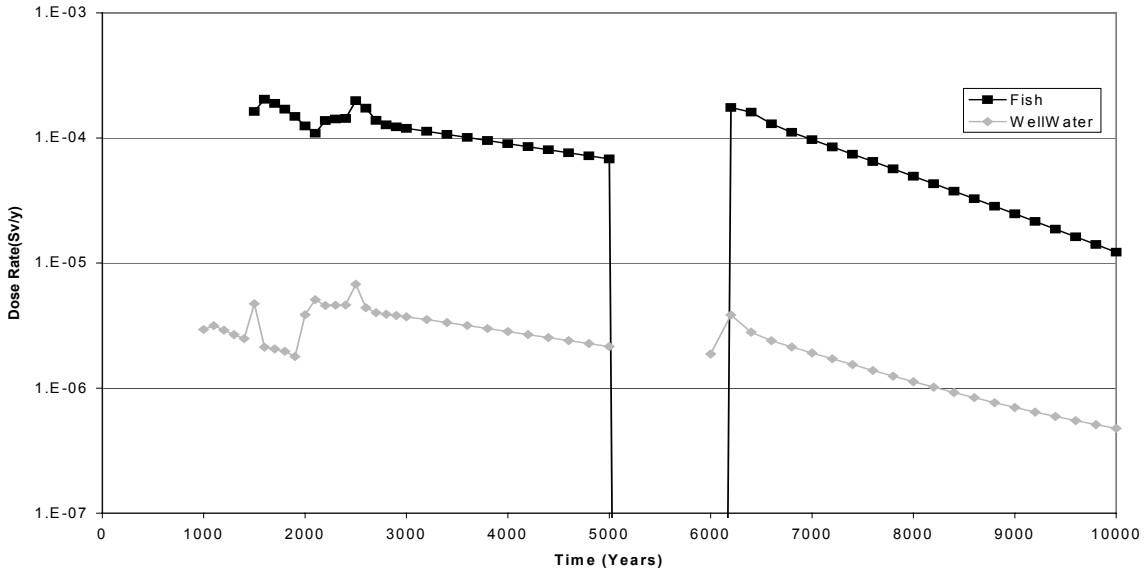

Figure 4.14 *Dose Rate for Terrestrial Pathways for the Permafrost Scenario*

Although the thawing of the permafrost results in a pulse of radioactivity entering the accessible environment, it does not result in peak dose rates that are higher than those calculated for the Reference Scenario (see Figure 4.4). As before, with the parameter values used, organic C-14 dominates the dose from the consumption of lake fish.

If there were discontinuous permafrost, it is possible that this could lead to channelled flow to a lake. The resulting dose rates would, however, not be expected to be any greater than those calculated for the reference scenario.

4.4 Very Long Term Calculations

A much simplified version of the AMBER Case File described in Section 2 has been used to investigate the hypothetical situation where all the radionuclides stay in the repository until activity reaches the surface on very long timescales due to surface erosion. This model is shown in Figure 4.15. A high erosion rate of 0.5 mm y^{-1} has been assumed, so that the repository begins to be exposed after 100 000 years. As the repository is eroded it is assumed that the radionuclides enter a region of soil of dimensions 300 m by 160 m. Subsequent radionuclide transfer mechanisms are

assumed to be for the terrestrial environment in the Reference Scenario. In reality surface erosion could be discontinuous, for example due to successive glaciations.

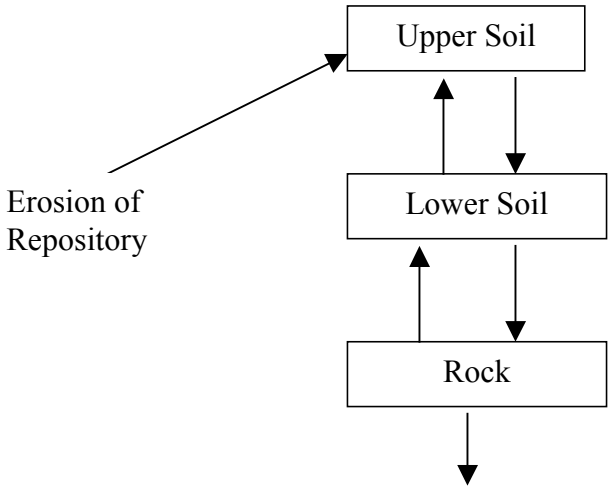

Figure 4.15 *Simplified Model for Very Long Term Calculations*

Figure 4.16 shows the total concentrations of radionuclides in the repositories as a function of time for this scenario. By the time that repository erosion commences at 100 000 years, radionuclide concentrations have reduced by around two-and-a-half orders of magnitude. Residual concentrations are dominated by very long-lived radionuclides such as Tc-99 and Ni-59.

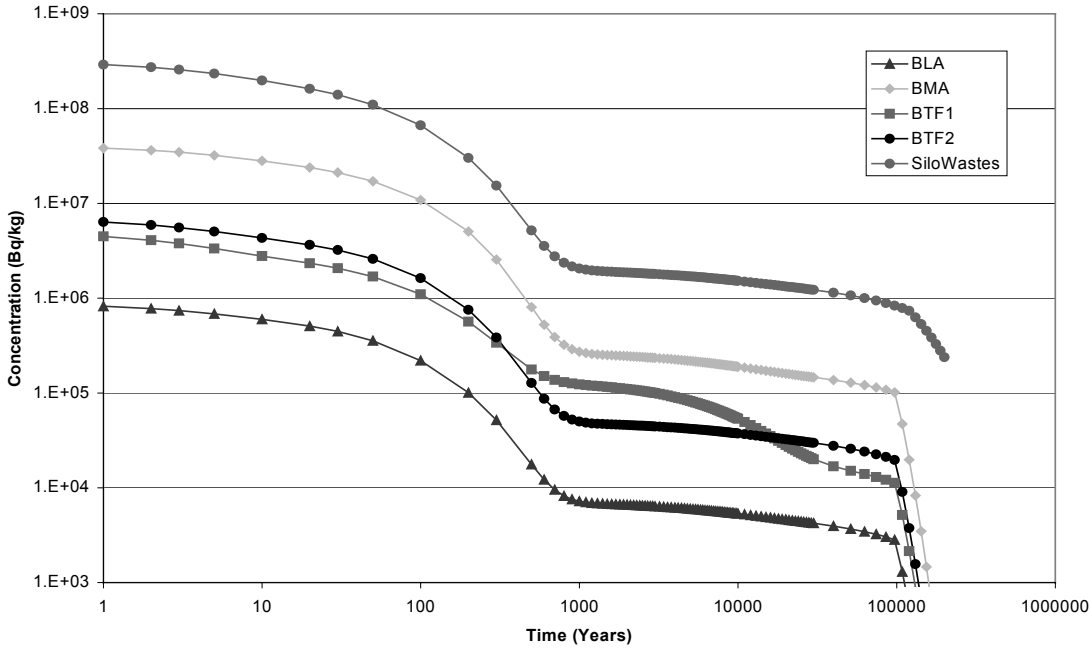

Figure 4.16 *Concentrations in Vaults for Very Long Term Calculations*

Figure 4.17 shows the calculated illustrative dose rates for Terrestrial pathways. These dose rates are much lower than those calculated for the Reference scenario, not exceeding 1 μSv y^{-1}. The important radionuclides are now very different from those that dominate the doses in the Reference scenario. Figure 4.18 shows the key radionuclides contributing to the dose calculations. As one would expect, they are all very long-lived isotopes: Nb-94, Tc-99, Ra-226, Th-229, Th-230, Pa-233, Np-237, Pu-239 and Pu-242.

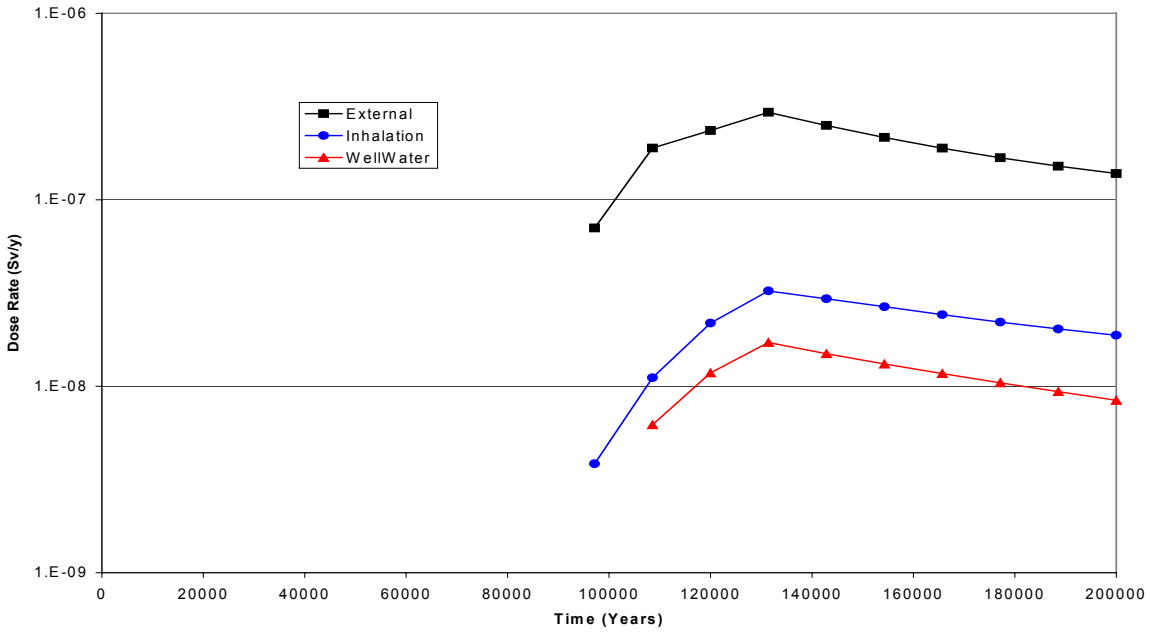

Figure 4.17 *Dose Rate for Terrestrial Pathways for Very Long Term Calculations*

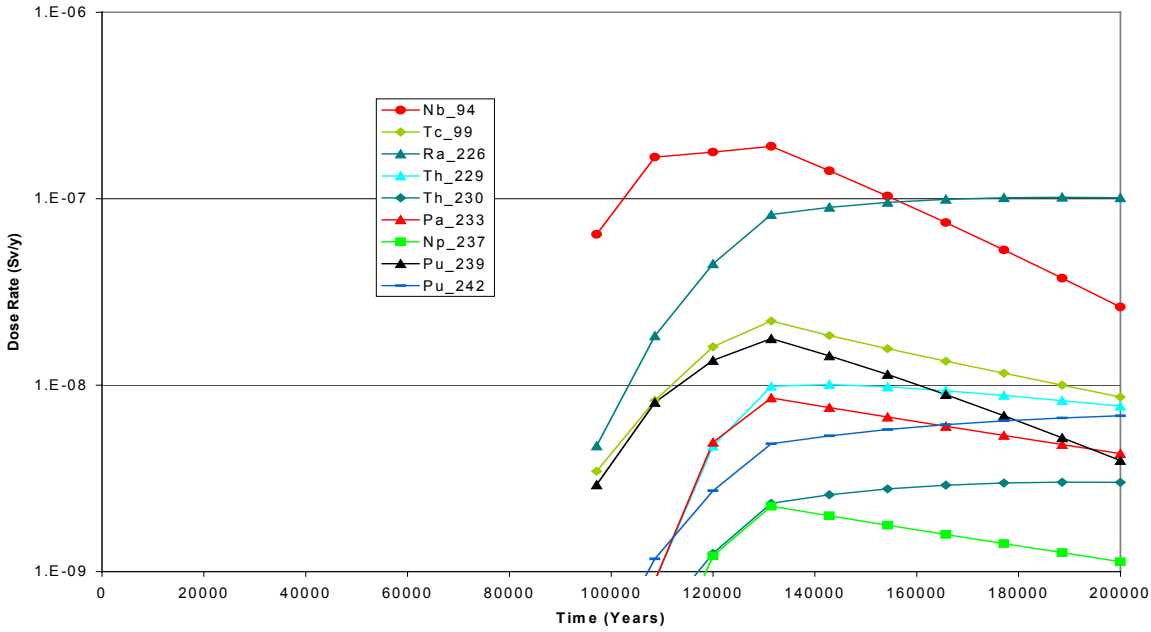

Figure 4.18 *Important Radionuclides for Very Long Term Calculations*

4.5 The Representation of Time Dependent Processes

As discussed in Section 1, a key feature of the PA methods that have been developed is to be able to represent time dependent processes explicitly in a continuous way. It is instructive to consider how the calculated impacts could differ if time dependent processes were represented in a discontinuous way, as many approaches to PA use such a 'snap shot'.

The Reference Scenario/Reference Case calculations have been rerun with time dependent parameters only being changed at specified intervals. Figure 4.19 shows the calculated flux of radionuclides from the different vaults with a 'snap shot' timescale of 1000 years; this can be compared directly with Figure 4.1.

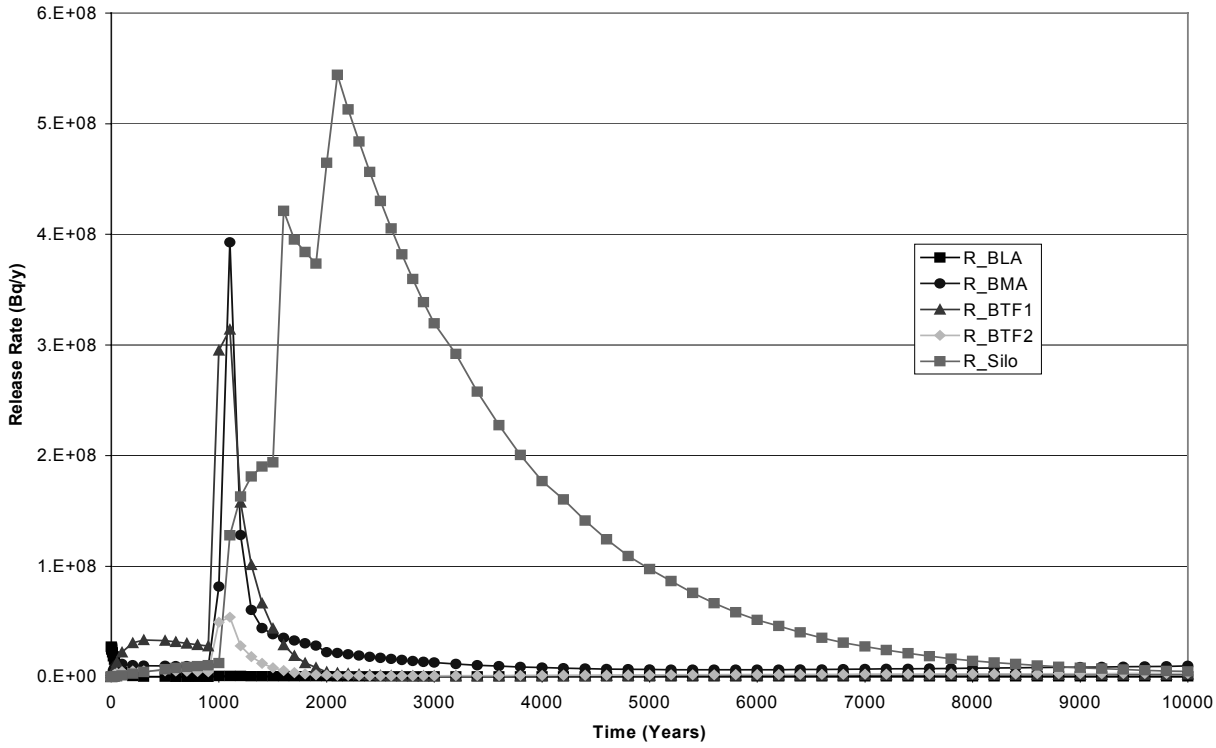

Figure 4.19 *Radionuclide Fluxes from the Vaults in the Reference Calculations with 1000 Year 'Snap Shots' for Time Dependent Parameters*

Comparing Figures 4.1 and 4.19 shows clearly how the 'snap shot' approach leads to a much more peaked profile of releases, particularly for the BMA and 1BTF. There is a possibility of unphysical fluxes being calculated with the snap shot approach, but whether or not this will be significant in terms of the calculated radiological impacts will depend upon the characteristics of the receiving biosphere at the time of peak discharges from the geosphere.

Figure 4.20 shows the calculated doses for terrestrial pathways with the 'snap shot' timescale of 1000 years; this can be compared directly with Figure 4.4.

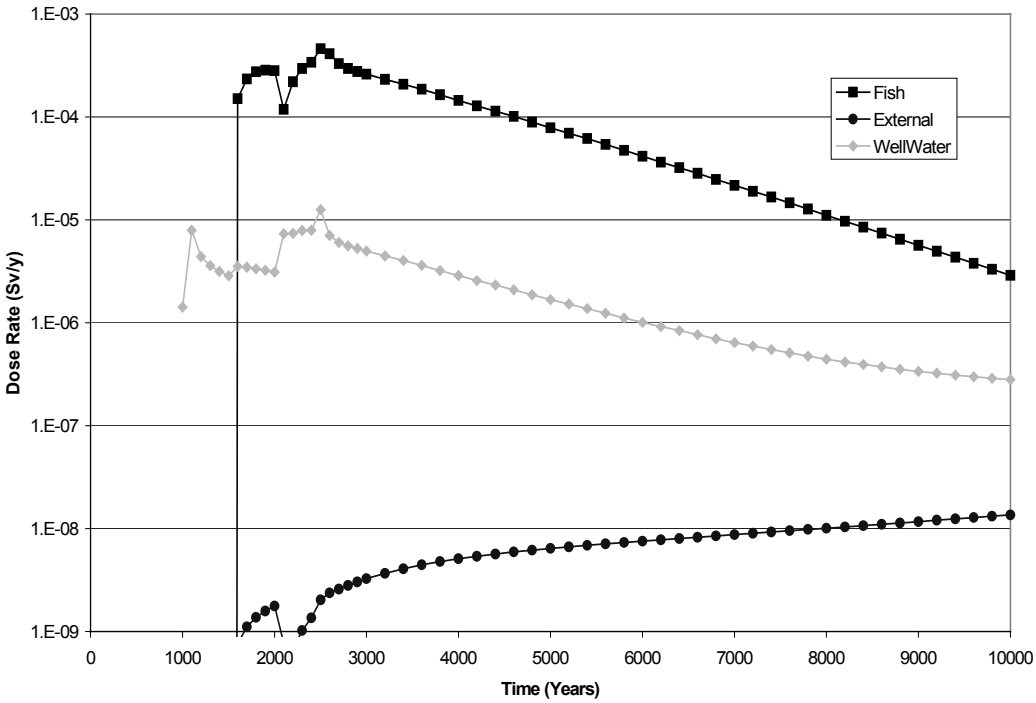

Figure 4.20 *Dose Calculations for Terrestrial Pathways the Reference Calculations with 1000 Year 'Snap Shots' for Time Dependent Parameters*

Comparing Figures 4.4 and 4.20 shows that the dose calculations for the 'continuous' and 'snap shot' calculations are generally similar; in particular, the peak dose rates for the three pathways shown are about the same. This is because the fluctuation in discharges from the vaults in the 'snap shot' case is calculated to occur when the facility is still below the Baltic, before the peak dose rates are incurred.

These calculations illustrate that although in general a 'snap shot' approach to the representation of continuously varying parameters may lead to unphysical estimates of

radionuclide transport, for the SFR 1 system the overall radiological impacts may not be significantly different from calculations made with a continuous representation of time dependent parameters.

4.6 Conclusions

10. With the reference set of assumptions employed, impacts appear to be dominated by long-lived beta-gamma radionuclides such as Mo-93, Nb-93m, Ni-59, Cl-36, Se-79, Cs-135 and C-14.

11. The use of water from a well could lead to relatively high dose rates. There are a number of modelling assumptions required to calculate impacts from this pathway (the type of well that could be present, the degree of dilution with uncontaminated groundwater etc.).

12. The assumed timing of engineered barrier degradation can be important. However, providing barrier degradation rates result in peak fluxes back into the accessible environment occurring after the Baltic has receded from the SFR 1 region, the peak impacts appear not be very sensitive to the details of the modelling assumptions.

13. Peak impacts are sensitive to the assumptions made about flow rates through the repositories.

14. The assumptions made about radionuclide sorption are most important for long-lived actinides. If conservative values are chosen, the relative importance of the release of such radionuclides from the Silo will increase, as illustrated in the Scoping calculations.

15. Illustrative calculations to investigate the potential importance of permafrost suggest that impacts are unlikely to be greater than those calculated for the Reference scenario.

16. Calculations to investigate potential impacts on very long timescales when the wastes may be brought close to the surface have shown that such impacts are small, being dominated by very long-lived radionuclides such as Nb-94, Tc-99, Ra-226, Th-229, Th-230, Pa-233, Np-237, Pu-239 and Pu-242.

17. A discontinuous ‘snap shot’ approach to the representation of continuously varying parameters may lead to unphysical estimates of radionuclide transport, but for the SFR 1 system (because the repository is under the Baltic at early times) the calculated radiological impacts may not be significantly different from calculations made with a continuous representation of time dependent parameters.

5 Overall Conclusions

Independent PA calculations having been undertaken for SFR 1. These calculations have been used to explore some of the key issues for the post-closure safety of this facility. The main findings can be summarised as follows:

18. The SFR 1 system has a number of different timescales that can affect the magnitude of potential radiological impacts. These include: repository resaturation and gas evolution timescales, the rate at which the Baltic is retreating, the rates of engineered barrier degradation, and groundwater residence times in the geosphere. It is important that all relevant time-dependent processes are represented in system modelling.

19. Because of the complexity of the system, it is not always possible to define what choices of modelling assumptions and parameter values can be regarded as 'conservative'.

20. Radiological impacts when radionuclide discharges are to the Baltic are likely to be orders of magnitude lower than those when the discharges are to the terrestrial environment.

21. If overpressurisation of the Silo takes place due to gas generation, this could lead to increased early releases of short-lived radionuclides into the environment, but this is unlikely to lead to significantly increased radiological impacts as these releases would take place when the SFR 1 is below the Baltic. Physical damage of the engineered barriers, might, however, be important on longer timescales by affecting groundwater flows through the facility.

22. Dose rates of the order of 0.1 mSv y^{-1} are possible when radionuclides from SFR 1 enter the terrestrial environment. The precise value of the calculated maximum dose rate will depend upon a number of assumptions about biosphere characteristics and critical group behaviour. The use of contaminated well water may give rise to significant exposures.

23. Long-lived actinide radionuclides (particularly in the Silo) may be retained by sorption processes on very long timescales. If this is the case, peak impacts are likely to be dominated by long-lived beta-gamma radionuclides such as Mo-93, Nb-93m, Ni-59, Cl-36, Se-79, Cs-135 and C-14.

24. For most of the PA calculations organic C-14 appears to be the dominant radionuclide primarily because it is assumed not to be sorbed in the near-field. Further consideration needs to be given to the behaviour of this radionuclide

throughout the system in order to be able to provide better estimates of potential radiological impacts.

25. Peak impacts are likely to be sensitive to the assumptions made about groundwater flow rates through the vaults.

26. Illustrative calculations to investigate the potential importance of permafrost suggest that impacts are unlikely to be greater than those calculated in its absence.

27. Calculations to investigate potential impacts on very long timescales when the wastes may be brought close to the surface by erosive processes have shown that such impacts are likely to be small, being dominated by very long-lived radionuclides and their daughters such as Nb-94, Tc-99, Ra-226, Th-229, Th-230, Pa-233, Np-237, Pu-239 and Pu-242.

These PA calculations are by no means comprehensive, and various issues could be investigated further if required.

References

Brydsten L (1999). Shore Line Displacement in Öregrunsgrepen. SKB Technical Report TR-99-16.

Chapman N A, Maul P R, Robinson P C and Savage D (2002). A Review of SKB's Project SAFE for the SFR Repository. To be published as an SKI Report.

Eckerman K F and Ryman J C (1993). External Exposure to Radionuclides in Air, Water and Soil. EPA Federal Guidance Report No. 12.

Egan M J (1999). Work in Support of Biosphere Assessments for Solid Radioactive Waste Disposal: Biosphere FEP List. QuantiSci Report to SSI. Report No. SSI-6181A-3, V 1.0.

Holmén J G and Stigsson M (2001). Modelling of Future Hydrogeological Conditions at SFR, Forsmark. SKB Report SKB R-01-02.

IAEA(1996). International Basic Safety Standards for Protection against Ionizing Radiation and for the Safety of Radiation Sources. International Atomic Energy Agency Safety, Series No. 115.

Maul P R and Cooper N S (1999). Development of a Performance Assessment Capability for SFR using the AMBER Code. QuantiSci report SKI-6246A-1 Version 1.0 for SKI.

Maul P R, Watkins B M and Egan M J (1999). Work in Support of Biosphere Assessments for Solid Radioactive Waste Disposal: Biosphere Modelling and Related AMBER Case Files. QuantiSci report SSI-6181A-4 Version 1.0 for SSI.

Maul P R (2000). Progress on Scoping Calculations and the Gas Pathway for SFR. QuantiSci report QSL-6246C-TN1 Version 1.0.

Maul P R and Robinson P C (2000). Scoping Calculations for the SFR Disposal Facility. QuantiSci report SKI-6246C-1 Version 1.0.

QuantiSci and Quintessa (2000). AMBER 4.3 Release Note. QuantiSci Report QSL-5046A-5 Version 1.0.

QuantiSci and Quintessa (2001). AMBER Verification: Summary. QuantiSci Report QSL-5046A-6 Version 1.0.

Robinson P C (2000). Stand-alone Modelling of Gas Issues in the SFR Silo. QuantiSci report QSL-6246C-TN2 Version 1.0.

Savage D and Stenhouse M (2001). SFR Database. Report to SKI.

Skagius K, Lindgren M and Pers K (1999). Gas Generation in SFL 3-5 and Effects on Radionuclide Release. SKB report R-99-16.

SKB (1987a). Data Base for the Radionuclide Transport Calculations for SFR by Wiborgh M and Lindgren M. Kemakta report SFR 87-09.

SKB (1987b). Radionuclide Release from the Near-field in SFR by Akke Bengtsson, Maria Lindgren, Karin Pers and Marie Wiborgh. SKB Report SFR 87-10.

SKB (1987c). Radiological Consequences to man due to Leakage from a Final Repository for Reactor Waste (SFR) by Ulla Bergström et al. SKB Report SFR 87-12.

SKB (1991). SFR in-depth safety assessment. SKB Report SFR 91-01.

SKB (2001). Project SAFE- Compilation of Data for Radionuclide Transport Analysis. SKB report R-01-14 .

SSI (1989). SFR-1, Environmental Impact by Hägg and G Johansson. SSI-rapport 89-13.

Stenhouse M, Miller W and Chapman N (2001). System Studies in PA: Development of Process Influence Diagram (PID) for SFR Repository: Near-field and Far Field. SKI Report 01:30.

Appendix A. Modelling SFR 1 with AMBER: Technical Details

In this Appendix some of the mathematical details are given for the general SFR 1 modelling with AMBER described in Section 2 of the main text. The nomenclature used is given in Table A1.

Table A1 *Nomenclature*

Parameter	Units	Definition
A	m^2	Area
a	m^{-1}	Flow wetted surface area per unit volume
B	$m^3\ y^{-1}$	Breathing rate
c	moles m^{-3}	Radionuclide concentration in liquid phase (per unit volume)
c^{sol}	moles m^{-3}	Elemental solubility limit
C_F	$m^3\ kg^{-1}$	Elemental concentration factor
d	m	Depth
D_e	$m^2\ y^{-1}$	Effective diffusion coefficient
D_m	$m^2\ y^{-1}$	matrix (porewater) diffusion coefficient
E	Sv y^{-1}	Dose rate
F	moles y^{-1}	Radionuclide flux
f	-	Repository Darcy flow as a fraction of flow through surrounding rock
f_0	-	Initial value of f
f_1	-	Final value flow of f
g	m s^{-2}	Acceleration due to gravity (9.8 m s^{-2})
G	Nm^3	Total volume of gas produced
h	m	Depth of gas layer at top of Silo
H	m	Height
I	kg y^{-1} or $m^3\ y^{-1}$	Ingestion or Inhalation rate
K_d	$m^3\ kg^{-1}$	Sorption coefficient
L	m	Compartment length

Parameter	Units	Definition
O	-	Occupancy factor
P_{atm}	Pa	Atmospheric pressure (0.1 MPa)
P_{ext}	Pa	Pressure outside the Silo in saturated groundwater
q	m y^{-1}	Infiltration rate
Q	moles	Radionuclide inventory
R	-	Elemental retardation coefficient
r	m^3 y^{-1}	Resaturation rate
S	kg m^{-3}	Suspended sediment load
t	y	Time since repository closure
t_{end}	y	Time when barriers have completely degraded physically
t_{start}	y	Time when barriers begin to degrade physically
U	m y^{-1}	Land uplift rate
v	m y^{-1}	Darcy velocity
v_g	Nm^3 y^{-1}	Gas production rate
V	m^3	Compartment volume
V_{free}	m^3	Volume of free water in Silo
V_g	Nm^3	Gas produced to time t
V_{gas}	Nm^3	Total volume of gas in the Silo
V_r	Nm^3	Residual volume of air at repository closure
V_{tot}	Nm^3	Total volume of gas generated
V_{water}	m^3	Total volume of water in the Silo
W	-	Well dilution factor
β	m y^{-1}	Bioturbation rate
γ	Sv y^{-1} per Bq kg^{-1}	External dose rate per unit soil concentration of radionuclide
χ	moles kg^{-1}	Mass-based radionuclide concentration in solid phase
δ	m	Depth of diffusion into rock matrix
Δ	m	Diffusion distance
ΔP_1	Pa	Overpressure required for gas to flow through the Silo lid
ΔP_2	Pa	Overpressure required for concrete walls to fail
ε	-	Degree of saturation

Parameter	Units	Definition
θ	-	Porosity
κ	m^3	Radionuclide capacity
κ^{ing}	Sv Bq^{-1}	Dose per unit activity ingested
κ^{inh}	Sv Bq^{-1}	Dose per unit activity inhaled
λ	y^{-1}	Radionuclide transfer rate
λ^{house}	y^{-1}	Turnover rate for air in the house.
ρ	kg m^{-3}	Bulk density
σ	kg m^{-2} y^{-1}	Sedimentation rate
τ	y	Timescale for gas generation
Φ	m^3 y^{-1}	Flux of water

Notes:

Units of Bq rather than moles are use in many algorithms; and conversions between the two sets of units is required.

A1 Evolution of the Silo System

The relatively short term evolution of the Silo is included in the AMBER Case file to investigate the importance of gas generation and resaturation effects. These effects are not modelled explicitly in the other vaults where it is assumed that resaturation is rapid and gas generation effects have not been considered. A modelling approach suitable for implementation in AMBER was described by Maul (2000) and compared with more detailed modelling in Robinson (2000).

It is assumed that when SFR 1 is closed there will initially be a residual volume V_r of air in the Silo at close to atmospheric pressure, and that water flows into the system at a specified rate r (m^3 y^{-1}) until the pressure increases to external saturated levels. Gas was assumed to be produced at a rate (Nm^3 y^{-1}) given by

$$vg(t) = G/\tau \exp(-t/\tau) \quad \text{(A1)}$$

Where G is the total volume of gas produced (Nm^3) and τ is a production timescale (y).

It was assumed that there will be a gas layer of depth h at the top of the Silo and that there will be an initial resaturation period during which water enters the Silo at the specified rate r (in reality this will not be constant but will depend upon the pressure differences between the Silo and the outside). As the Silo resaturates the gas pressure increases and one can envisage four possible states of the system:

28. Initial resaturation is taking place and there is no gas flow through the lid (the overpressure is less than that required to initiate flow or barrier failure).
29. Initial resaturation is taking place at the same time that gas flow has been initiated.
30. Initial resaturation has been completed but there is no gas flow.
31. Initial resaturation has been completed and there is gas flow through the lid. When gas flow starts this may result in a further flow of groundwater into the system.

Various criteria were specified to determine at any given time t the state the system is in.

1. If $t > V_r / r$ the initial resaturation period must have come to an end.

2. If the time is less than that given in 1 and there is an overpressure in the gas, initial resaturation must have been completed. This is so when

$P_{atm}\ V_{gas}\ (t)/\ (V_r\text{-}rt) > \quad P_{ext}+H\ (V_r\text{-}rt)\ \rho\ g/V_{free,}$ where ρ is the density of water.

3. If initial resaturation is still taking place, then gas flow will take place at the same time if

$P_{atm}\ V_{gas}/\ (V_r\ -\ r\ t) >\ P_{ext}+\ \Delta P_1$ (or ΔP_2).

4. If initial resaturation is complete then gas flow will take place if $h\ \rho\ g > \Delta P_1$ (or ΔP_2).

For the four system states *h* and other parameters can be estimated as follows:

State 1: initial resaturation, no gas flow

h is simply determined from $H\ (V_r\text{-}rt)\ /\ V_{free}$.

State 2: initial resaturation with gas flow

h is similarly determined from $H\ (V_r\text{-}rt)\ /\ V_{free}$.

State 3: initial resaturation complete with no gas flow

h is determined from

$(h)^2\ +\ h\ \{P_{ext}/\ (\rho\ g)\}\ -\ V_g\ P_{atm}\ H\ /\ (V_{free}\ \rho\ g)\ \ =\ \ 0$

The rate of expulsion of (potentially contaminated) water can be calculated from the gas volume production rate at the prevailing pressure:

$G/\tau\ \ exp\ (-\ t/\tau)\ [P_{atm}\ /\ (P_{ext}\ +\ h\ \rho\ g)]$.

State 4: initial resaturation complete with gas flow

h is taken to be the larger of $\Delta P\ /\ (\rho\ g)$ and $H\ (V_r\text{-}rt)\ /\ V_{free}$. The second case corresponds to the situation where the release of gas requires a further flow of groundwater into the Silo.

The governing equations implied in this simplified model are summarised in Table A2.

The simple model is capable of producing estimates of the release with time of gas from the Silo and also of expelled water, which may be contaminated. It is also

capable of calculating when barrier degradation could result in an advective flow path being opened up. These are the quantities of most relevance to PA calculations.

A2 Flows in Near-Field Rock

The flows through the vaults are taken to vary linearly from values assumed for the Saltwater Period to values assumed for the Inland Period over a specified time period. The engineered barriers were assumed to start degrading physically at a time t_{start} and to complete degrading at a time t_{end}. For the Silo these timescales refer to the engineered barriers as a whole, although in reality the concrete and bentonite barriers may degrade at different rates. It was assumed that the degradation timescales for the other repositories (BMA, 1BTF, 2BTF and BLA) are the same. The flow rates (Darcy velocities) through the vaults were taken to be a fraction (f) of the flow rate (Darcy velocity) through the near-field rock.

$$f(t) = \begin{cases} f_0 & t < t_{start} \\ f_0 + \dfrac{(f_1 - f_0)\,(t - t_{start})}{(t_{end} - t_{start})} & t_{start} \le t \le t_{end} \\ f_1 & t > t_{end} \end{cases} \qquad \text{(A2)}$$

SKB (1987a) gave, for the Silo $f_0 = 0$ and $f_1 = 2$, $t_{start} = t_{end} = 1000$ years, and $f_0 = 2$ and $f_1 = 20$, $t_{start} = t_{end} = 100$ years for the other vaults.

These flows are resolved into vertical and horizontal components, using the same directional angle as the Darcy flow in the near-field rock. In some cases water flows from one donor compartment needed to be split between two receiving compartments according to geometrical factors.

Tables A3 and A4 give details of how the flows in the near-field rock have been represented. This is a very simple approach aimed to conserve overall water flows.

Table A2 *Governing Equations in the Simplified Model for the Evolution of the Silo System*

$\frac{\partial V_{water}}{\partial t} = r, \quad P_{gas} < \rho(h+d)g$
$\frac{\partial V_{water}}{\partial t} = \quad 0, \qquad P_{gas} = \rho\,(h+d)\,g$
$\frac{\partial V_{water}}{\partial t} = \quad -\frac{v_g\ P_{atm}}{P_{gas}}, \qquad P_{gas} > \rho\,(h+d)\,g$
$V_{water} = \quad V_{silo} - \frac{h\,V_{free}}{H}$
$P_{gas} = \frac{P_{atm}\,V_{gas}\,H}{V_{free}\,h}$
$\frac{\partial V_{gas}}{\partial t} = \quad v_g, \qquad P_{gas} < \rho\,d\,g + \Delta\,P_1$
$\frac{\partial V_{gas}}{\partial t} = \quad 0, \qquad P_{gas} \geq \rho\,d\,g + \Delta\,P_1$
$P_{gas}(0) = P_{atm} \qquad\qquad V_{gas}(0) = V_r$
$h(0) = \quad \frac{H\,V_r}{V_{free}}$

Table A3 *Horizontal Darcy Velocities in Near-field Rock Compartments*

Donor	**Receptor**	**Horizontal Darcy Velocity factor when f<1**	**Horizontal Darcy Velocity factor when f>1**
Above Left Silo Rock	Above Silo Rock	1	1
Above Silo Rock	Above Right Silo Rock	1	1
Above Right Silo Rock	Geosphere	1	1
Left Silo Rock	Silo Backfill	1+ (1-f)H[Bentonite]/H[Backfill]	f
Left Silo Rock	Left Silo Bentonite	f	f
Silo Backfill	Right Silo Rock	1+ (1-f)H[Bentonite]/H[Backfill]	f
Right Silo Bentonite	Right Silo Rock	f	f
Right Silo Rock	Geosphere	1	f
Below Left Silo Rock	Below Silo Rock	1	1
Below Silo Rock	Below Right Silo Rock	1	1
Below Right Silo Rock	Geosphere	1	1

Note: H refers to compartment height

Table A4 *Vertical Darcy Velocities between Near-field Rock Compartments*

Donor	**Receptor**	**Vertical Darcy Velocity factor when f<1**	**Vertical Darcy Velocity factor when f>1**
Above Left Silo Rock	Geosphere	1	1
Above Silo Rock	Geosphere	1	f
Above Right Silo Rock	Geosphere	1	1
Left Silo Rock	Above Left Silo Rock	1	1
Silo Backfill	Above Silo Rock	1	f
Right Silo Rock	Above Right Silo Rock	1	1
Below Left Silo Rock	Left Silo Rock	(L[Below Left Rock]+ L[Below Right Rock]+ (1-f)L[Below Rock])/ (L[Below Left Rock]+ L[Below Right Rock])	1
Below Silo Rock	Silo Base	f	f
Below Right Silo Rock	Right Silo Rock	(L[Below Left Rock]+ L[Below Right Rock]+ (1-f)L[Below Rock])/ (L[Below Left Rock]+ L[Below Right Rock])	1

Note: L refers to compartment length

A3 Radionuclide Transfers in the Near-Field

The concept of Capacity is useful when describing radionuclide transport in the near-field. This parameter κ has units of m^3 and is defined as:

$$\kappa = V(\theta + \rho K_d) \tag{A3}$$

where V is the volume of material in the compartment, θ is the porosity, K_d is the distribution coefficient for a given element and ρ is the bulk density. All the AMBER compartments are assumed to be composed of a single material. The capacity of a compartment is related to the retardation coefficient for radionuclide transport, R, for the material involved.

$$\kappa = V \theta R \tag{A4}$$

$$R = 1 + \frac{\rho K_d}{\theta} \tag{A5}$$

The concentration, c, of radionuclides in the porewater of any compartment (moles m^{-3}) can be obtained from

$$c = (\frac{Q}{\kappa}, c^{sol}) \tag{A6}$$

where Q is the total amount of radioactivity in the compartment and c^{sol} is the appropriate solubility limit (which may be a fraction of the elemental limit if there is more than one radionuclide for the given element).

If the flux of radionuclides between two compartments is diffusive, that flux can be approximated by:

$$F = \frac{A D_e \Delta c}{\Delta} \tag{A7}$$

where A is the cross-sectional area relevant to the transport, D_e is the effective diffusion coefficient, Δc is the difference in concentrations between the two compartments, and Δ is a representative diffusion length. Employing the expression above for the porewater concentration, the expression used in AMBER for diffusive transfers between compartments becomes:

$$\lambda = \frac{A D_e}{\kappa \Delta} \quad \text{(A8)}$$

The diffusive flux is represented by the combination of a 'forward' and 'backward' exchange coefficient.

The corresponding expression for an advective flux, is:

$$F = A v c \quad \text{(A9)}$$

$$\lambda = \frac{A v}{\kappa} \quad \text{(A10)}$$

where v is the Darcy velocity. Alternatively this can be expressed as

$$\lambda = \frac{v}{\theta R L} \quad \text{(A11)}$$

where L is the length of the donor compartment in the direction of radionuclide transport.

A4 Radionuclide Transfers in the Geosphere

Advective transfers between compartments in the geosphere are modelled using a similar approach to that used for the near-field. Radionuclide sorption on the fracture surfaces is neglected.

The transfer rate from a fractured rock compartment into the associated matrix compartment is taken as

$$\lambda_{rm} = \frac{2 a \theta_m D_m}{\theta \delta} \quad \text{(A12)}$$

where a is the flow wetted surface area per unit volume (m^{-1}), θ is the fracture porosity, θ_m is the matrix porosity, D_m is the matrix diffusivity ($m^2\ y^{-1}$), and δ is the depth of the matrix compartment (m).

The reverse transfer rate from a matrix compartment back to the rock fracture is taken as

$$\lambda_{mr} = \frac{2\,D_m}{R_m\,\delta^2} \qquad \text{(A13)}$$

where R_m is the retardation coefficient of the radionuclide in question in the matrix.

A5 Radionuclide Transfers in the Terrestrial Biosphere Sub-System

Transfers when the Land is Under the Sea

When any of the four areas of land are under seawater, radionuclides transferred from the Geosphere sub-system to the Terrestrial Biosphere sub-model will be transported according to the general hydrogeological regime assumed. For simplicity, it is assumed that in these conditions radionuclides will be transported upwards through the sediments into the sea according to the magnitude of the geosphere Darcy velocity.

The advective vertical transfer rate between the compartments is then

$$\lambda = \frac{v}{\theta\,R\,H} \qquad \text{(A14)}$$

where v is the magnitude of the Darcy velocity (m y^{-1}), θ is the porosity of the donor compartment, R is the retardation factor for the radionuclide concerned in the donor compartment, and H is the depth of the donor compartment. In the Terrestrial Biosphere sub-system it is assumed that whilst land is under the sea, groundwater movement is vertically upwards. This algorithm is also relevant to the transfer from the upper sediments compartments into the sea.

In addition to advective transfers of radionuclides, it is assumed that there are additional transfers due to bioturbation and other related processes. In this case the transfer is represented by

$$\lambda = \frac{\beta}{H} \qquad \text{(A15)}$$

where β is a bioturbation rate (m y^{-1}). This transfer can also be used to represent transport due to processes such as variations in the depth of the water table. There is a transfer back from the marine environment to the Upper Sediments as a result of sedimentation- this is specified in the section on the Marine Biosphere sub-system.

Transfers when the Sea has Receded

When the sea has receded and the land is not covered with water, vertical transfers towards the water table are defined by:

$$\lambda = \frac{q}{\theta \varepsilon R H} \quad \text{(A16)}$$

where q is the infiltration rate (m y^{-1}) and ε is the degree of saturation of the donor compartment. In addition 'bioturbation' transfers are represented, as in the period when the sea is under the land, but it is possible to employ a different bioturbation rate if required.

Aquatic Environment Transfers

The transfer of radionuclides from the land to the Lake is represented in the same way as when the Sea is present. The flux of radionuclides from the Sea or Lake back to the Upper Sediments compartments is determined by the scavenging rate

$$\lambda = \frac{K_d \sigma}{(1 + K_d S) H} \quad \text{(A17)}$$

where K_d is the appropriate sorption coefficient for the radionuclide in question on suspended sediment, S is the suspended sediment load (kg m^{-3}) and σ is the sedimentation rate (kg m^{-2} y^{-1}). The net flux from the Lake to Upper Sediments is apportioned to Areas 3 and 4 on the basis of area.

Radionuclides are assumed to leave the Lake and be transferred directly to the Regional Waters compartment in the Marine Biosphere sub-system. This transport will be in a small river, but this is not modelled explicitly as transfer rates would be very rapid, and radionuclide concentrations in the Lake are of more interest for radiological assessments than those in the river.

The transfer rate from the Lake to the Biosphere sub-model is represented by a simple turnover rate.

Transfers between other compartments are assumed to be the same in the presence of the Lake as when the area concerned was under the sea.

Gas

The concentration of gas (total and C-14) in a house assumed to be situated above the Silo was calculated by assuming that the flux into the house is a fraction of the total

volume of gas leaving the surface determined by the relative areas of the top of the Silo and the House itself. The concentration is then:

$$c^{house} = \frac{F\ A^{house}}{A^{Silo}\ V^{house}\lambda^{house}} \quad \text{(A18)}$$

where F is the flux from the surface, A^{house} is the area of the house, A^{silo} is the area of the top of the Silo, V^{house} is the volume of the house, and λ^{house} is the turnover rate for air in the house. Concentrations could possibly be higher if the gas were 'focussed', for example by being transported through a particular fracture.

A6 Individual Dose Calculations

For Terrestrial pathways, a potentially exposed group is assumed to be exposed by external irradiation over contaminated soils, inhalation of contaminated soils, drinking contaminated groundwater from a well and consumption of lake fish (when applicable). These pathways give indications of the possible radiological impacts, without the need for detailed biosphere modelling. It would be straightforward to add other pathways (such as crop and animal product consumption) if required.

The external exposure dose rate is calculated from

$$E = \gamma\ \chi\ O \quad \text{(A19)}$$

where γ is the external dose rate per unit soil concentration (Sv y^{-1} per Bq kg^{-1}), χ is the bulk concentration of the radionuclide in soil (Bq kg^{-1}) and O is an occupancy factor giving the fraction of time spent over the area in question. The factor γ is taken for an assumed semi-infinite mass geometry. The corresponding expression for inhalation doses is given by

$$E = \kappa\ \chi\ O\ I \quad \text{(A20)}$$

where κ is the dose per unit activity inhaled (Sv Bq^{-1}), I is the dust inhalation rate (kg y^{-1}), χ is the concentration of the radionuclide on soil grains (Bq kg^{-1}) and O is an occupancy factor giving the fraction of time spent over the area in question.

Drinking water doses are calculated from

$$E = \frac{\kappa\ I\ c}{W} \quad \text{(A21)}$$

where κ is the dose per unit activity ingested (Sv Bq^{-1}), I is the consumption rate for water (m^3 y^{-1}), c is the relevant radionuclide concentration in the geosphere (Bq m^{-3}) and W is a well dilution factor. The value of c is taken to be the maximum groundwater concentration in the geosphere compartments below the area in question. The dilution factor can be estimated depending on the flux of water through the contaminated region and the pumping rate of the well,

The dose rate due to consumption of lake fish is given by

$$E = \kappa I C_F c \qquad \text{(A22)}$$

where κ is the dose per unit activity ingested (Sv Bq^{-1}), I is the ingestion rate for the fish (kg y^{-1}), C_F is the relevant concentration factor for the fish (m^3 kg^{-1}) and c is the radionuclide concentration in filtered lake water (Bq m^{-3}).

For Marine pathways a potentially exposed group is assumed to be exposed by external irradiation over contaminated sediments, inhalation of contaminated soils and consumption of sea fish caught in the Regional Waters compartment. The algorithms used to calculate these doses are similar to those used for the Terrestrial group. Again, other pathways (such as consumption of crustacea and mollusca) could readily be considered.

For the gas pathway potential doses for C-14 are calculated from

$$E = \kappa B O c^{house} \qquad \text{(A23)}$$

where B is the breathing rate (m^3 y^{-1}).

A7 Default Data Values

Table A5 gives details of the input parameters for the AMBER Case File together with details of the default parameter values employed. This is supplemented by data information in Tables A6-A9.

Table A10 gives details of the default parameters used to define the compartment properties. Each compartment has an associated material type. For cementitious materials in the repository two groups of materials have been considered: ‘cements’ and ‘concretes’. ‘Cements’ include the porous concrete in the Silo and any material used to grout waste packages. ‘Concretes’ include all structural cementitious materials.

In the Final calculations described in Section 4, the radionuclide inventory given in SKB (2001) was used. This is reproduced in Table A11. Earlier calculations used the inventory given in SKB (1987b), reproduced in Appendix B.

Table A5 *Default Model Input Parameters*

AMBER parameter	Symbol/Units	Description	Default Value(s)	Data sources
Area	A (m^2)	Compartment area. Used in diffusive transfers in near-field	Compartment Properties Table A6	Near-field data derived from SFR 87-10
B_BalticSSL	S (kg m^{-3})	Suspended sediment load in the Baltic	0.001	SKB R-01-14
B_BalticSedimentation	σ (kg m^{-2} y^{-1})	Sedimentation rate in the Baltic	3.2	SKB R-01-14 (assuming a sediment density of 1600 kg m^{-3})
B_BalticTurnover	λ (y^{-1})	Turnover rate of Baltic waters	0.045	SKB R-01-14
B_RegionalSSL	S (kg m^{-3})	Suspended sediment load in the Regional Waters	0.005	SKB R-01-14
B_RegionalSedimentation	σ (kg m^{-2} y^{-1})	Sedimentation rate in Regional Waters	0.1	SFR 87-12
B_RegionalWatersTurnover	λ (y^{-1})	Turnover rate of Regional Waters	30	SKB R-01-14
BulkDensity	ρ (kg m^{-3})	Bulk density of different media	Media Properties Table A9	Near-field materials taken from SKI vault database
D_ConcentrationFactor	C_F- (-or m^3 kg^{-1} [fish])	Concentration factors	Element Properties Table A8	Taken from a review of a number of studies. Some data from SKI R-01-14
D_Consumption Rates	I (kg y^{-1} or m^3 y^{-1})	Critical group consumption rates	Water 0.6 m^3 y^{-1} Lake and Sea Fish 30 kg y^{-1}	SSI 89-13
D_DustInhalationRate	I (kg y^{-})	Dust inhalation rate	5E-4	Indicative value
D_ExtDosSF	γ (Sv kg Bq^{-1} y^{-1})	External dose per unit soil concentration	Radionuclide Properties Table A6	
D_FarmingOccupancyFactor	O	Fraction of time that the Terrestrial group is exposed to external exposure pathway	0.23	Indicative value
D_InhalationRate	B (m^3 y^{-1})	Average human respiration rate	8766	equivalent to 1 m^3 h^{-1}
D_MarineOccupancyFactor	O	Fraction of time exposed to external exposure pathway for Marine group	0.23	Indicative value

AMBER parameter	Symbol/Units	Description	Default Value(s)	Data sources
D_king	κ^{ing} (Sv Bq^{-1})	Ingestion dose factor	Radionuclide Properties Table A6	
D_kinh	κ^{inh} (Sv Bq^{-1})	Inhalation dose factor	Radionuclide Properties Table A6	C gas assumed to be in the form of methane
G_AngleEnd	(radians)	Final direction of Darcy velocity	0.05	Modelling assumption
G_AngleStart	(radians)	Initial direction of Darcy velocity	$\pi/2$-0.05	Modelling assumption
G_DarcyEnd	v_{end} (m y^{-1})	Final magnitude of Darcy velocity	0.005	SKB Hydrogeology studies
G_DarcyStart	v_{start} (m y^{-1})	Initial magnitude of Darcy velocity	0.0005	SKB Hydrogeology studies
G_DarcyStartTime	t_{start}(y)	Time after repository closure when Darcy velocity starts to change	0	Modelling assumption
G_DiffusionDepth	δ (m)	Diffusion depth into rock matrix	0.1	
G_FlowWettedArea	a (m^{-1})	Flow wetted surface area	0.2	
G_FracturePorosity	θ (-)	Fracture porosity	0.001	SKI vault database
G_MatrixPorosity	θ (-)	Matrix porosity	0.005	SKI vault database
Height	H (m)	Compartment heights	Compartment Properties Table A10	
I_HouseGasTurnover	λ^{house} (y^{-1})	Turnover rate for gas in house	8766	equivalent to 1 h^{-1}
I_InfiltrationRate	q (m y^{-1})	Infiltration rate when land is not covered by water	0.1	Indicative value
I_InitialLakeDepth	d (m)	Initial depth of lake	1.4	Brydsen (1999)
I_InitialLakeTurnoverRate	λ (y^{-1})	Initial turnover rate for lake	1	Indicative value
I_InitialSeaDepth	d (m)	Initial depth of sea for 4 terrestrial biosphere regions	6, 9, 12, 12	Based on information in Brydsen (1999)
I_LakeSSL	S (kg m^{-3})	Suspended sediment load in the lake	0.002	SKB R-01-14
I_LakeSedimentation	σ (kg m^{-2} y^{-1})	Sediment rate in the lake	6.4	SKB R-01-14 (assuming a density of 1600 kg m^{-3})
I_LandUpliftRate	U (m y^{-1})	Rate of land uplift	0.006	Brydsen (1999)
I_SoilSaturation	ε (-)	Degree of soil saturation	0.4	Indicative value
I_bioturb	β (m y^{-1})	Bioturbation rate	0.003	

AMBER parameter	Symbol/Units	Description	Default Value(s)	Data sources
Kd	K_d (m^3 kg^{-1})	Distribution coefficients	Sorption Properties Table A7	SKI vault database SKB R-01-14
Length	L (m)	Compartment lengths (horizontal dimension)	Compartment Properties Table A10	
P_atm	P_{atm} (Pa)	Atmospheric pressure	1E5	
P_ext	P_{ext} (Pa)	External pressure at top of Silo	5.9E5	
Porosity	θ (-)	Porosity of different media	Material Properties Table A9	SKI vault database SKB R-01-14
R_CrackFlowFraction	α (-)	Fraction of flow through Silo following over-pressurisation and wall cracking	0.1	Postulated value
R_DL_BLA_Waste	Δ (m)	Diffusion length for BLA waste	1.2	assumed geometry
R_DL_BMA_Waste	Δ (m)	Diffusion length for BMA waste	0.55	assumed geometry
R_DL_BTF1_Waste	Δ (m)	Diffusion length for 1BTF waste	1.15	assumed geometry
R_DL_BTF2_Waste	Δ (m)	Diffusion length for 2BTF waste	1.15	assumed geometry
R_DL_Silo_IW	Δ (m)	Diffusion length for Silo internal walls	1.4	assumed geometry
R_DL_Silo_Package	Δ (m)	Diffusion length for Silo package	0.09	assumed geometry
R_DL_Silo_Waste	Δ (m)	Diffusion length for Silo waste	0.55	assumed geometry
R_DPFlowVents	ΔP_1 (Pa)	Over-pressure required for gas flow through the Silo lid	5	Maul (2000)
R_DPFlowWalls	ΔP_2 (Pa)	Over-pressure required for gas flow through the Silo walls	5E5	Maul (2000)
R_Diff	D_e (m^2 y^{-1})	Effective diffusivities	Elemental Properties Table A8	SKI vault database
R_InventoryBq	Q (Bq)	Radionuclide inventories	See Table A11	
R_ResaturationRate	r (m^3 y^{-1})	Silo resaturation rate	1	Postulated value
R_SiloDiameter	- (m)	Silo diameter	28	SKB R-01-14
R_SiloFlowStartTime	t_{start} (y)	Time when Silo barriers start to degrade physically and allow water to flow	1000	Postulated value
R_SiloHeight	H (m)	Silo height	53	SKB R-01-14

AMBER parameter	Symbol/Units	Description	Default Value(s)	Data sources
R_SiloPhysDegradation	- (y)	Time for Silo barriers completely to degrade physically	500	Postulated value
R_SiloStage2	- (y)	Time when Stage II of cement evolution starts in the Silo	1000	Postulated value
R_SiloStage3	- (y)	Time when Stage III of cement evolution starts in the Silo	50 000	Postulated value
R_TotalGasVolume	G (Nm^3)	Total volume of gas produced in the Silo	8E5	Maul (2000)
R_TunnelLength	- (m)	Vault lengths	160	SKB R-01-14
R_VaultFlowStartTime	t_{start} (y)	Time when Vault barriers start to degrade physically and allow water to flow	0	Postulated value
R_VaultPhysDegradation	- (y)	Time for Vault barriers completely to degrade physically	1000	Postulated value
R_VaultStage2	- (y)	Time when Stage II of cement evolution starts in the Vaults	1000	Postulated value
R_VaultStage3	- (y)	Time when Stage III of cement evolution starts in the Vaults	50 000	Postulated value
R_V_{free}	V_{free} (m^3)	Volume of free water in the Silo	1410	Maul (2000)
R_Vr	V_r (Nm^3)	Initial gas volume present in the Silo	500	Maul (2000)
R_f0	f_0 (-)	Initial fractional flow through repositories compared with surrounding rock	0 (all vaults)	Postulated value
R_f1	f_1 (-)	Final fractional flow through repositories compared with surrounding rock	2 (all vaults)	Postulated value
R_tau	τ (y)	Gas generation timescale for the Silo	2000	Maul (2000)
Solubility	c^{sol} (moles m^{-3})	Elemental solubility limits	See Elemental Properties Table A8	SKI vault database SKB R-01-14
Volumes	V (m^3)	Compartment volumes	See Compartment Properties Table A10	
WellDilutionFactor	W (-)	Dilution of contaminated groundwater	300	Assumes a well pumping rate of around 1E4 m^3 y^{-1}
g	g ($m\ s^{-2}$)	Acceleration due to gravity	9.8	Standard constant
pi	π (-)		3.1415927	Standard constant

Table A6 *Radionuclide-specific Parameters*

Radionuclide	**Ingestion Dose Factor** **(Sv Bq^{-1})**	**Inhalation Dose Factor** **(Sv Bq^{-1})**	**External Irradiation** **(Sv kg y^{-1} Bq^{-1})**
H-3	1.8E-11	4.5E-11	0
C-14 organic	5.8E-10	2.0E-9	3.6E-12
C-14 inorganic	5.8E-10	2.0E-9	3.6E-12
C gas	-	6.4E-14	-
Cl-36	9.3E-10	7.3E-9	6.5E-10
Co-60	3.5E-9	1.0E-8	4.4E-6
Ni-59	6.3E-11	1.3E-10	0
Ni-63	1.5E-10	4.8E-10	0
Se-79	2.9E-9	1.1E-9	5.0E-12
Sr-90	3.4E-8	3.8E-8	6.7E-9
Zr-93	1.1E-9	1.0E-8	0
Nb-93m	1.2E-10	1.8E-9	2.8E-11
Nb-94	1.7E-9	4.9E-8	2.6E-6
Mo-93	3.1E-9	2.3E-9	1.6E-10
Tc-99	6.4E-10	4.0E-8	3.4E-11
Pd-107	5.5E-10	3.7E-10	0
Ag-108m	2.3E-9	3.7E-8	0
Cd-113m	2.3E-8	3.1E-8	0
Sn-126	5.5E-9	2.8E-8	3.2E-6
I-129	1.1E-7	3.6E-8	3.5E-9
Cs-135	2.E-9	6.9E-10	1.0E-11
Cs-137	1.3E-8	4.6E-9	9.2E-7

Radionuclide	Ingestion Dose Factor ($Sv\ Bq^{-1}$)	Inhalation Dose Factor ($Sv\ Bq^{-1}$)	External Irradiation ($Sv\ kg\ y^{-1}\ Bq^{-1}$)
Sm-151	9.8E-11	4.0E-9	2.7E-13
Eu-152	1.4E-9	4.2E-8	1.9E-6
Eu-154	2.0E-9	5.3E-8	2.1E-6
Ho-166m	2.0E-9	1.2E-7	1.9E-6
Po-210	1.2E-6	1.2E-6	1.4E-11
Pb-210	6.9E-7	3.3E-6	1.6E-9
Ra-226	2.8E-7	3.5E-6	3.0E-6
Ra-228	6.9E-7	2.6E-5	1.6E-6
Th-228	2.1E-7	4.0E-5	2.7E-6
Th-229	7.3E-7	8.6E-5	4.3E-7
Th-230	2.1E-7	1.4E-5	3.3E-10
Th-232	2.3E-7	2.5E-5	1.4E-10
Ac-227	1.3E-6	5.7E-4	5.4E-7
Pa-231	7.1E-7	1.4E-4	5.2E-8
Pa-233	8.7E-10	3.9E-9	2.8E-7
U-233	5.1E-8	3.6E-6	3.8E-10
U-234	4.9E-8	3.5E-6	1.1E-10
U-235	4.7E-8	3.1E-6	2.0E-7
U-236	4.7E-8	3.2E-6	5.8E-11
U-238	4.8E-8	2.9E-6	4.1E-8
Np-237	1.1E-7	2.5E-5	3.0E-7
Pu-238	2.3E-7	4.6E-5	4.1E-11
Pu-239	2.5E-7	5.0E-5	8.0E-11
Pu-240	2.5E-7	5.0E-5	4.0E-11
Pu-241	4.8E-9	9.0E-7	5.1E-12

Radionuclide	Ingestion Dose Factor ($Sv\ Bq^{-1}$)	Inhalation Dose Factor ($Sv\ Bq^{-1}$)	External Irradiation ($Sv\ kg\ y^{-1}\ Bq^{-1}$)
Pu-242	2.4E-7	4.8E-5	3.5E-11
Am-241	2.0E-7	9.6E-5	1.2E-8
Am-242m	1.9E-7	9.2E-5	1.8E-8
Am-243	2.0E-7	9.6E-5	2.4E-7
Cm-244	1.2E-7	5.7E-5	3.4E-11

Ingestion and Inhalation factors are taken from IAEA(1996).
External Irradiation factors are taken from Eckerman and Ryman (1993)

Table A7 *Equilibrium Sorption Parameters*

Element	Bentonite	Sand	Sand/ Bentonite	Cement	Concrete	Rock	Soil	Lake Sediment	Marine Sediment
H	0	0	0	0	0	0	0	0	0
C (organic)	0	0	0	0	0	0	0	0	0
C (inorganic)	0	0	0	0.5, 0.5, 0.01	0.5, 0.5, 0.01	0.001	0.001	0.001	0.001
Cl	0	0	0	0.006	0.006	0	0.001	1	0.001
Fe	0.1	0.04	0.05	0.1, 0.1, 0.01	0.1	0.02	10	10	10
Ni	0.1	0.04	0.05	0.1, 0.1, 0.01	0.1	0.02	10	10	10
Co	0.1	0.04	0.05	0.1, 0.1, 0.01	0.1	0.02	1	1	1
Se	0	0.0005	0.0005	0.006	0.006	0.001	0.01	5	5
Sr	0.01	0.001	0.002	0.005	0.005	0.0002	0.1	0.1	0.05
Zr	0.05	0.5	0.5	0.5	0.5	1.0	1	1	50
Mo	0	0	0	0.006	0.006	0	0.1	0.001	0.001
Nb	0.2	0.05	0.065	0.5,0.5,0.1	0.5,0.5,0.1	1.0	10	10	10
Tc	0.1	0.05	0.06	1	1	1	0.1	0.1	0.05
Pd	0	0.001	0.0009	0.04	0.04	0.01	0.2	2	10
Ag	0	0.01	0.009	0.001	0.001	0.05	0.1	2	1
Cd	0.02	0.01	0.01	0.04	0.04	0.02	0.1	0.1	5
Sn	0.01	0	0.001	0.5	0.5	0.001	0.1	50	50
I	0	0	0	0.02,0.02,0.01	0.02,0.02,0.01	0	0.1	0.1	0.05
Cs	0.05	0.001	0.006	0.001,0.001,0.005	0.001,0.001,0.005	0.05	5	5	3
Sm	0.2	1	0.9	5	5	0.2	1	5	100
Eu	0.2	1	0.9	5	5	2	10	0.5	10
Ho	0.2	1	0.9	5	5	2	1	0.3	0.1
Pb	0.5	0.05	0.1	0.5,0.5,0.1	0.5,0.5,0.1	1	10	10	10

Element	Bentonite	Sand	Sand/ Bentonite	Cement	Concrete	Rock	Soil	Lake Sediment	Marine Sediment
Po	0.5	0.05	0.1	0.5,0.5,0.1	0.5,0.5,0.1	1	10	10	10
Ra	0.01	0.003	0.004	0.05	0.05	0.02	10	10	10
Ac	3	1	1	0.25,0.25,0.05	5,5,1	3	10	10	10
Th	3	1	1	0.25,0.25,0.05	5,5,1	5	10	10	10
Pa	0.3	0.1	0.1	0.5,0.5,0.1	0.5,0.5,0.1	1	10	10	10
Np	3	1	1	5,5,1	5,5,1	5	10	10	10
U	1	1	1	5,5,1	5,5,1	5	10	10	10
Pu	3	0.5	0.75	0.25	5,5,1	5	10	10	10
Am	3	1	1	0.25,0.25,0.05	5,5,1	3	10	10	10
Cm	3	1	1	0.25,0.25,0.05	5,5,1	3	10	10	10

All values are in units of $m^3 kg^{-1}$

Where 3 values are given for Kd values for cement and concrete, these refer to the 3 stages of chemical degradation

Redox-sensitive values for Tc, U and Np are assumed to be for reducing conditions

All data taken from the SKI vault database (Savage and Stenhouse, 2001)

Table A8 *Element-specific Parameters*

Element	**Solubility (moles m^{-3})**	**Concentration Factor for Lake Fish (m^3 kg^{-1})**	**Concentration Factor for Sea Fish (m^3 kg^{-1})**
H	unlimited	0.001	0.001
C (organic)	0.07	9	20
C (inorganic)	0.07	9	20
Cl	unlimited	0.05	0.001
Fe	0.02	0.1	0.3
Ni	0.02	0.1	0.3
Co	0.02	0.3	1
Se	unlimited	2	4
Sr	0.1	0.06	0.002
Zr	0.1	0.2	0.1
Mo	unlimited	0.01	0.01
Nb	unlimited	0.3	0.01
Tc	4E-5	0.01	0.03
Pd	3E-4	0.1	0.01
Ag	unlimited	0.005	0.5
Cd	1	0.02	0.2
Sn	unlimited	3	1
I	unlimited	0.03	0.01
Cs	unlimited	2	0.2
Sm	unlimited	0.025	0.03
Eu	unlimited	0.05	0.1
Ho	unlimited	0.025	0.025

Element	Solubility (moles m^{-3})	Concentration Factor for Lake Fish (m^3 kg^{-1})	Concentration Factor for Sea Fish (m^3 kg^{-1})
Pb	1E-3	0.3	0.2
Po	unlimited	0.05	2
Ra	1E-3	0.05	0.5
Ac	3E-6	0.8	0.05
Th	6E-7	0.03	0.6
Pa	2E-5	0.01	0.05
Np	5E-6	0.01	0.01
U	1E-5	0.01	0.001
Pu	1E-7	0.004	0.04
Am	2E-6	8e-5	0.05
Cm	2E-6	0.03	0.05

Data for Solubilities taken from the highest values in the SKI vault database (Savage and Stenhouse, 2001). For elements not included in the database, values have been taken from SKB R-01-14 (SKB, 2001).

Concentration Factor data taken from a review of a number of studies. Data for Cl, Ni, Se, Zr, Mo, Pd, Ag, Cd, Sn, Sm, Eu, Ho and Cm taken from SKB R-01-14 (SKB, 2001).

Table A9 *Material-specific Parameters*

	Bentonite	Sand	Sand/ Bentonite	Cement	Concrete	Rock	Soil	Lake Sediment	Marine Sediment
Bulk Density ($kg\ m^{-3}$)	2070	1855	1065	1200,1200,960	2100, 2100, 1800	2697	1600	1600	1600
Porosity	0.25	0.3	0.6	0.5,0.5,0.6	0.125, 0.125, 0.25	0.005	0.4	0.4	0.4
Effective Diffusivity ($m^2\ y^{-1}$)	0.003	0.02	0.003	0.02	8E-5, 8E-4, 4E-3	2E-6	-	-	-

Where 3 values are given for values for cement and concrete, these refer to the 3 stages of chemical degradation

Values are from SKI vault database (Savage and Stenhouse, 2001) and SFR 87-10

Table A10 *Compartment Properties*

Compartment	Description	Sub-Model	Material	Height (m)	Length (m)	Area (m^2)	Volume (m^3)	Comment/Data Source
R_Silo_Waste	Silo Waste	Silo Engineering	Cement	1.0	1.0	67 500	9000	SFR 87-09
R_Silo_Package	Silo Waste Packages	Silo Engineering	Concrete	0.1	0.1	97 000	9000	SFR 87-09
R_Silo_PorousConcrete	Silo Porous Concrete	Silo Engineering	Cement	51	26	-	3500	SFR 87-09
R_Silo_InternalWalls	Silo Internal Walls	Silo Engineering	Concrete	51	0.2	35000	3500	SFR 87-09
R_Silo_Bentonite_left	Left half of Silo bentonite	Silo Engineering	Bentonite	53	1.2	geometry	geometry	
R_Silo_Bentonite_right	Right half of Silo bentonite	Silo Engineering	Bentonite	53	1.2	geometry	geometry	
R_Silo_Wall_left	Left half of Silo wall	Silo Engineering	Concrete	53	0.8	geometry	geometry	
R_Silo_Wall_right	Right half of Silo wall	Silo Engineering	Concrete	53	0.8	geometry	geometry	
R_Silo_Bottom	Silo Bottom	Silo Engineering	Concrete	1.0	28	geometry	geometry	
R_Silo_Lid	Silo Lid	Silo Engineering	Concrete	1.0	28	geometry	geometry	
R_Silo_Base	Silo Base	Silo Engineering	Sand/Bentonite	1.5	28	geometry	geometry	
R_Silo_Cover	Silo Cover	Silo Engineering	Sand/Bentonite	1.5	32	geometry	geometry	
R_Silo_Backfill	Silo Backfill	Silo Engineering	Sand	10	32	geometry	6000	SFR 87-09
R_BMA_Waste	BMA Waste	BMA Engineering	Cement	1.0	1.0	45 000	8 723	SFR 87-09
R_BMA_Package	BMA Waste Packages	BMA Engineering	Concrete	7.3	15	-	5 127	SFR 87-09
R_BMA_Sand_left	Left half of BMA sand	BMA Engineering	Sand	8.5	2	geometry	geometry	
R_BMA_Sand_right	Right half of BMA sand	BMA Engineering	Sand	8.5	2	geometry	geometry	
R_BMA_Wall_left	Left half of BMA wall	BMA Engineering	Concrete	7.3	0.4	geometry	geometry	
R_BMA_Wall_right	Right half of BMA wall	BMA Engineering	Concrete	7.3	0.4	geometry	geometry	
R_BMA_Lid	BMA Lid	BMA Engineering	Concrete	0.95	16	1900	geometry	SFR 87-09
R_BMA_Base	BMA Base	BMA Engineering	Concrete	0.25	16	1900	geometry	SFR 87-09
R_BMA_Backfill	BMA Backfill	BMA Engineering	-	8	20	1900	17 420	SFR 87-09

Compartment	Description	Sub-Model	Material	Height (m)	Length (m)	Area (m^2)	Volume (m^3)	Comment/Data Source
R_BTF1_Waste	1BTF Waste	1BTF Engineering	Cement	2.0	3.0	17380	4700	Same for 2BTF
R_ BTF1_Package	1BTF Waste Packages	1BTF Engineering	Concrete	4.6	13.2	-	3200	" "
R_BMA_Wall_left	Left half of BTF1 wall	1BTF Engineering	Concrete	5.7	0.4	geometry	geometry	" "
R_ BTF1_Wall_right	Right half of BTF1 wall	1BTF Engineering	Concrete	5.7	0.4	geometry	geometry	" "
R_ BTF1_Lid	BTF1 Lid	1BTF Engineering	Concrete	0.4	15	geometry	geometry	" "
R_ BTF1_Base	BTF1 Base	1BTF Engineering	Concrete	0.4	15	geometry	geometry	" "
R_ BTF1_Backfill	BTF1 Backfill	1BTF Engineering	Sand	3.8	15	geometry	geometry	" "
R_BLA_Waste	BLA Waste	BLA Engineering	Cement	4.6	15	-	geometry	
R_ BLA _Backfill	BLA Backfill	BLA Engineering	-	3.8	15	-	geometry	
R_AL_Silo	NF rock above left of Silo	Silo NF Rock	Rock	26.5	50	-	geometry	
R_A_Silo	NF rock above Silo	Silo NF Rock	Rock	26.5	30	-	geometry	
R_AR_Silo	NF rock above right of Silo	Silo NF Rock	Rock	26.5	220	-	geometry	
R_R_Silo	NF rock right of Silo	Silo NF Rock	Rock	69	220	-	geometry	
R_BR_Silo	NF rock below right of Silo	Silo NF Rock	Rock	50	220	-	geometry	
R_B_Silo	NF rock below Silo	Silo NF Rock	Rock	50	30	-	geometry	
R_BL_Silo	NF rock below left of Silo	Silo NF Rock	Rock	50	50	-	geometry	
R_L_Silo	NF rock left of Silo	Silo NF Rock	Rock	69	50	-	geometry	
R_AL_BMA	NF rock above left of BMA	BMA NF Rock	Rock	10	15	-	geometry	
R_A_ BMA	NF rock above BMA	BMA NF Rock	Rock	10	20	-	geometry	
R_AR_ BMA	NF rock above right of BMA	BMA NF Rock	Rock	10	15	-	geometry	
R_R_ BMA	NF rock right of BMA	BMA NF Rock	Rock	16.5	15	-	geometry	
R_BR_ BMA	NF rock below right of BMA	BMA NF Rock	Rock	120	15	-	geometry	

Compartment	Description	Sub-Model	Material	Height (m)	Length (m)	Area (m^2)	Volume (m^3)	Comment/Data Source
R_B_ BMA	NF rock below BMA	BMA NF Rock	Rock	120	20	-	geometry	
R_BL_ BMA	NF rock below left of BMA	BMA NF Rock	Rock	120	20	-	geometry	
R_L_ BMA	NF rock left of BMA	BMA NF Rock	Rock	16.5	15	-	geometry	
R_AL_BTF1	NF rock above left of BTF1	1BTF NF Rock	Rock	17	30	-	geometry	
R_A_ BTF1	NF rock above BTF1	1BTF NF Rock	Rock	17	45	-	geometry	
R_AR_ BTF1	NF rock above right of BTF1	1BTF NF Rock	Rock	17	140	-	geometry	
R_R_ BTF1	NF rock right of BTF1	1BTF NF Rock	Rock	11	140	-	geometry	
R_BR_ BTF1	NF rock below right of BTF1	1BTF NF Rock	Rock	120	140	-	geometry	
R_B_ BTF1	NF rock below BTF1	1BTF NF Rock	Rock	120	45	-	geometry	
R_BL_ BTF1	NF rock below left of BTF1	1BTF NF Rock	Rock	120	45	-	geometry	
R_L_ BTF1	NF rock left of BTF1	1BTF NF Rock	Rock	11	30	-	geometry	
R_AL_BTF2	NF rock above left of BTF2	2BTF NF Rock	Rock	17	15	-	geometry	
R_A_ BTF2	NF rock above BTF2	2BTF NF Rock	Rock	17	45	-	geometry	
R_AR_ BTF2	NF rock above right of BTF2	2BTF NF Rock	Rock	17	80	-	geometry	
R_R_ BTF2	NF rock right of BTF2	2BTF NF Rock	Rock	11	80	-	geometry	
R_BR_ BTF2	NF rock below right of BTF2	2BTF NF Rock	Rock	120	80	-	geometry	
R_B_ BTF2	NF rock below BTF2	2BTF NF Rock	Rock	120	45	-	geometry	
R_BL_ BTF2	NF rock below left of BTF2	2BTF NF Rock	Rock	120	45	-	geometry	
R_L_ BTF2	NF rock left of BTF2	2BTF NF Rock	Rock	11	15	-	geometry	
R_AL_BLA	NF rock above left of BLA	BLA NF Rock	Rock	14	15	-	geometry	
R_A_ BLA	NF rock above BLA	BLA NF Rock	Rock	14	15	-	geometry	
R_AR_ BLA	NF rock above right of BLA	BLA NF Rock	Rock	14	50	-	geometry	
R_R_ BLA	NF rock right of BLA	BLA NF Rock	Rock	14.5	50	-	geometry	

Compartment	Description	Sub-Model	Material	Height (m)	Length (m)	Area (m^2)	Volume (m^3)	Comment/Data Source
R_BR_ BLA	NF rock below right of BLA	BLA NF Rock	Rock	120	50	-	geometry	
R_B_ BLA	NF rock below BLA	BLA NF Rock	Rock	120	15	-	geometry	
R_BL_ BLA	NF rock below left of BLA	BLA NF Rock	Rock	120	15	-	geometry	
R_L_ BLA	NF rock left of BLA	BLA NF Rock	Rock	14.5	15	-	geometry	
G_Rock_13	Fractures in block 13	Geosphere	Water	15	300	-	geometry	
G_Matrix_13	Rock in block 13	Geosphere	Rock	15	300	-	geometry	
G_ Rock _14	Fractures in block 14	Geosphere	Water	15	300	-	geometry	
G_Matrix_14	Rock in block 14	Geosphere	Rock	15	300	-	geometry	
G_ Rock _21	Fractures in block 21	Geosphere	Water	120	500	-	geometry	
G_Matrix_21	Rock in block 21	Geosphere	Rock	120	500	-	geometry	
G_ Rock _22	Fractures in block 22	Geosphere	Water	20	500	-	geometry	
G_Matrix_22	Rock in block 22	Geosphere	Rock	20	500	-	geometry	
G_ Rock _23	Fractures in block 23	Geosphere	Water	15	500	-	geometry	
G_Matrix_23	Rock in block 23	Geosphere	Rock	15	500	-	geometry	
G_ Rock _31	Fractures in block 31	Geosphere	Water	120	500	-	geometry	
G_Matrix_31	Rock in block 31	Geosphere	Rock	120	500	-	geometry	
G_ Rock _32	Fractures in block 32	Geosphere	Water	20	500	-	geometry	
G_Marix_32	Rock in block 32	Geosphere	Rock	20	500	-	geometry	
G_ Rock _41	Fractures in block 41	Geosphere	Water	120	500	-	geometry	
G_Matrix_41	Rock in block 41	Geosphere	Rock	120	500	-	geometry	
I_TopRock1	Rock in Region 1	Terrestrial Bios.	Rock	2.4	300	-	geometry	
I_LowerSediments1	Lower Sediments in Region 1	Terrestrial Bios.	Soil	0.3	300	-	geometry	
I_UpperSediments1	Upper Sediments in Region 1	Terrestrial Bios.	Soil	0.3	300	-	geometry	
I_TopRock2	Rock in Region 2	Terrestrial Bios.	Rock	2.4	500	-	geometry	

Compartment	Description	Sub-Model	Material	Height (m)	Length (m)	Area (m^2)	Volume (m^3)	Comment/Data Source
I_LowerSediments2	Lower Sediments in Region 2	Terrestrial Bios.	Soil	0.3	500	-	geometry	
I_UpperSediments2	Upper Sediments in Region 2	Terrestrial Bios.	Soil	0.3	500	-	geometry	
I_TopRock3	Rock in Region 3	Terrestrial Bios.	Rock	2.4	500	-	geometry	
I_LowerSediments3	Lower Sediments in Region 3	Terrestrial Bios.	Soil	0.3	500	-	geometry	
I_UpperSediments3	Upper Sediments in Region 3	Terrestrial Bios.	Soil	0.3	500	-	geometry	
I_TopRock4	Rock in Region 4	Terrestrial Bios.	Rock	2.4	500	-	geometry	
I_LowerSediments4	Lower Sediments in Region 4	Terrestrial Bios.	Soil	0.3	500	-	geometry	
I_UpperSediments4	Upper Sediments in Region 4	Terrestrial Bios.	Soil	0.3	500	-	geometry	
I_Lake	Lake	Terrestrial Bios.	Water	1.4	1000	1.6E5	geometry	
House	House	Terrestrial Bios.	Air	8	10	100	geometry	
B_RegionalWaters	Regional waters	Marine Biosphere	Water	7.5	-	2.3E8	geometry	
B_RegionalSediment	Regional sediments	Marine Biosphere	Mar.Sediment	0.3	-	2.3E8	geometry	
B_RegionalDeepSediment	Regional deep sediments	Marine Biosphere	Mar.Sediment		-	2.3E8	-	Effective sink
B_Baltic	Baltic waters	Marine Biosphere	Water	56	-	3.8E11	geometry	
B_ BalticSediment	Baltic sediments	Marine Biosphere	Mar.Sediment	0.3	-	3.8E11	geometry	
B_ BalticDeepSediment	Baltic deep sediments	Marine Biosphere	Mar.Sediment	-	-	3.8E11	-	Effective sink
B_Oceans	Oceans	Marine Biosphere	Water	-	-	-	-	Effective sink

Table A11 *Radionuclide Inventory used in Final Calculations*

Radionuclide	Silo	BMA	1BTF	2BTF	BLA
H-3	5.8E11	3.3E10	3.3E9	5.3E9	6.6E8
C-14 inorganic	2.0E13	1.9E12	2.3E12	2.7E11	3.9E10
C-14 organic	1.8E12	1.7E11	1.8E11	3.0E10	3.3E7
Cl-36	4.7E10	3.4E9	3.0E8	5.4E8	8.2E7
Co-60	1.8E15	7.1E13	5.4E12	9.1E12	1.0E12
Ni-59	2.1E13	2.1E12	1.8E11	3.0E11	3.9E10
Ni-63	3.6E15	3.2E14	2.9E13	4.7E13	6.2E12
Se-79	1.9E10	1.4E9	1.2E8	2.2E8	3.3E7
Sr-90	2.4E14	1.4E13	1.3E12	2.3E12	3.6E11
Zr-93	2.1E10	2.1E9	1.8E8	3.0E8	3.9E7
Nb-93m	7.6E12	4.9E11	4.7E10	7.6E10	9.7E9
Nb-94	2.1E11	2.1E10	1.8E9	3.0E9	3.9E8
Mo-93	1.1E11	1.0E10	9.1E8	1.5E9	1.9E8
Tc-99	2.4E13	1.7E12	1.5E11	2.7E11	4.1E10
Pd-107	4.7E9	3.4E8	3.0E7	5.4E7	8.2E6
Ag-108m	1.2E12	1.2E11	1.0E10	1.7E10	2.2E9
Cd-113m	8.2E11	3.6E10	3.6E9	6.4E9	1.0E9
Sn-126	2.4E9	1.7E8	1.5E7	2.7E7	4.1E6
I-129	1.4E9	1.0E8	9.1E6	1.6E7	2.5E6
Cs-135	2.4E10	1.7E9	1.5E8	2.7E8	4.1E7
Cs-137	2.5E15	1.4E14	1.4E13	2.4E13	3.7E12
Sm-151	1.1E13	7.5E11	6.9E10	1.2E11	1.9E10
Eu-152	9.2E10	4.0E9	4.4E11	7.1E8	1.1E8
Eu-154	7.9E13	2.7E12	2.8E11	4.8E11	7.6E10
Ho-166m	8.4E10	8.2E9	7.2E8	1.2E9	1.5E8
U-232	2.0E7	1.1E6	8.1E4	6.3E4	6.1E4
U-234	8.4E8	4.5E7	3.5E6	2.7E6	2.5E6
U-235	1.7E7	8.9E5	7.1E4	5.4E4	5.1E4
U-236	2.5E8	1.3E7	1.1E6	8.2E5	7.6E5
U-238	3.3E8	1.8E7	1.4E6	1.1E6	1.0E6
Np-237	3.3E8	1.8E7	1.4E6	1.1E6	1.0E6
Pu-238	2.8E12	1.5E11	1.1E10	8.9E9	8.5E9
Pu-239	2.8E11	1.5E10	1.2E9	9.1E8	8.5E8
Pu-240	5.6E11	3.0E10	2.4E9	1.8E9	1.7E9
Pu-241	3.1E13	1.6E12	1.0E11	8.2E10	8.8E10
Pu-242	2.5E9	1.3E8	1.1E7	8.2E6	7.6E6
Am-241	6.1E12	4.3E10	3.4E9	2.6E9	2.5E9
Am-242m	7.5E9	4.0E8	3.1E7	2.4E7	2.3E7
Am-243	2.5E10	1.3E9	1.1E8	8.1E7	7.6E7
Cm-243	1.0E10	5.3E8	3.8E7	3.0E7	3.0E7
Cm-244	1.1E12	5.9E10	3.9E9	3.1E9	3.3E9

Radionuclide	Silo	BMA	1BTF	2BTF	BLA
Cm-245	2.5E8	1.3E7	1.1E6	8.1E5	7.6E5
Cm-246	6.7E7	3.6E6	2.8E5	2.2E5	2.0E5

Notes:

All units are Bq.

Data taken from SKB (2001).

C-14 inventory is assumed to be 10% organic and 90% inorganic.

Appendix B. Demonstration Calculations

B1 Introduction

In 1999 a number of Demonstration calculations were undertaken with the aim of reproducing with AMBER the key features of calculations undertaken by SKB at the time of the original authorisation of SFR 1 SKB, 1991). This work is reported in Maul et al. (1999).

The modelling undertaken at the time of the original safety case submission for SFR 1 considered two periods: the Saltwater Period, when fluxes of radionuclides to the biosphere entered the local marine environment, and the Inland Period, when radionuclides entered a lake or a well. The change occurred due to land rise resulting in changes in the surface environment. It should be noted that two separate sets of calculations were undertaken for the two different periods; no attempt was made to model the transition between the two cases.

The inventory used for these calculations is given in Table B1. This inventory was also used in the calculations describe in Appendices C and D.

B2 The AMBER Model

For the near-field, the models and data described by SKB (1987a and 1987b) provided the basis for the AMBER models. A very simple geosphere model was used, based on that employed by SSI (1989). The biosphere model employed was also taken from SSI (1989).

The Silo Model

Figure B1 shows the model that was used for the engineered parts of the Silo system. Compared with the general model described in Section 2, it can be seen that:

- The Silo Contents were represented as a single compartment; no distinctions were made between the waste, package and porous concrete;
- The Silo walls were represented as a single compartment;
- The Gas vents in the Silo lid were represented separately; and
- There was no backfill at the top.

Table B1 *Radionuclide Inventory of SFR 1 used in Preliminary Calculations*

Radionuclide	Silo	BTF	BMA	BLA
H-3	1.3E14			
C-14	6.8E12	1.3E11	2.9E11	2.6E9
Co-60	1.8E15	4.0E13	2.6E14	5.8E12
Fe-55	7.1E14	1.7E13	1.0E14	2.3E12
Ni-59	6.8E12	1.5E11	1.0E12	2.3E10
Ni-63	6.3E14	1.5E13	8.8E13	1.9E12
Sr-90	6.8E9	1.5E8	1.0E9	2.3E7
Nb-94	6.8E9	1.5E8	1.0E9	2.3E7
Tc-99	3.3E11	3.6E9	8.8E9	1.1E8
I-129	1.9E9	2.2E7	4.7E7	6.4E5
Cs-134	8.1E14	1.1E13	2.2E12	2.6E11
Cs-135	1.9E10	2.2E8	5.3E8	6.4E6
Cs-137	4.9E15	5.3E13	1.3E14	1.4E12
Pu-238	1.2E12	1.7E10	3.1E10	4.7E8
Pu-239	3.8E11	6.9E9	1.2E10	1.9E8
Pu-240	7.8E11	1.1E10	1.9E10	2.9E8
Pu-241	4.2E13	5.4E11	9.4E11	1.5E10
Am-241	1.0E12	1.3E10	2.4E10	3.8E8
Cm-244	1.2E11	1.5E9	2.8E9	4.4E8

Notes:

All units are Bq.

Data taken from SKB (1987b).

C-14 inventory is assumed to be 10% organic and 90% inorganic.

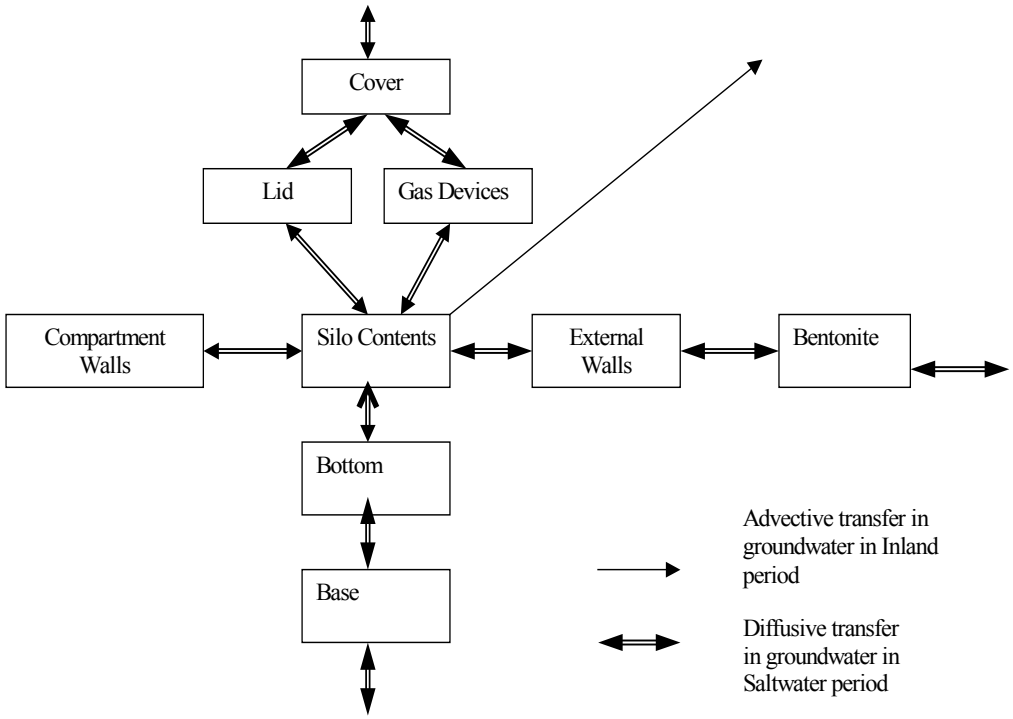

Figure B1 *The Silo Model used in the Demonstration Calculations*

Inside the Silo the compartment walls were assumed initially to be uncontaminated; these were represented in the AMBER model by a single compartment.

In the Saltwater Period, all the barriers were assumed to be intact, so that the only transport mechanisms are by diffusion.

The fluxes of radionuclides from the edge of the near-field (the bentonite buffer around the mantle (sides), and the sand and bentonite layers under the base and over the top of the Silo) into the geosphere depend upon the boundary conditions that are assumed. In the SKB calculations the diffusive flux of radionuclides F (Bq y^{-1}) across the boundary depended on the 'equivalent water flow rate', Φ (m^3 y^{-1}), assumed to be flowing past the relevant boundary and the radionuclide concentration c_g (Bq m^{-3}) in the groundwater:

$$F = \Phi c_g \qquad \text{(B1)}$$

In the AMBER modelling the flux was taken to depend linearly on the difference between c_g and c_n, the concentration in the relevant near-field compartment (Bq m^{-3}). One then has:

$$\Phi\, c_g \;=\; \frac{A\, D_e}{\Delta}(c_n - c_g) \qquad \text{(B2)}$$

where A is the area for the diffusive flux, D_e is the effective diffusion coefficient, and Δ is a diffusion length scale. Using this assumption the diffusive flux can be represented

$$F \;=\; \frac{\dfrac{A\, D_e}{\Delta}\, c_n}{1 + \dfrac{A\, D_e}{\Phi\, \Delta}} \qquad \text{(B3)}$$

The values used by SKB for the equivalent water flow rate were 2 $m^3\ y^{-1}$ for the top of the Silo, 0.064 $m^3\ y^{-1}$ for the mantle and 0.02 $m^3\ y^{-1}$ for the bottom of the Silo. These values are critical in determining the flux of radionuclides out of the near-field in the Saltwater Period.

In the Inland Period, the barriers were assumed to be ineffective and an advective transfer of radionuclides was initiated from the Silo to the geosphere depending on the assumed groundwater flux through the system.

Rock Vault for Intermediate Level Waste (BMA)

Figure B2 shows the model that was used for the engineered parts of the BMA system.

The contents of the vault (waste matrix, compartment construction and water inside the compartment) were assumed to act as a uniformly mixed ‘soup’; represented in the AMBER model by three compartments with rapid exchanges between the compartments to ensure that porewater concentrations are the same in each. Inside the vault the internal walls were assumed initially to be uncontaminated; these were represented in the AMBER model by a single compartment. The void space above at the top of the vault was assumed to be filled with water.

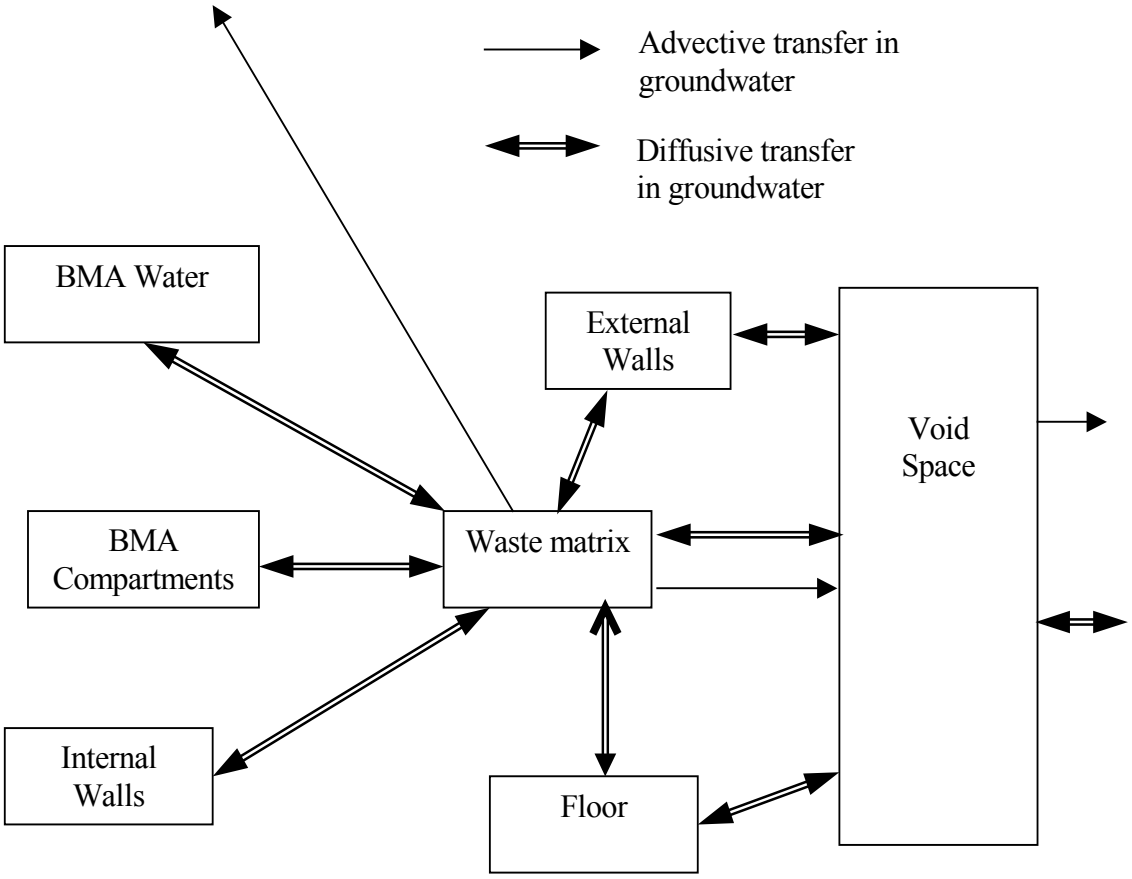

Figure B2 *The BMA Model used in the Demonstration Calculations*

Compared with the general model described in Section 2, it can be seen that the main differences are:

- Internal walls were directly represented;
- There was no representation of a lid;
- The BMA external walls were represented as a single well-mixed compartment;
- There was no representation of sand placed around the walls; and
- There was no representation of backfill above the BMA, with a void space being assumed.

Rock Vault for Concrete Tanks (BTF)

Figure B3 shows the model that was used for the engineered parts of the BTF vaults.

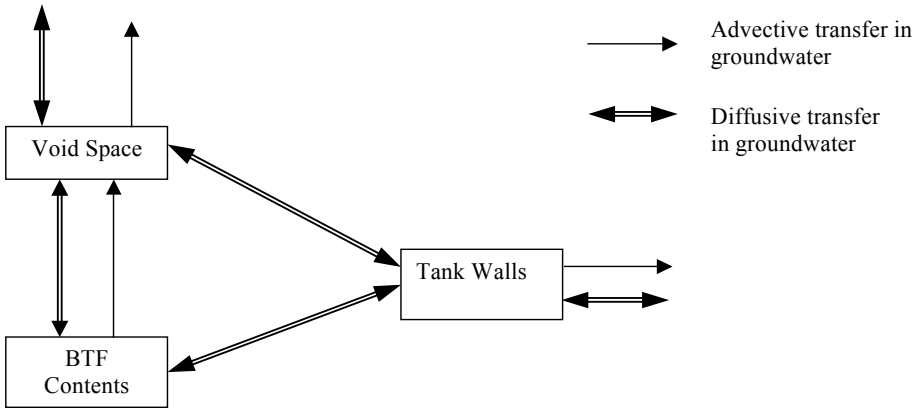

Figure B3 *The BTF Model used in the Demonstration Calculations*

The waste contents of the tanks were included in a single compartment. No sorption was assumed in this compartment, so the AMBER parameters reflect that water-filled volume available. The walls of the tanks were represented by a separate compartment. For a short period (taken to be 100 years) the sole release mechanism considered was diffusion through the tank walls directly into the geosphere. For that period the walls were assumed to have the properties of fresh concrete.

After the integrity of the tanks walls was assumed to breakdown, for the remainder of the Saltwater Period it was assumed that both diffusive and advective processes transport radionuclides into the water-filled void in the cavern. For this period the tank walls were assumed to have the properties of aged concrete.

In the Inland Period equilibrium was assumed between the tank internals, the tank walls and the void space. This was simulated in AMBER by rapid exchanges between the three compartments.

Compared with the general model described in Section 2, it can be seen that the main differences are:

- There was no representation of a lid;
- The external walls were represented as a single well-mixed compartment;
- There was no representation of backfill, with a void space being assumed.

Rock Vault for Low Level Waste (BLA)

This was the simplest model because a single compartment was used for all the BLA contents with no allowance for sorption, and advection was assumed to directly to the geosphere.

The Geosphere

In the safety assessments carried out at the time of the original safety submission for SFR 1, little credit was taken for the geosphere barrier. SSI (1989) assumed a simple transfer rate between the geosphere and the biosphere for all radionuclides of 0.003 y^{-1} in the Saltwater Period, and 0.0017 y^{-1} in the Inland Period. These simple assumptions were retained in the AMBER Case File.

The Biosphere

The Marine biosphere model used in the Demonstration calculations was very similar to that described in Section 2, although a Bothnian Sea compartment was included between the Regional Waters (Öregrundsgrepen) and the Baltic Sea. For the Inland Period a Lake was considered with similar characteristics to the Lake in the Terrestrial Biosphere sub-system described in Section 2.

In the Saltwater Period the release from the geosphere was assumed to enter the Öregrundsgrepen. In the Inland Period, the release from the geosphere was assumed to enter the Lake directly.

B3 Model Calculations

Some example calculations are shown here to illustrate the good correspondence between the AMBER model and the original SKB models.

Saltwater Period Releases

Figure B4 shows the total flux of radionuclides from the Silo near-field for the Saltwater Period. The general features of this Figure compare well with Figure 6.3 of SKB (1987b).

Figure B5 shows the fractional release rate of organic carbon from the Silo near-field for the Saltwater Period. This compares well with Figure 6.8 of the SKB (1987b).

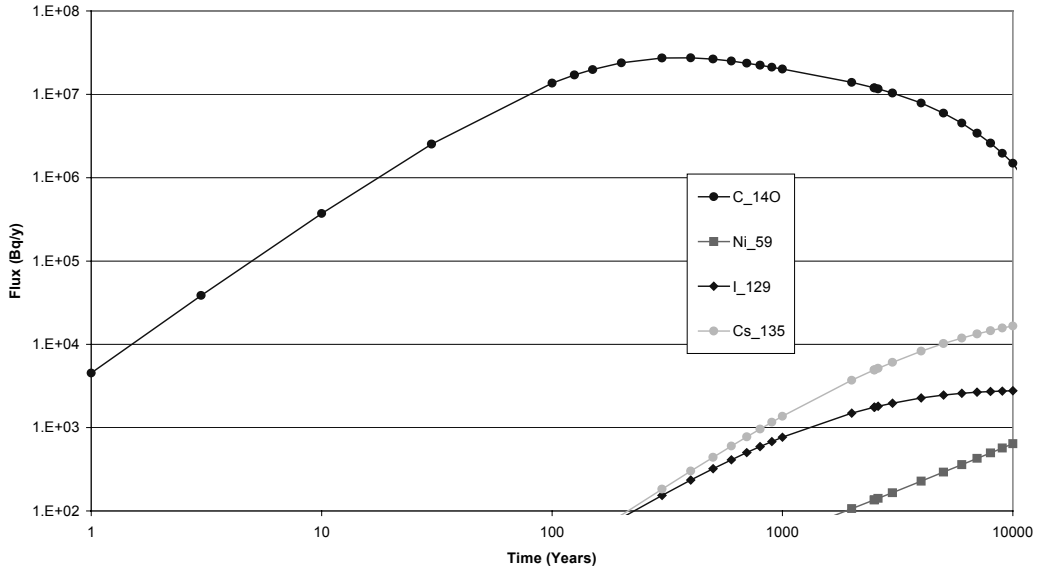

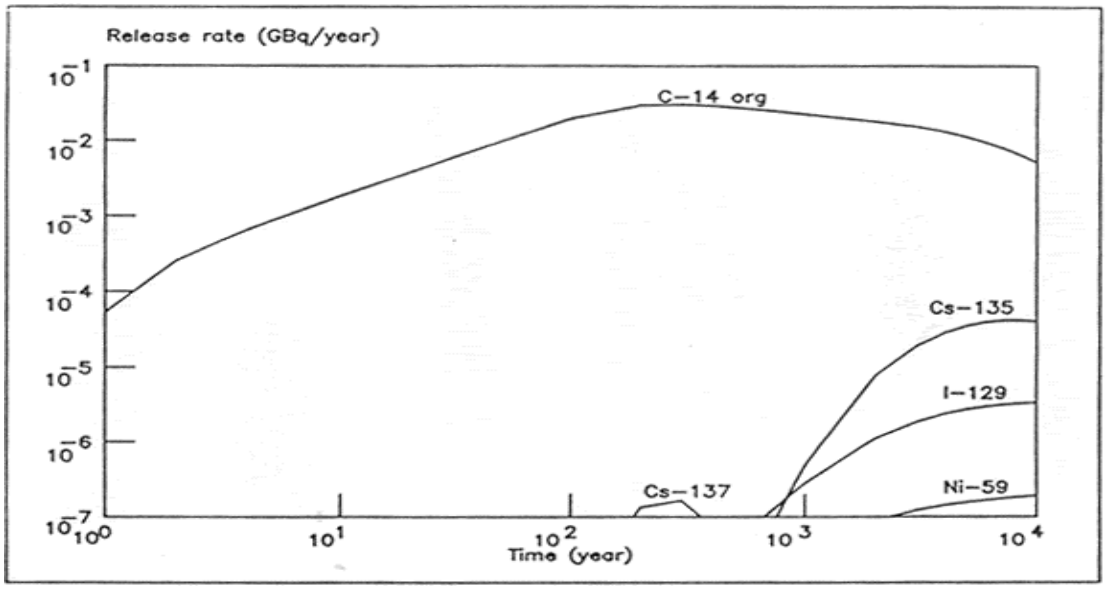

Figure B4 *Flux from the Silo in the Saltwater Period in the Demonstration Calculations*

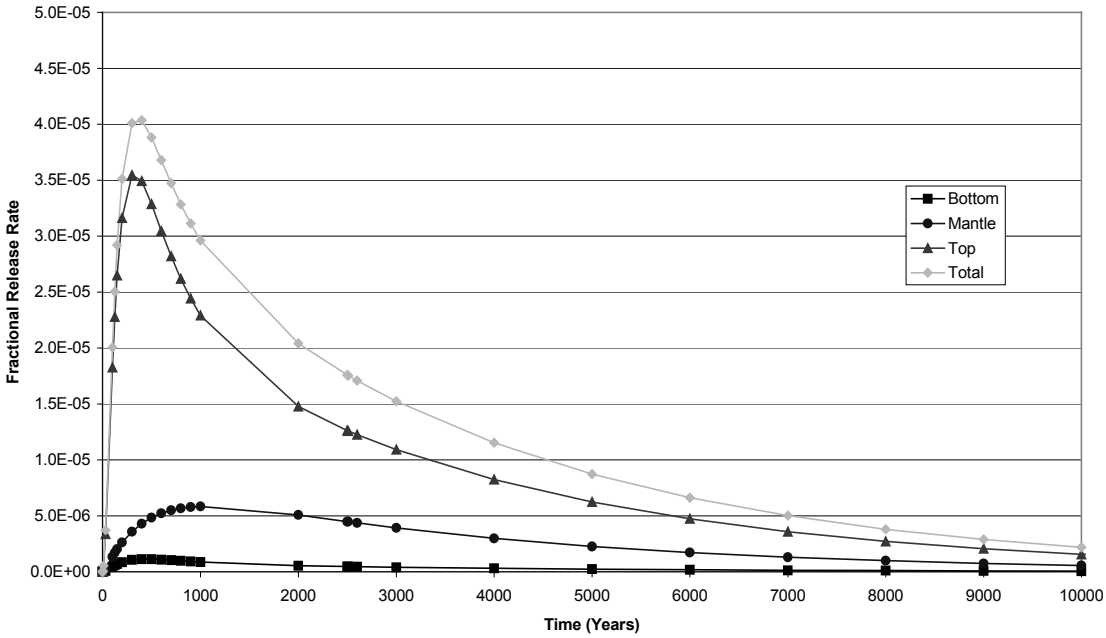

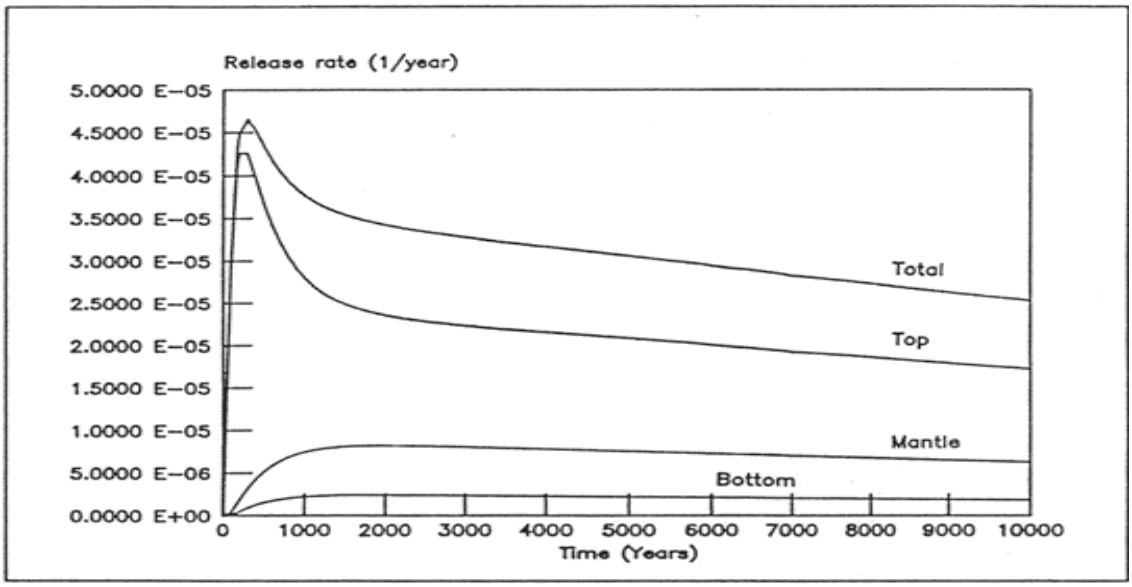

Figure B5 *Flux of Organic Carbon from the Silo in the Saltwater Period in the Demonstration Calculations*

Inland Period Releases

Figure B6 shows release rates from the Silo during the Inland Period for selected radionuclides. This is compared with Figure 6.13 of the SKB (1987b). The peak release rates of the key radionuclides are very similar.

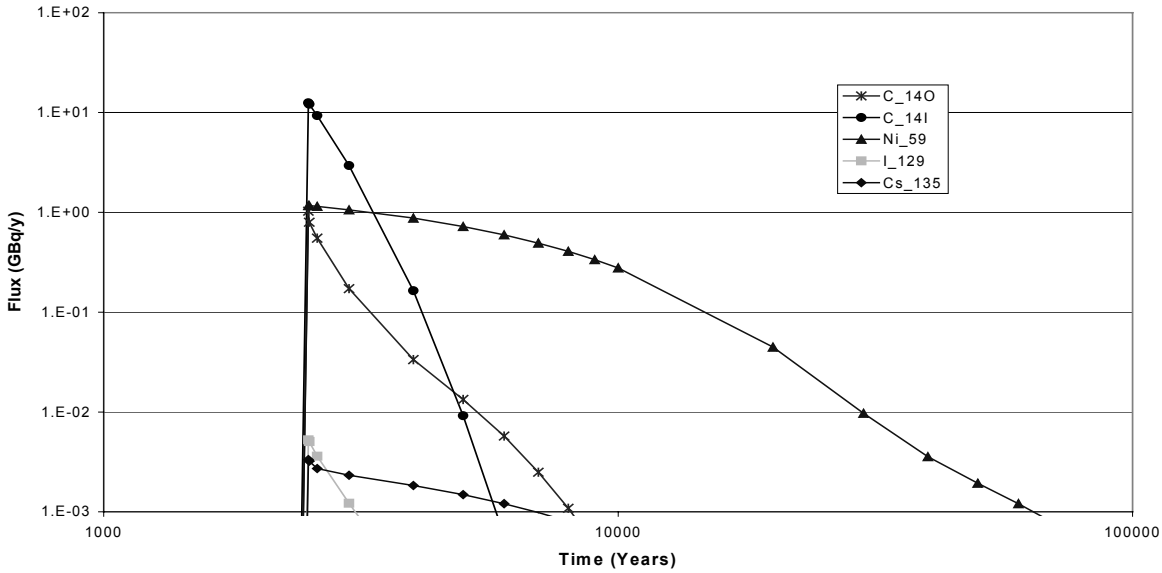

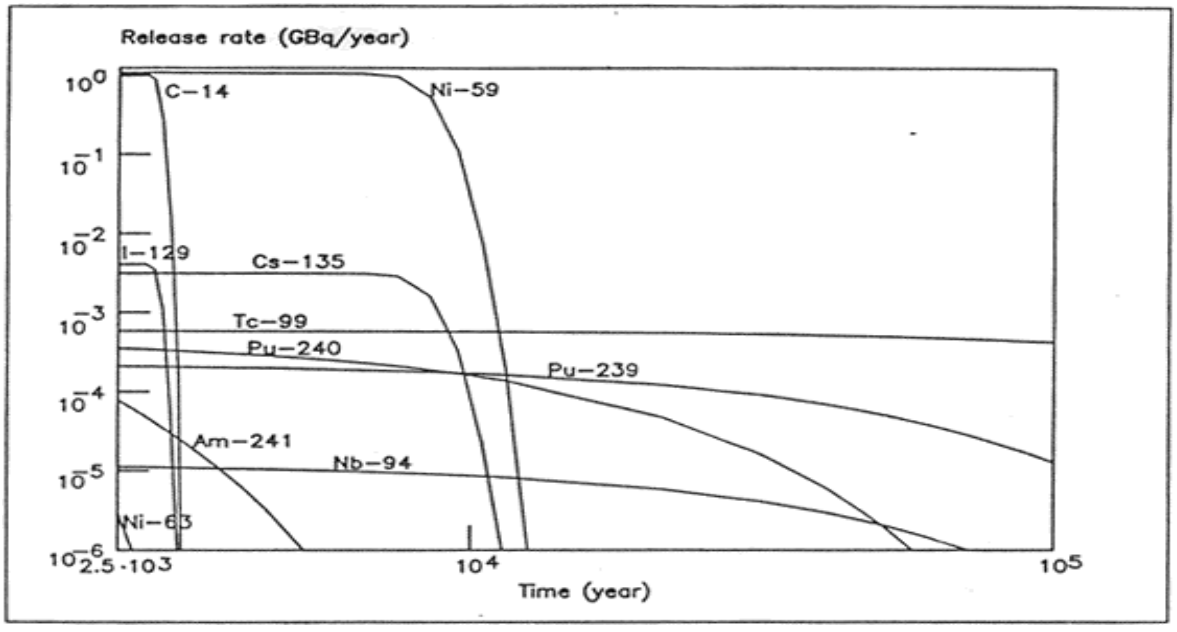

Figure B6 *Flux from the Silo in the Inland Period in the Demonstration Calculations*

For long-lived radionuclides that are assumed to be sorbed onto the degraded concrete (e.g., Tc-99, Pu-239 and Pu-240), the shapes of the curves are similar. For radionuclides that are not so strongly sorbed (e.g., organic C-14, Cs-135 and Ni-59), the shapes of the curves are rather different; the SKB calculation showed a 'flat' release rate followed by a rapid decay, whilst the AMBER calculations showed a more steady gradual reduction in release rate. This difference was due to the assumption in the AMBER calculations that radionuclides remain uniformly mixed throughout the Silo. In the SKB calculations the profile of radioactivity is initially uniform, but subsequently the profile becomes non-uniform due to the combined effects of advection from one end of the Silo and diffusion inside it. The SKB calculations could have been more closely simulated by splitting the AMBER compartments into a number of sub-compartments.

Total Releases

Figure B7 gives the total releases into the geosphere for each repository for the Saltwater Period. This compares well with Figure 10.1 of SKB (1987b); there are some detailed differences for relatively short timescales, but in the period 100 to 2500 years, the total releases are remarkably similar.

Figure B8 gives the corresponding total releases for the Inland Period. Again, these compare well with Figure 10.2 of SKB (1987b). The detailed differences in the shapes of the curves for the Silo are for the reasons previously discussed.

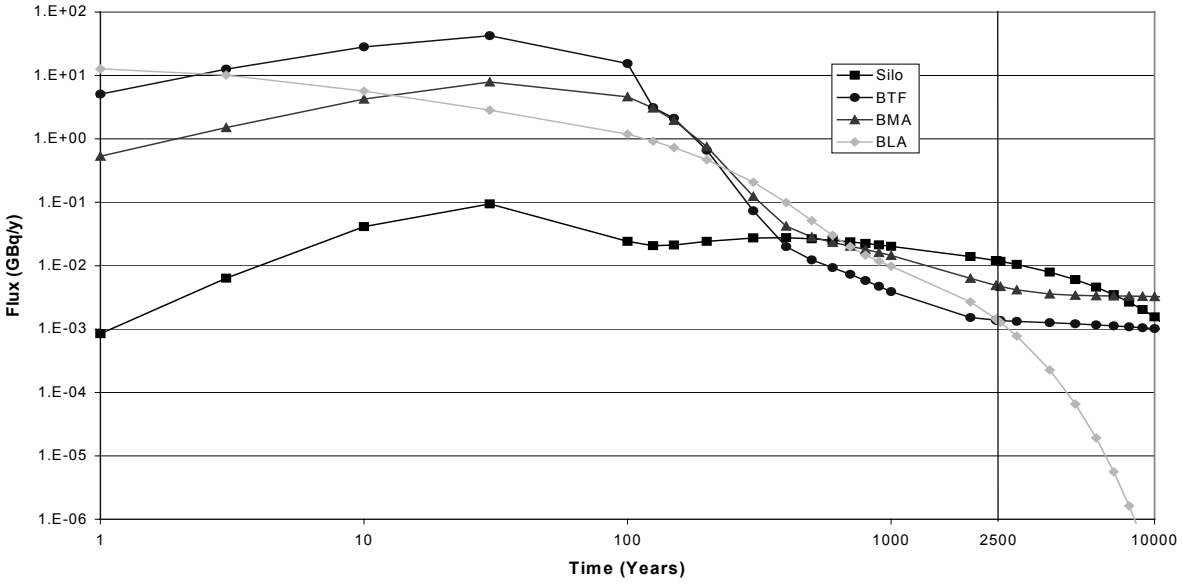

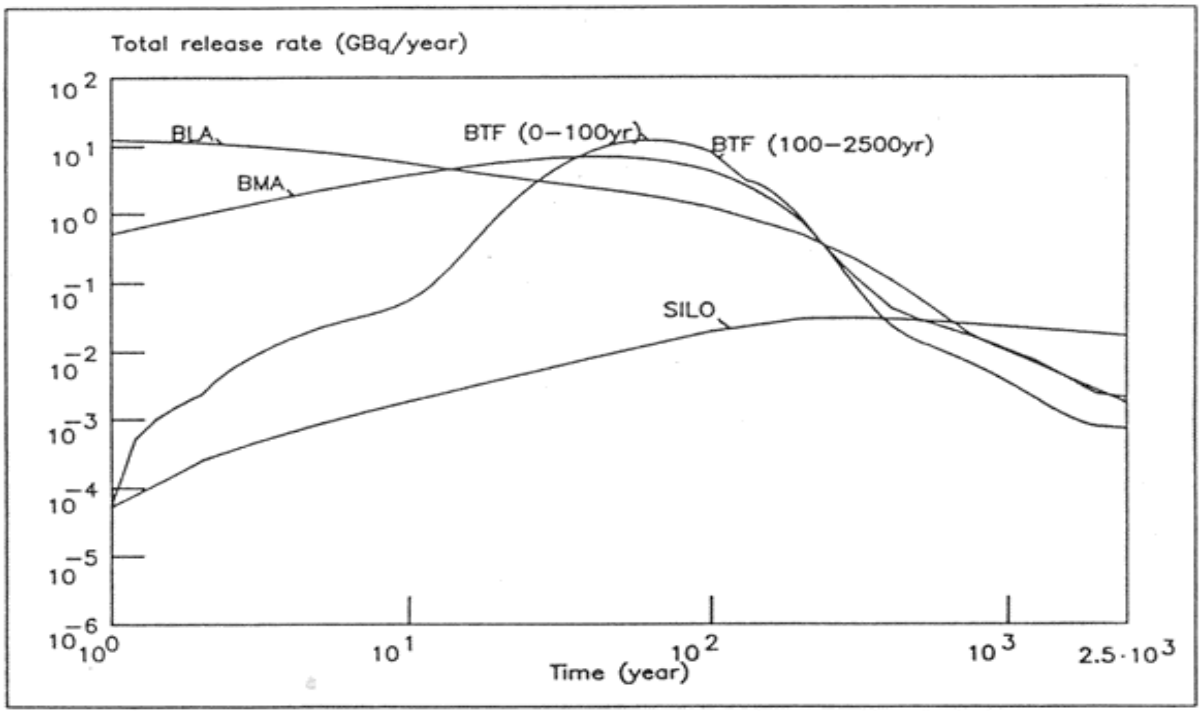

Figure B7 *Total Releases in the Saltwater Period Demonstration Calculations*

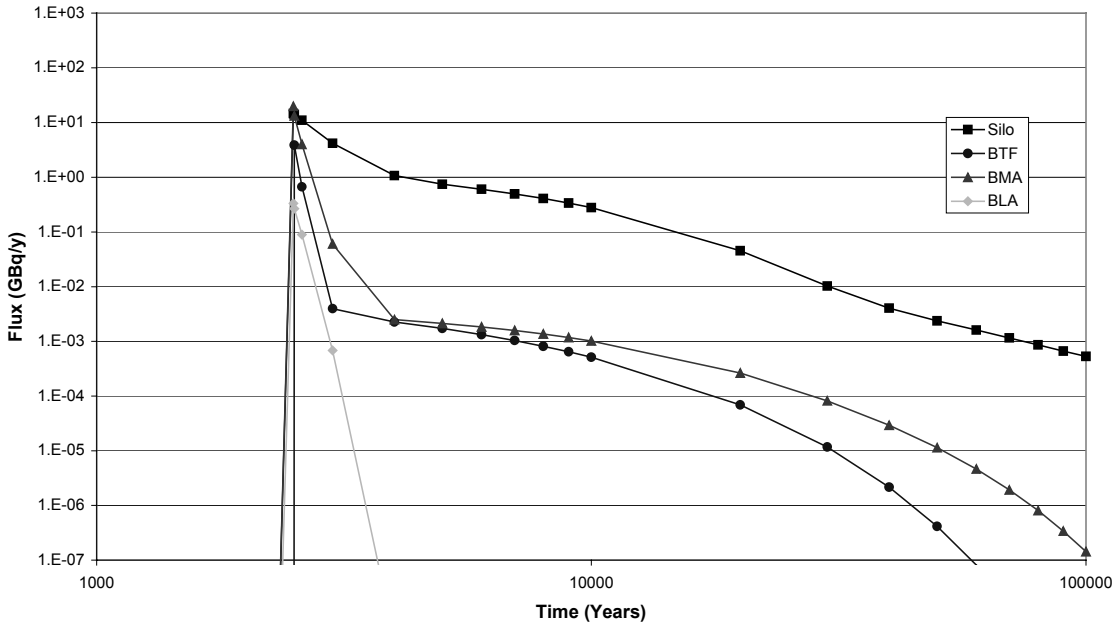

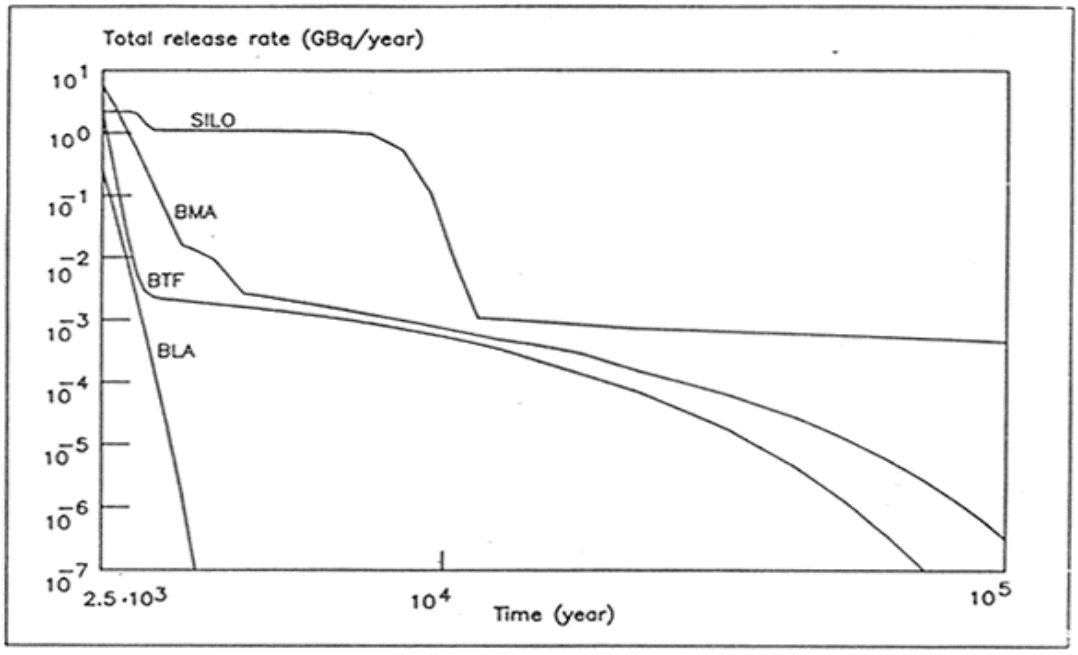

Figure B8 *Total Releases in the Inland Period Demonstration Calculations*

Critical Group Doses: Saltwater Period

Calculations of critical group doses from the consumption of fish from regional seawaters in the Saltwater Period were compared with those given in SSI (1989). Because of the different near-field models used (the SSI calculations used radionuclide-independent transfer rates out of the near-field), the calculations were not directly comparable, but similar magnitudes and patterns of doses were seen. Figure B9 shows the calculated doses for the most significant radionuclide in this period, Cs-137. In this case the calculations compare reasonably closely with Figure A6 of SSI (1989).

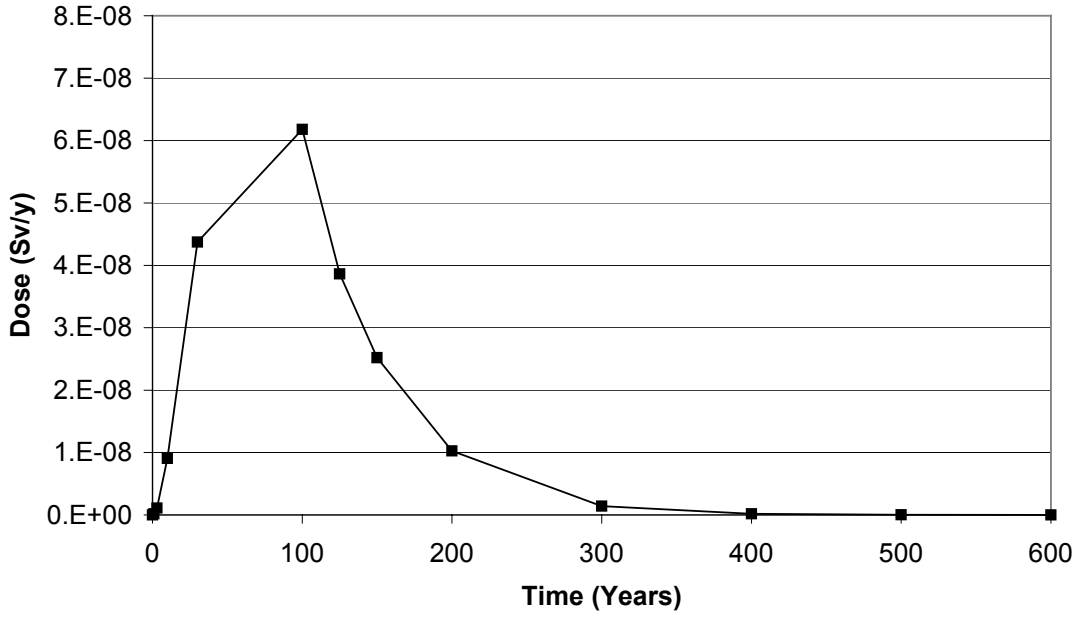

Figure B9 *Cs-137 Doses in the Saltwater Period Demonstration Calculations*

Critical Group Doses: Inland Period

Calculations of critical group doses from the consumption of fish from the lake in the Inland Period were compared with those given in SSI (1989). Figure B10 shows the calculated doses for Pu-239. In this case the AMBER calculations were around two orders of magnitude lower than those shown in Figure A18 of SSI (1989), as SSI assumed a simplified near-field that gave much faster releases.

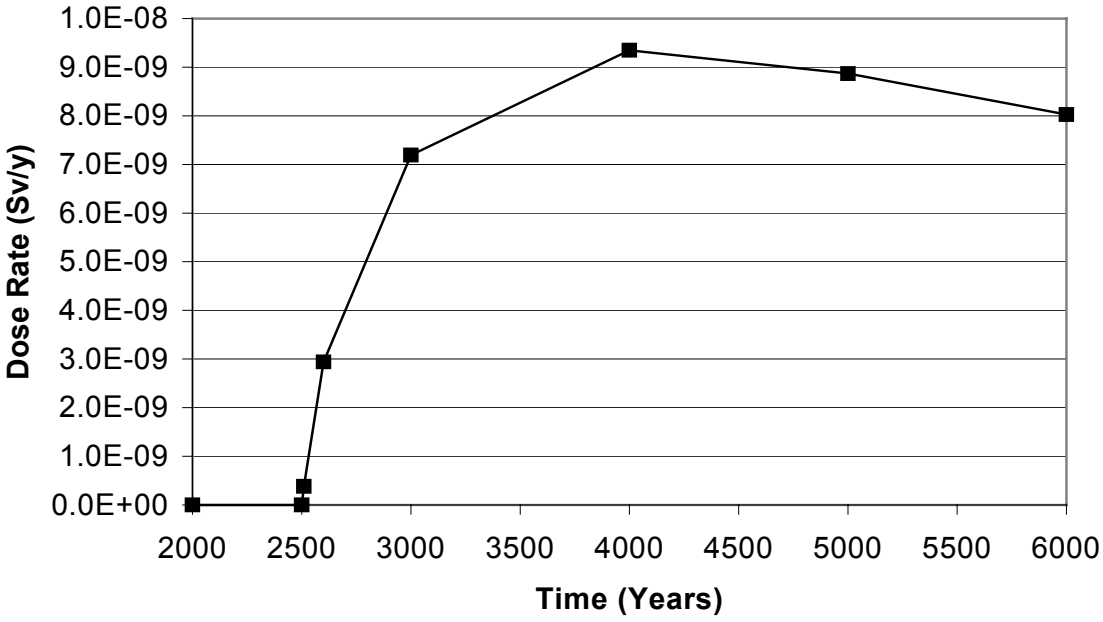

Figure B10 *Pu-239 Doses in the Inland Period Demonstration Calculations*

B4 Conclusions

32. Despite a number of simplifying assumptions, the demonstration AMBER calculations were able to reproduce satisfactorily near-field and biosphere calculations produced by SKB and SSI.

33. The reproduction of the SKB calculations provided confidence in the use of AMBER for PA calculations for SFR 1.

34. The lack of full time dependency in the original SKB calculations, with a simple representation of Saltwater and Inland conditions, could be a significant limitation in the representation of potential radiological impacts, and this would need to be investigated in AMBER models.

Appendix C. Prototype Calculations

C1 Introduction

In 1999 a first set of Prototype calculations were undertaken under contracts with SKI and SSI. The main aim of this work was to set up PA models for SFR 1 that did not rely on previous work undertaken by SKB in order to investigate whether AMBER could be used effectively as a system-level code with a full representation of the time-dependency of all the important processes. At the time that these calculations were undertaken many important input data items had not been defined; the emphasis was on investigating AMBER's modelling capabilities rather than on producing a detailed set of PA calculations. This work is reported in Maul and Cooper (1999) and Maul et al. (1999).

C2 The AMBER Model

The sub-models used were very similar to those described in Section 2, although there was no consideration given to gas generation in the Silo or to radionuclide solubility limits. Model data were taken from the same sources as for the Demonstration calculations; i.e., mainly from SKB (1987a) and SSI (1989). A single BTF repository was considered.

It was decided to include the representation of groundwater flows from one vault to another through near-field rock compartments. As the flow was assumed to vary between being vertically upwards (during the Saltwater Period) though to being off-shore (away from the coast during the Inland Period) the flow within the Repository sub-model was similarly limited to one quadrant as discussed in Section 2. It was also assumed that, within the near-field, horizontal flow was directed from the Silo towards (and past) the tunnels.

In the Prototype model it was assumed that flow through backfill parts of repositories was determined by the flow through the general repository flows.

C3 Model Calculations

The Prototype model was used to investigate radionuclide transport in different parts of the system and the resulting potential individual radiation doses. The illustrative example calculations that were presented in Maul and Cooper (1999) and Maul et al. (1999) are reproduced here.

Figures C1-C3 give examples of the type of information that can readily be obtained for a particular radionuclide (Cs-135). Figure C1 shows the total fluxes of the radionuclide out of each of the engineered repositories.

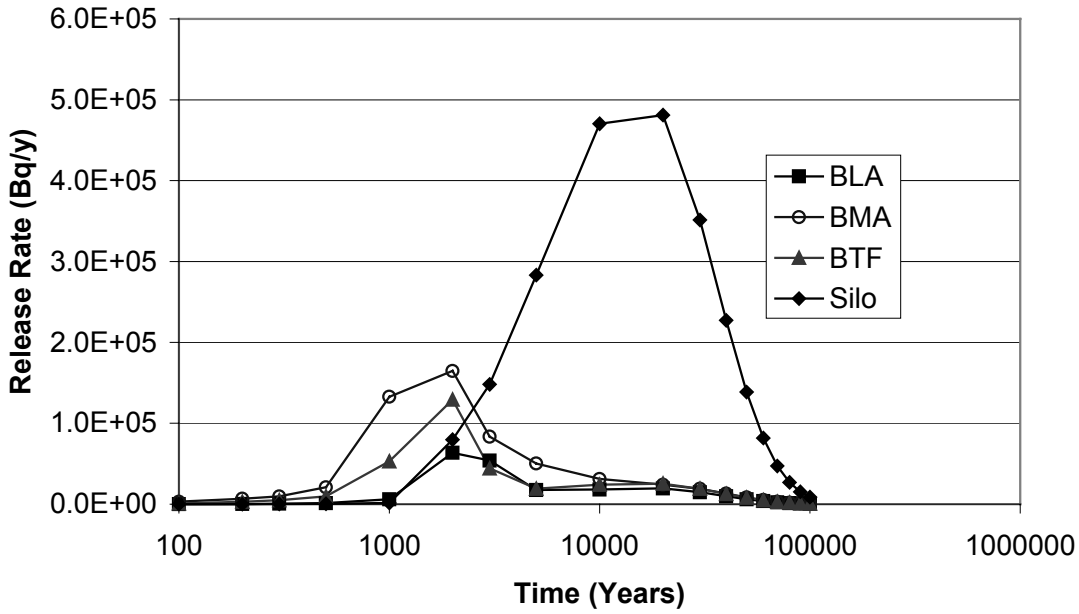

Figure C1 *Releases of Cs-135 from the Near-Field*

As one would expect, the peak fluxes from BLA, BMA and BTF occur before that for the Silo, due to the shorter lifetime assumed for the engineered barriers. The peak Silo flux is larger than the others, however, because of the larger initial inventory of the radionuclide.

Figures C2 and C3 show the inventories of Cs-135 in the two 'extreme' geosphere compartments 'G_Rock14' and 'G_Rock41' shown in Figure 2.17 of the main text.

Figure C2 shows the inventory in the compartment immediately above SFR 1 (Rock14 in Figure 2.17 in the main text), and Figure C3 gives corresponding information for the compartment that is furthest from the facility (Rock41 in Figure 2.17 in the main text). There is a relatively early narrow peak of activity in the first compartment (Figure C2), obtained when groundwater transport has a significant vertical component. The peak for the second compartment (Figure C3) is much later and flatter, reflecting the transport over longer periods when groundwater flow is essentially horizontal.

Figure C4 shows calculated concentrations of Cs-135, in two of the soil/sediment compartments in the Terrestrial Biosphere sub-system. The peak concentration appears in the Lower Sediments compartment in the first Terrestrial Biosphere region much

earlier than the corresponding peak in the Lower Sediments compartment in the fourth Terrestrial Biosphere region. This is because of the time-dependent nature of the groundwater flow regime, with transport to the first region occurring relatively early on, when there is a significant vertical component to the Darcy velocity. Transport to the fourth region occurs later, when the Darcy velocity is essentially horizontal. This type of calculation could be used for comparisons with naturally occurring radionuclide concentrations in the environment.

Figure C5 shows calculated total drinking water doses, summed over radionuclides. As a result of changing groundwater flow conditions, the concentrations of radionuclides in well water vary with time and location. With the parameter values chosen, the highest doses were calculated to arise in the second region of the Terrestrial Biosphere sub-system around 2000 years after repository closure.

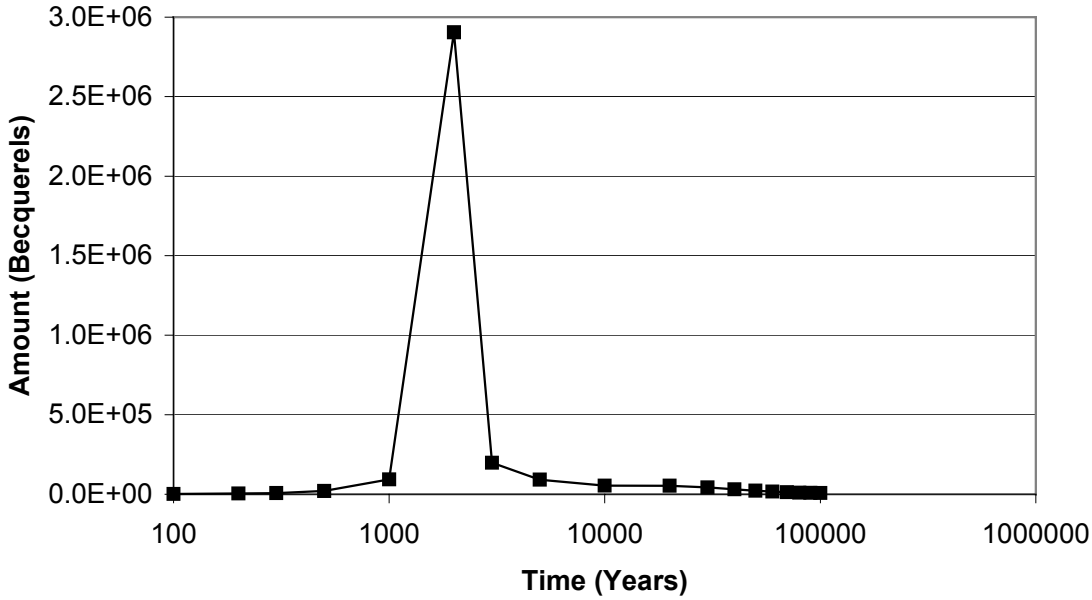

Figure C2 *Amount of Cs-135 in the Compartment G_Rock14*

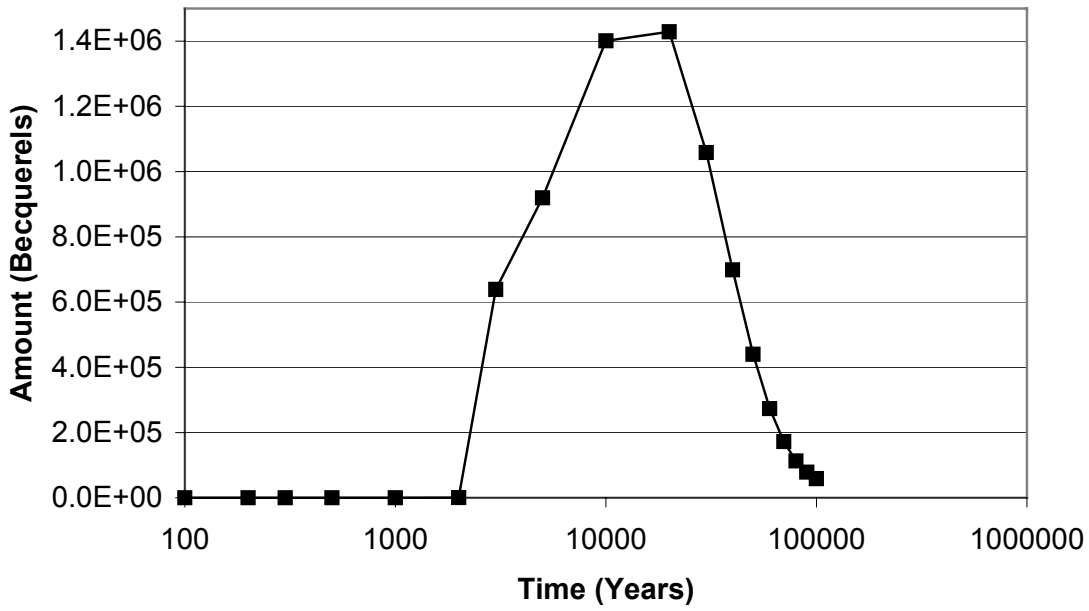

Figure C3 *Amount of Cs-135 in the Compartment G_Rock41*

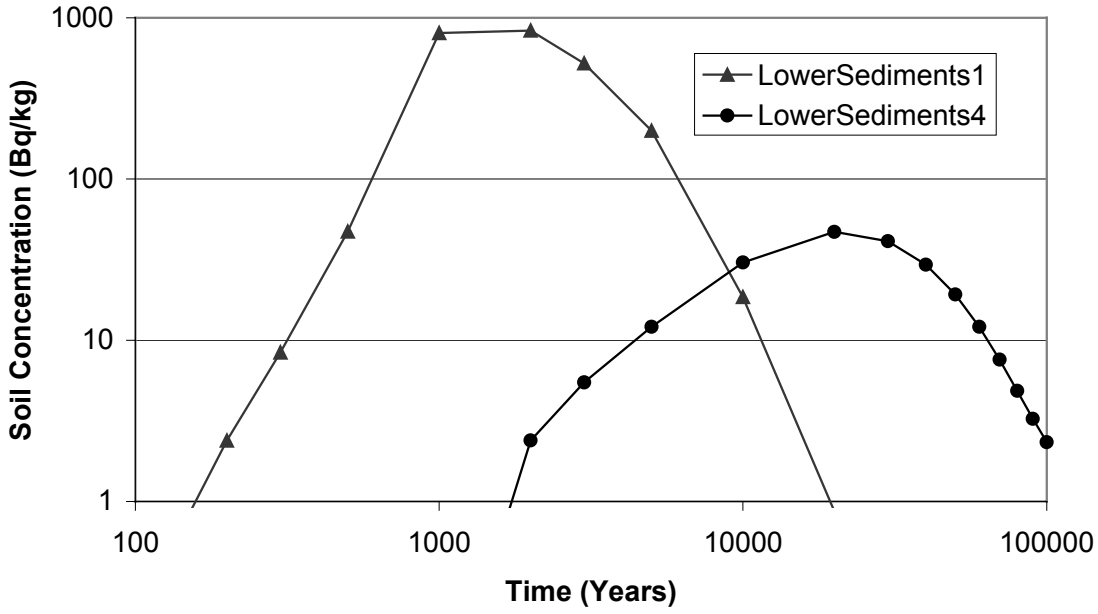

Figure C4 *Concentration of Cs-135 in Soil in the Prototype Calculations*

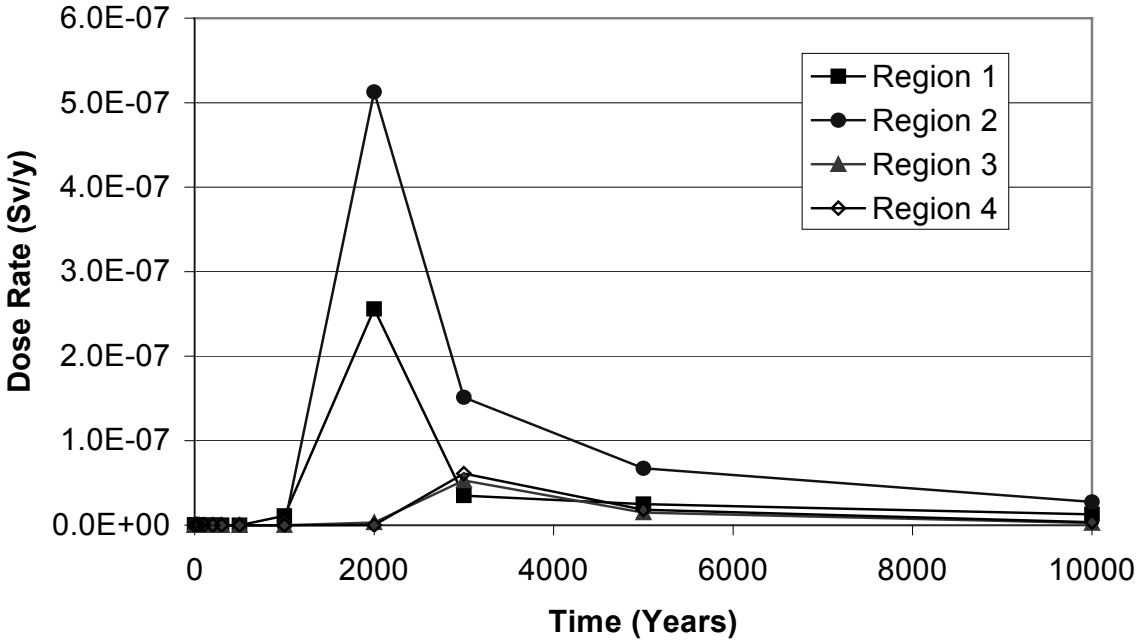

Figure C5 *Drinking Water Doses in the Prototype Calculations*

Figure C6 shows calculated doses for all the Marine pathways, summed over radionuclides. It is interesting to note that these dose rates were calculated to continue to increase (although still to relatively low values) over very long timescales (peaking at 90 000 years). This is because of the ingrowth and transport of long-lived daughters of actinides in the SFR 1 inventory.

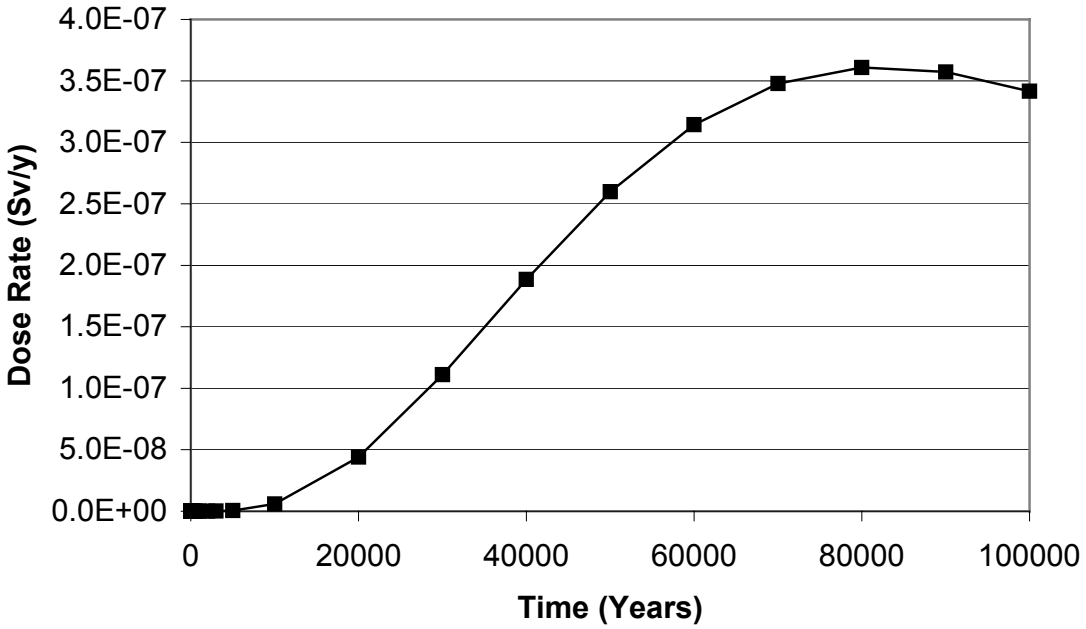

Figure C6 *Marine Doses the Prototype Calculations*

C4 Conclusions

35. The Prototype calculations demonstrated AMBER's capability to model full system time dependency. This gave confidence in the continued use of AMBER for SFR 1 PA calculations.

36. The Prototype calculations illustrated the range of model end-points that can be calculated, and how these could be used to help assess the key issues for the safety of SFR 1.

Appendix D. Scoping Calculations

D1 Introduction

Maul and Robinson (2000) built on the work undertaken in 1999 and 2000 to produce a first set of Scoping calculations to investigate some of the key PA issues for SFR 1. An AMBER Case File was produced that was in some respects simpler than that used for the Prototype calculations (by considering only the Silo repository), but which incorporated a number of refinements including the representation of gas generation and transport and radionuclide solubility limitations. Use of the data in Savage and Stenhouse (2001) avoided the need to rely totally on SKB data, but some information on gas generation was taken from Skagius et al. (1999).

SKI had identified the effects of gas generation as one area where they wished to see independent PA calculations. Detailed discussions of the importance of gas have been described in Maul (2000) and Robinson (2000).

D2 The Scoping Calculations Model

The model for the system followed that described in Section 2, but only the Silo repository was considered. The depth of the two-dimensional plane was taken to be that of the Silo itself; this is an appropriate simplification although three-dimensional processes could be represented if the required data were available.

Material Properties

In the Scoping calculations the three stages of chemical evolution of the Silo concrete were associated with the assumed rates for the physical degradation of the barriers, i.e.:

$t < t_{start}$ Stage 1 properties

$t_{start} < t < t_{end}$ Stage 2 properties

$t > t_{end}$ Stage 3 properties

Where t_{start} is the time when physical degradation is assumed to commence, and t_{end} is the time when physical degradation is assumed to be complete.

Gas Production and Transport

In the Scoping calculations the total volume of gas produced was modelled together with volume of gaseous C-14. It was conservatively assumed that all the organic C-14 present in the Silo inventory could be released in gaseous form; there was thus an intentional double counting with the groundwater pathway.

Once gas has been transported through the lid it was assumed that it would be quickly transported towards the surface.

D3 Scoping Calculation Results

In order to keep the number of calculation cases to a manageable number, a reference calculation was undertaken, and in the light of the results obtained from that case a number of variant calculations were undertaken.

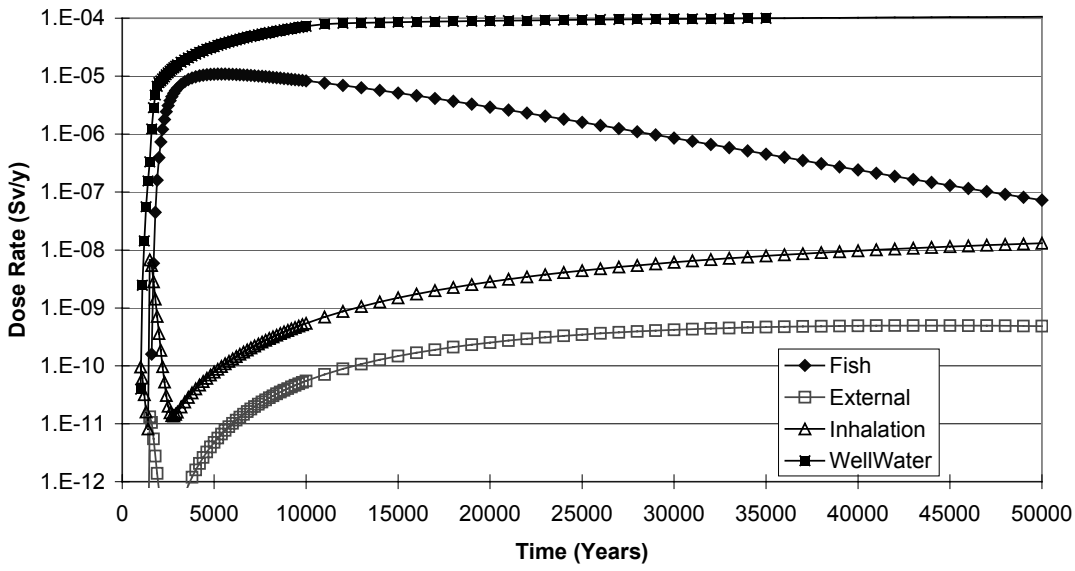

Figure D1 *Reference Scoping Calculations: Terrestrial Pathways*

Figure D1 gives details of the calculated doses for Terrestrial pathways. This suggests that the drinking water and lake fish consumption pathways are likely to be important once the sea has retreated. In both cases the dose calculations are likely to be overestimates due to some of the simplifying assumptions retained. In particular, for the drinking water pathway:

- No consideration was given to whether a well would actually be present. If not, the drinking water doses would not be incurred.
- No allowance was made for transverse spreading of the plume which could reduce the concentrations of contaminants in the well.
- No allowance was made for the sorption of radionuclides on the surface of fractures (although matrix diffusion is modelled).

For the lake fish consumption pathway a relatively slow turnover rate for the lake water was assumed (1 y^{-1}); a more rapid rate would result in reduced calculated doses.

The drinking water dose was dominated by the two radionuclides Tc-99 and I-129. Both these radionuclides are long-lived and assumed to be poorly sorbed in both the near-field and the geosphere. Oxidising conditions were, pessimistically, assumed to be applicable in the near-field for Tc-99. In fact, reducing conditions can be expected to be present in the repository soon after closure, and this would greatly reduce the flux of Tc-99 into the accessible environment (reducing conditions were assumed in the Final PA calculations presented in Section 4 of the main text). The doses presented here are much greater than those shown for the Prototype calculations because of the different sorption characteristics assumed for these two radionuclides.

The lake fish doses are dominated by C-14 as suggested in the Demonstration calculations. C-14 is relatively mobile and the concentration factor assumed for fish is high.

Figure D2 gives details of the calculated doses for Marine pathways. These doses are much lower than those calculated for Terrestrial pathways and take much longer to build up to peak values; negligible radioactivity was calculated to enter the marine environment before the sea retreated from the SFR 1 region. Sea fish consumption doses are dominated by C-14. Doses for the inhalation pathway are dominated by Tc-99, but long-lived alpha-emitting radionuclides are only just beginning to enter the marine environment at the end of the 50 000 year calculational period. These radionuclides could make a substantial contribution to the dose from the inhalation pathway. Doses for the external pathway are less than 1E-15 Sv y^{-1} throughout.

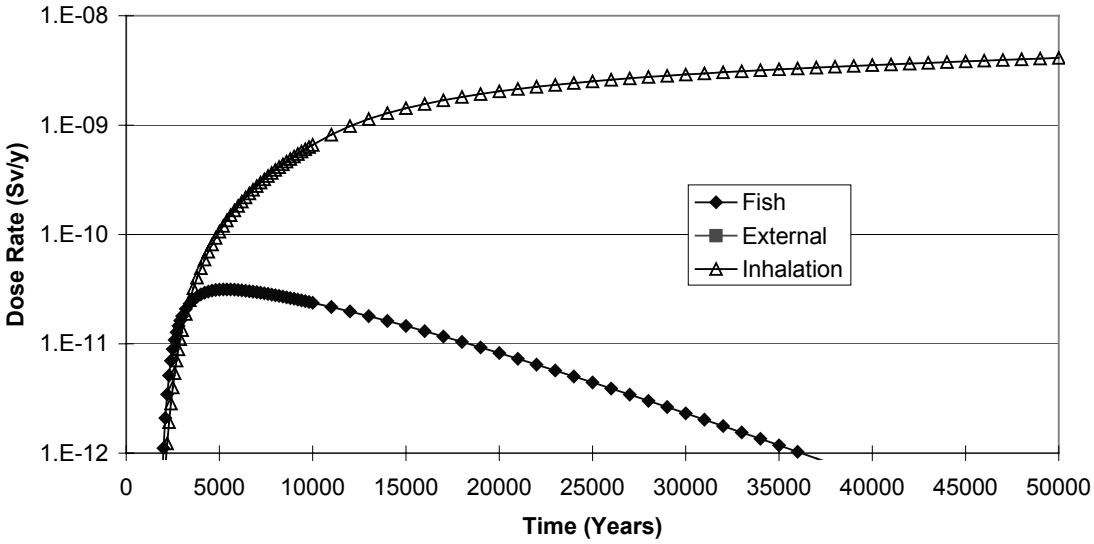

Figure D2 *Reference Scoping Calculations: Marine Pathways*

Figure D3 gives details of the calculated dose due to the inhalation of C-14 gas. No dose is incurred until the sea has retreated from above SFR 1 and it was assumed that a house is constructed immediately above the facility. Calculated doses are very low, but the magnitude of the dose is critically dependent on the form assumed for the gas. The dose per unit activity inhaled used assumes that the gas is in the form of methane. Carbon dioxide would have a value around 100 times higher, and much higher values still are obtained if the C-14 were assumed to be in the form of soluble organic material. Doses drop to zero at about 22 000 years when it is assumed that gas production has ceased.

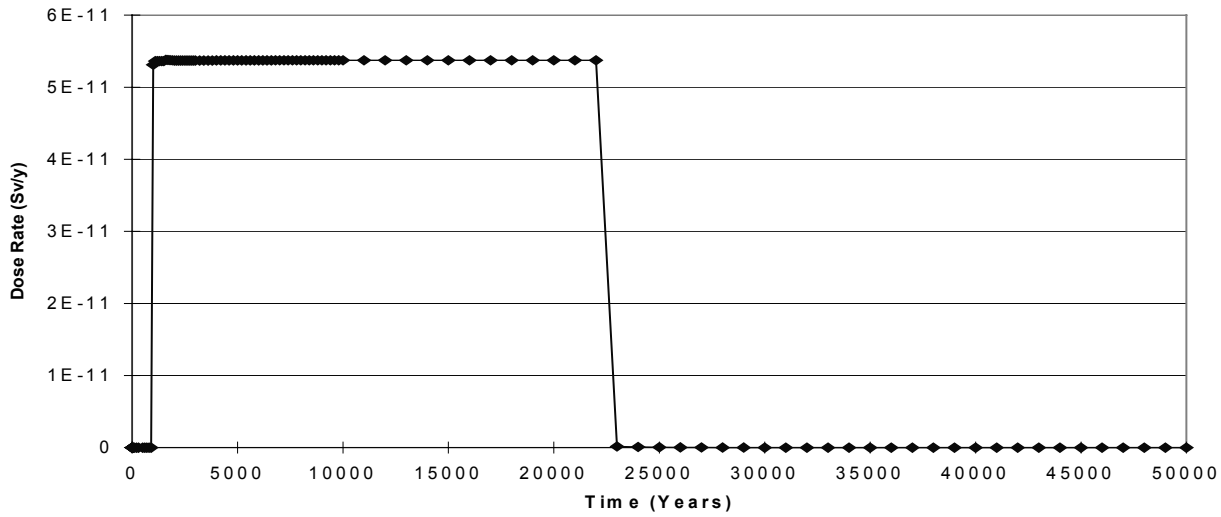

Figure D3 *Reference Scoping Calculations: Doses from C-14 Gas Inhalation*

In addition to presenting the results for individual doses, AMBER can provide information on a number of intermediate endpoints. Figure D4 shows the total flux of radionuclide calculated to leave the Silo as a function of time. Very low fluxes were calculated until the engineered barriers were assumed to start to degrade after 1000 years. Release rates peak at around 3400 years and there is a 'kink' in the curve where the inventory of Tc-99 remaining in the Silo is essentially depleted around 10 000 years. As noted previously, if near-field sorption parameters for Tc are taken for reducing conditions, much lower releases are calculated.

Another example of such an intermediate endpoint is given in Figure D5 where the total inventory of radionuclides in the Terrestrial Biosphere sub-system is presented. This underlines the long timescales over which radioactivity released from the Silo may build up; the peak inventory is not reached until 11 000 years after repository closure.

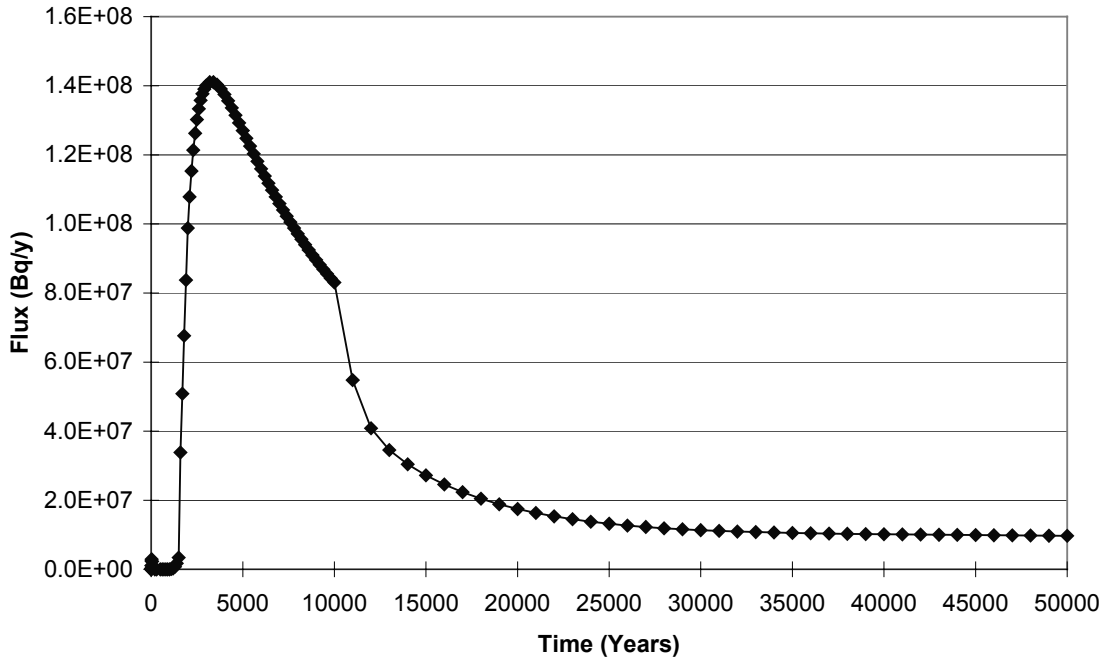

Figure D4. Reference Scoping Calculations: Total Releases from the Silo

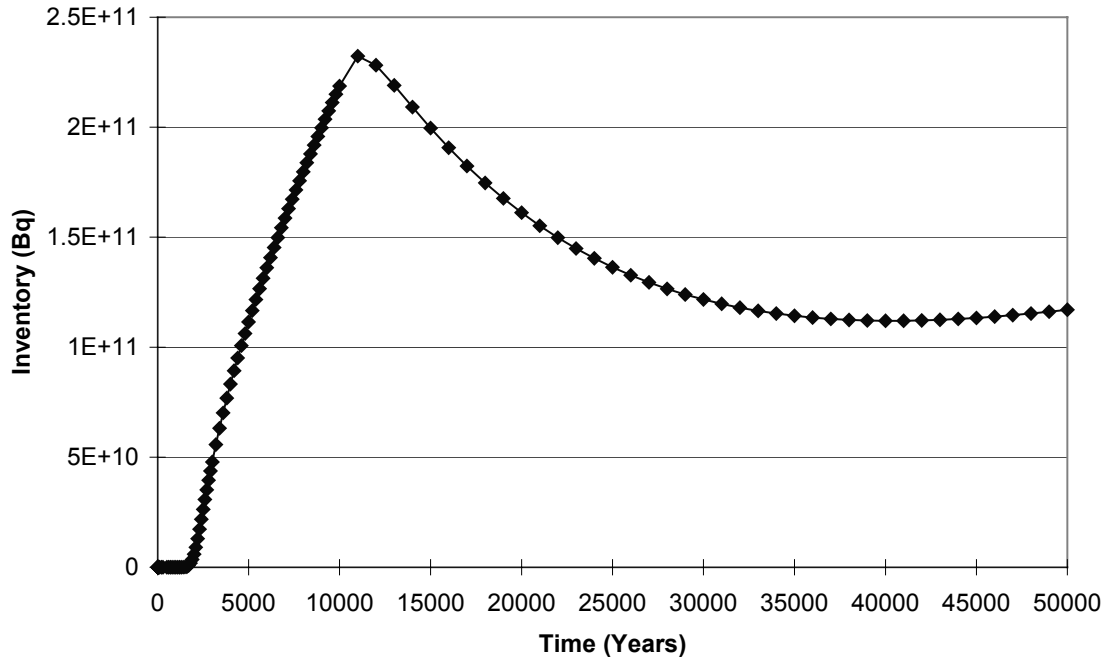

Figure D5 *Reference Scoping Calculations: Total Inventory in the Terrestrial Biosphere Region*

Blocked Gas Vents Variant

Figure D6 gives details for the total flux of radionuclides from the Silo if it is assumed that the gas vents are blocked (by taking the overpressure required for flow through the vents to be greater than that through the Silo walls). This Figure can be compared with Figure D4, although logarithmic scales have had to be used in order to show the new pattern of radionuclide releases. Now there is an early peak corresponding to releases of relatively short-lived radionuclides such as Cs-137 and Sr-90 following damage to the walls of the Silo from gas overpressurisation. The later peak of relatively long-lived radionuclides following the gradual degradation of the engineered barriers is little changed.

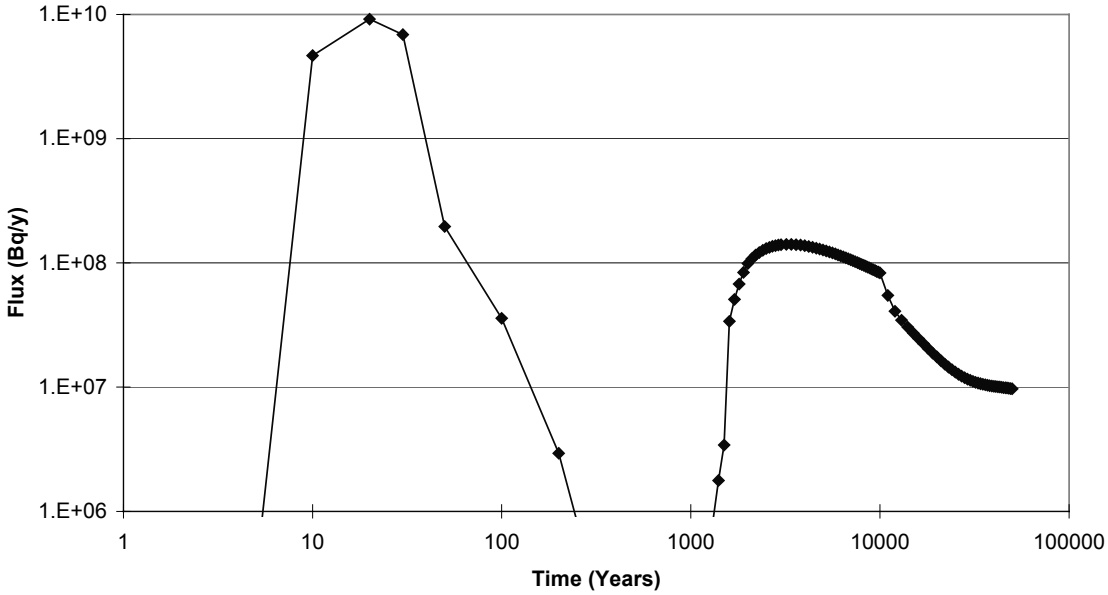

Figure D6 *Blocked Gas Vents Scoping Calculations: Total Releases from the Silo*

Although there is an increased flux of radionuclides from the Silo, the change to the calculated doses compared with the reference calculation (Figures D2-D4) was very small. This is because the new early flux of relatively short-lived radionuclides into the environment occurs when SFR 1 is still below the Baltic, and the radiological consequences are small as radionuclides are rapidly dispersed in the marine environment.

Low Near-field Sorption Variant

A variant on the reference calculations was undertaken by using the 'pessimistic' values for near-field sorption given in Savage and Stenhouse (2001) rather than the 'best estimate' values.

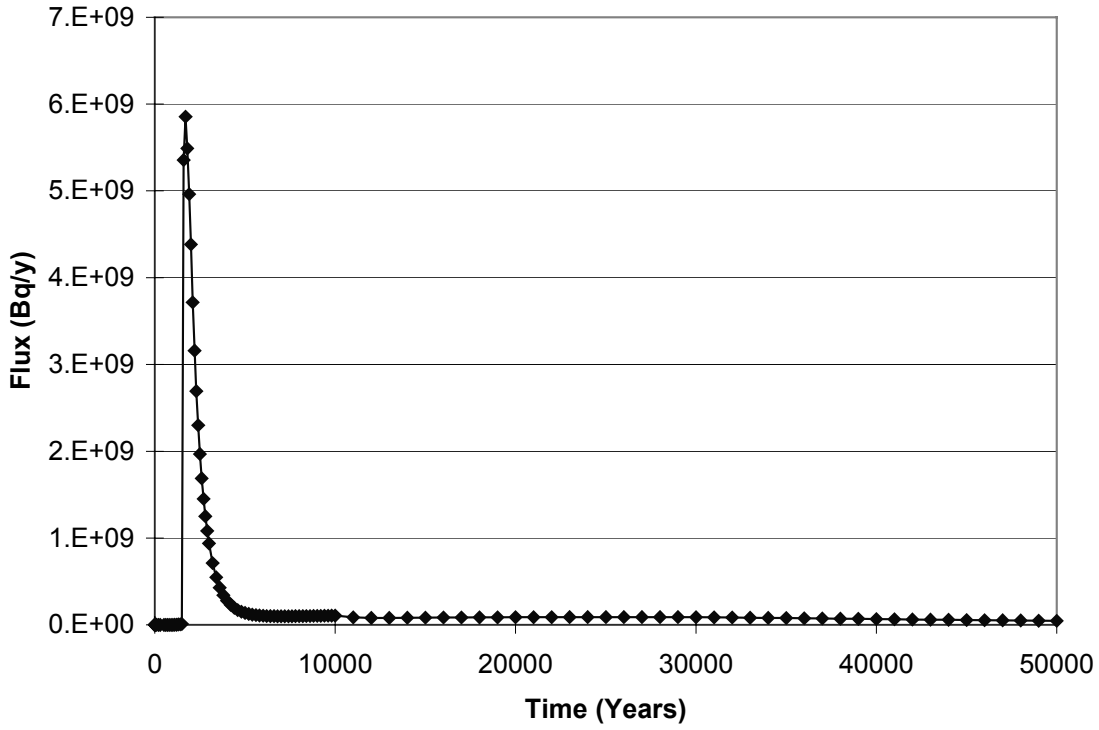

Figure D7 *Low Near-Field Sorption Scoping Calculations: Total Releases from the Silo*

Figure D7 shows that with these reduced sorption values the release of radionuclides from the Silo is much more rapid than for the reference calculations (Figure D4). The peak flux is about a factor of 40 higher and this occurs much earlier. This increased flux of radionuclides into the environment is reflected in higher calculated doses. Figure D8 shows the calculated doses for Terrestrial pathways; these are around an order of magnitude higher than those for the reference calculations (Figure D1).

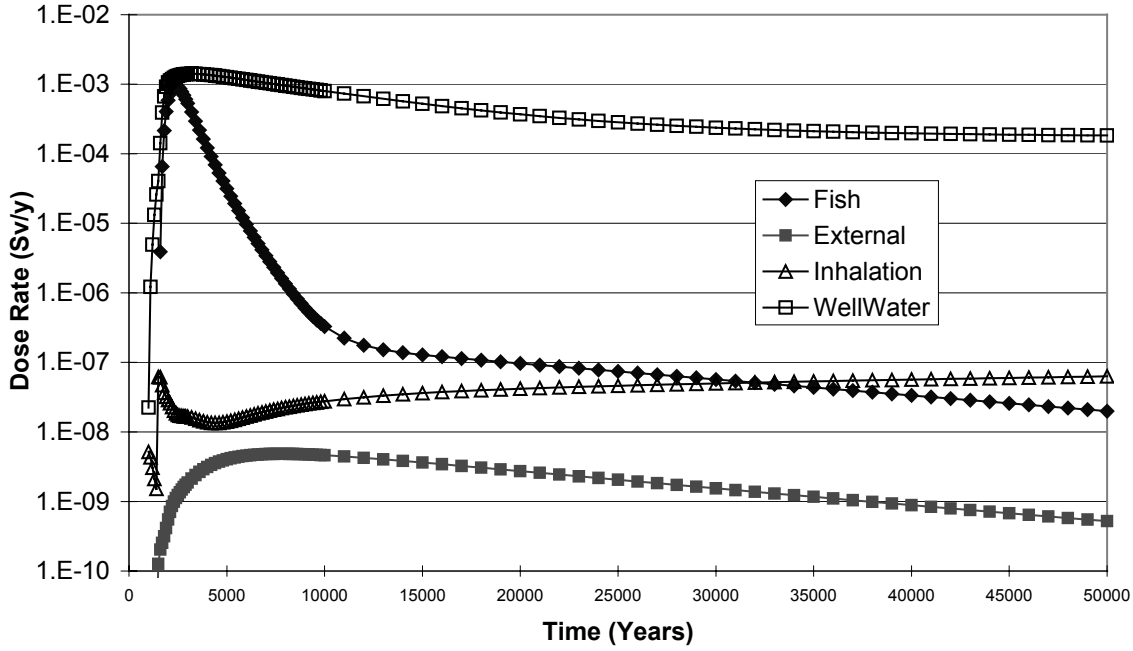

Figure D8 *Low Near-Field Sorption Scoping Calculations: Terrestrial Pathways*

Long-lived Barriers Variant

Figure D9 gives details of calculated doses for Terrestrial pathways if the engineered barriers are assumed to degrade much more slowly than in the Reference calculations. Here the barriers are assumed to start to degrade after 3000 years, and to be completely degraded by 10 000 years (compared with corresponding timescales of 1000 and 1500 years in the reference calculations). Comparing Figure D9 with Figure D1 it is interesting to note that although the peak dose rates are not incurred until much later, the magnitude of the peak doses is little altered. This is because of the importance of the long-lived radionuclides such as I-129.

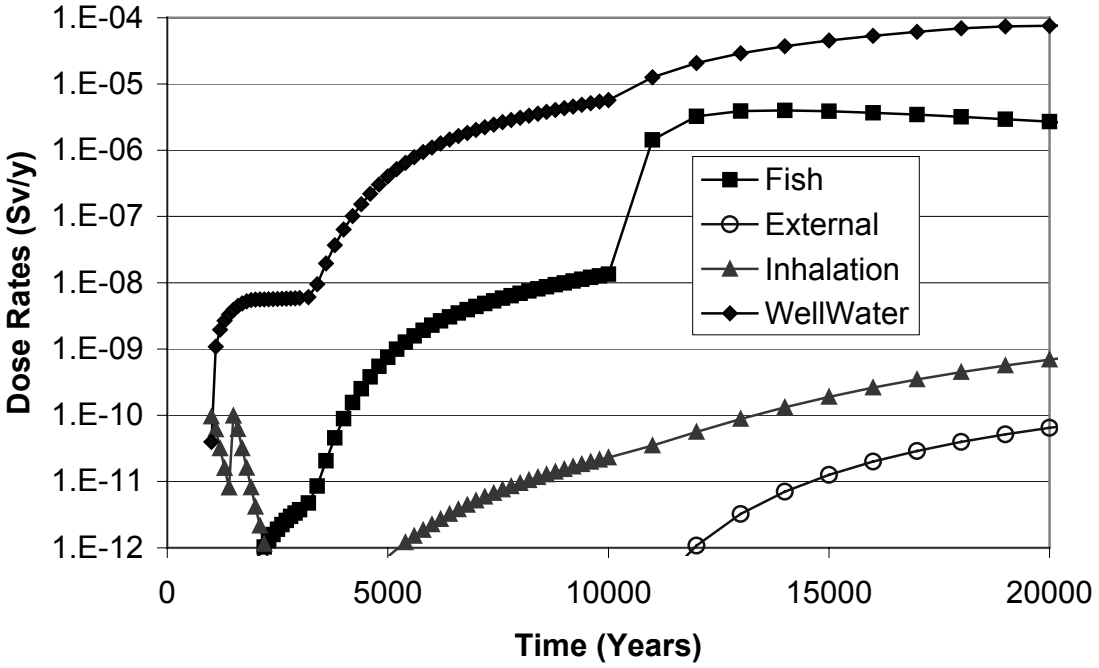

Figure D9 *Calculations with Long-Lived Engineered barriers: Terrestrial Pathways*

Other Variants

A large number of variant calculations are possible, but many do not add any additional insight into the performance of the system and have not been presented here. Some of the ways that the variation of particular parameters affects the behaviour of the system are summarised below.

37. Variation of the land uplift rate (U) affects the time when the sea retreats from above SFR 1 and when the new lake is formed. However, within the possible range of effective uplift rates the resulting variation in calculated doses is not very great; peak dose rates are similar, although the timing of the peak is affected.

38. Parameters affecting the evolution of the near-field (such as the resaturation rate, and the overpressure needed for gas to flow through the gas vents) can affect the time history of radionuclide fluxes from the Silo on relatively short timescales, but do not generally result in major changes to calculated doses. For example, porewater can be expelled through the base of the Silo due to the build up of gas pressure, and this leads to a flux of short-lived radionuclides out of the Silo in a similar way to that calculated for the Blocked Gas Vents variant.

39. Varying the assumed timescales for barrier degradation will change the timing of the flux of relatively long-lived radionuclides but the general magnitude of peak radionuclide fluxes from the Silo and the resulting potential doses to individuals do not vary very much. The implication appears to be that the sorption properties of the near-field materials are more important than their ability to limit groundwater flows.

40. The only radionuclides that are solubility limited in the waste in the reference calculations were isotopes of plutonium, and the resulting reduction in radionuclide releases was small. Sensitivity studies were not undertaken for solubility limit parameters, but it is unlikely that varying these parameters within reasonable ranges would significantly affect the performance of the system.

D4 Conclusions

41. The reference set of Scoping calculations suggested that potential doses would be very small when SFR 1 is below the Baltic, but once the sea has retreated dose rates of around 0.1 mSv y^{-1} are possible.

42. For the reference calculations one of the most significant pathways could be the consumption of contaminated drinking water, although it is not certain that this pathway would actually be present.

43. Doses from long-lived mobile radionuclides such as C-14, Tc-99 and I-129 may be dominant.

44. If overpressurisation of the Silo takes place this could lead to increased short term releases of short-lived radionuclides into the environment, but this is unlikely to lead to significantly increased radiological impacts as these releases take place when SFR 1 is below the Baltic and radionuclides released into the sea are rapidly dispersed.

45. The (chemical) sorbing properties of engineered barriers appear to be at least as important as their (physical) ability to limit groundwater flows. Calculated peak dose rates are sensitive to the choice of radionuclide sorption coefficients.